OBSERVING PRESSURED SEA ICE IN THE HUDSON STRAIT USING RADARSAT: IMPLICATIONS FOR SHIPPING

Olivia Mussells

A thesis submitted to
The Faculty of Graduate and Postdoctoral Studies
In partial fulfillment of the requirements for the degree of
Master of Science in Geography with Specialization in Environmental Sustainability

Department of Geography

Faculty of Arts

University of Ottawa

ABSTRACT

Pressured and ridged ice is a dangerous hazard facing ships in the Arctic. Ships can become stuck or beset in these conditions, which is environmentally and economically costly. Understanding where and when ridges form as a result of pressured ice is important for ensuring safe winter shipping operations; however there have been few studies to date regarding the distribution of ridges and their impacts within a geographic region. The Hudson Strait, which connects Hudson Bay and the Atlantic Ocean, is the site of ongoing winter shipping, where vessels frequently encounter pressured ice. This thesis addresses two questions: where and when do ridges occur in the Hudson Strait and what are their impacts on an ice strengthened vessel traveling through the Strait. To answer the first question, ridges were manually identified in RADARSAT-1 and -2 images during the winter months (December to May) from 1997-2012. Ridge counts and densities for each winter season were calculated and their spatial distribution was mapped. A 30-year sea ice climatology of the Hudson Strait was also created in order to understand ongoing trends in freeze-up and breakup timing in the region. Recurring patterns in the location and timing of ridging were found in the Hudson Strait, specifically in areas where shearing and bottlenecks created pressure. Ridge densities were correlated with sea level pressure, air temperature and wind NCEP reanalysis data to look to for connections between these factors and ridge densities. Some connections were found between freeze-up dates, sea level pressure and ridge densities.

The second half of this thesis focuses on how ridges impact the voyage of an ice-strengthened vessel. Log books from the *MV Arctic*, a cargo ship that makes two winter transits through the Hudson Strait every year, were used to plot the movement of the ship and where and when it became beset. These data were examined for temporal and spatial patterns in besetting events. Most besetting events took place in February and March. They typically occurred in the eastern and western ends of the Strait. These voyages were compared to ridge data from the first half of thesis, and there were good correlations between the presence of high ridge densities and ship besetting events, demonstrating that ridge densities identified in satellite imagery can act as a proxy when forecasting hazardous ice conditions.

This research fills an important knowledge gap in understanding where and when pressured ice forms in the Hudson Strait and what factors play a role in creating this hazardous ice condition. It also addresses the impacts that ridges have on ship transits through the Strait.

ACKNOWLEDGEMENTS

This thesis would not have been possible without the support and encourage of many people. I'd like to thank Jackie Dawson, my co-supervisor, for her guidance and feedback during this process. I have learned so much from you and greatly appreciate all the opportunities you have presented to me. I would also like to thank my other co-supervisor, Steve Howell, for his patience in teaching me more than I ever thought I would know about sea ice. Thank you as well to my committee members for their advice and insight along the way. Thanks to Fednav for their contributions to this project and for the opportunity to travel north and see the beauty of the ice in person.

To Larissa Pizzolato, without whom I would have given up on GIS long ago, thank you. Thanks to Brigitte Champaigne for her help digitizing the logbooks of the *MV Arctic*. I would like to extend a thank you as well to all the geography graduate students who were there for long chats, about work and otherwise, and for the trips to Cafe Nostalgica necessary to maintain morale.

Finally, I would like to acknowledge my close friends and family. Thank you for support and encouragement through times of stress, which made all those times of success possible.

Table of Contents

Table of Figures

TABLE OF TABLES

CHAPTER 1: INTRODUCTION

1.1 INTRODUCTION

Arctic shipping in Canadian waters has increased significantly since 2007 (Pizzolato et al., 2014). Pressured ice and ridges are a serious hazard facing ships operating in this Arctic region (Kubat et al.; Kubat et al., 2011; Kwok, 2014). These conditions occur when convergent forces act upon the ice, putting it under pressure and causing it to ridge (Marchenko, 2008; Timco et al., 1997). Ridging can be a result of winds, tides and currents, aided in part by the geography of coasts and islands (Kubat et al., 2012). This situation makes it difficult for a ship to transit the ice and can cause the vessel to become beset, which is environmentally and economically costly, and puts crews and cargo at risk (Kubat and Sudom, 2008). Pressured ice and ridges can even hinder the passage of highly ice-strengthened ships. Therefore, it is critical to understand where and when these ice hazards are occurring and how they can impact a vessel transiting ice infested waters. In the Hudson Strait region, there tends to be common yet unpredictable ice pressure events that have created challenges for year-round shipping to mining operations in Deception Bay, Quebec (P. Bourbonnais, personal communication, January 24th, 2014). These pressure events occur when the ice concentration in the region is high. While traveling through ice-infested waters, captains most commonly use operational ice charts that are produced by the Canadian Ice Service (CIS) as sources of information for navigational decision-making. These charts include information on sea ice concentration and stage of development. However, they have a relatively coarse spatiotemporal resolution and do not capture the intricacies of sea ice dynamics such as ice ridging, convergent and divergent ice patterns, and areas of pressure. Therefore there is an urgent need for better information about ice pressure at the ship scale.

Currently, there are only a very limited number of studies examining ice under pressure as it relates to shipping in the Canadian Arctic (Kubat et al., 2008; Xue et al., 2011; Kubat et al., 2012; Kubat et al., 2013). Previous studies have typically focused on ridge size and shape for the purpose of understanding loads that ridges can place on ships or offshore structures, as opposed to the distribution of ridges in a region (Kwok, 2014). In a survey of captains and ship operators who worked in the Arctic conducted by Kubat et al. (2008), respondents noted that ice pressure can be extremely hazardous to ships and

that more information is urgently needed about where and when pressure is developing. Many of the models that have been developed for understanding pressured ice are at the scale of several kilometres, whereas ships experience pressure at much smaller scales (Kubat et al., 2012). This thesis research addresses this knowledge gap in two parts: first it aims to understand where and when ridges, which are an indicator of pressured ice, are occurring in the Hudson Strait using RADARSAT-1 and -2 imagery. Second, it addresses how these ridges and hazardous ice conditions impact a vessel at the ship scale by analyzing winter shipping voyages through the Hudson Strait.

1.2 Physical Properties of Ice

It is important to understand the physical properties of sea ice before examining the causes of sea ice pressure. Sea ice is made up of ice crystals, solid salts, air, and brine. It is typically classified by age; first year (FYI), second year and multiyear ice (MYI).

1.2.1 Sea Ice Thermodynamics

Sea ice thermodynamics define the growth of sea ice as a result of heat loss from the ocean and sea ice. Sea ice thermodynamics have less of a direct role in putting ice under pressure than do sea ice dynamics. However, thermodynamics remain important in determining ice coverage and thickness, both of which are characteristics that interact with dynamic factors to create pressure.

Arctic waters are stratified by salinity rather than temperature. As surface air temperatures (SATs) drop in the autumn, the surface layer cools, becomes denser and sinks, but is prevented from sinking completely by the density stratification determined by each layer's salinity. So rather than mixing, the top layer can thus cool below freezing point and ice can form before the entire column is cooled, allowing a lot of ice to form quickly. As described in Serreze and Barry (2005), sea ice formation begins with a slush of ice crystals on the surface of the water called frazil ice. Wind and wave action push the crystals together into chunks of semi-consolidated ice called pancake ice, which are about 0.3 to 3.0 m in diameter. The pancake ice eventually congeals together to form FYI. In calm waters, the ice crystals form thin sheets of ice called nilas ice, which thickens into

FYI. FYI thickens throughout the winter. Accretion continues from the bottom and is dependent on the temperature gradient between air temperatures and water temperatures. The rate slows as the heat from the ocean must first be lost through the insulating layer of ice before the water temperature can decrease to the freezing point and ice can be formed. Snow cover on the ice is a strong insulator and decreases the temperature gradient and slows the ice growth. As the ice thickens and ages, it also freshens as brine and salt are rejected downwards through the ice (Wadhams, 2000).

Melt is initiated once the surface energy budget becomes positive; melt from the bottom of the ice begins once the oceanic heat flux is greater than the flux of heat through the ice (Eicken, 2003). The presence of open water decreases the albedo of the ocean surface (from 0.4-0.7 for ice down to 0.15-0.4 for open water) and initiates the sea-ice albedo feedback mechanism (Maykut, 1986; Curry et al., 1995). More solar radiation is absorbed, the oceanic heat flux is enhanced and this increases the rate of bottom and side ice melting. This is a positive feedback cycle as increased melting increases the open water area available for solar radiation absorption (Curry et al., 1995). As the surface of the ice melts, ponds of water form in shallow depressions. The ponds decrease the albedo of the surface and increase solar radiation absorption. The melt pond reduces the albedo of sea ice, increases solar radiation, so the ice under the pond melts 2-3 times faster than bare ice, thus deepening the depression (Fetterer and Untersteiner, 1998).

1.2.2Sea Ice Dynamics

Sea ice dynamics are the key forces that put ice under pressure and therefore an understanding of sea ice dynamics highly important for this study. When ice is not land-fast, it is in constant dynamic motion. The ice is subject to convergent and divergent forces that influence the ice thickness, distribution and the level of pressure it is under.

1.2.2.1Divergence

Divergent forces act to thin the ice concentration and release ice pressure. Both divergent and convergent forces are illustrated in Figure 1.1. Winds and currents with divergent patterns can create areas of open water within the ice called leads and polynyas (Wadhams, 2000). Leads are linear openings in the ice and they re-freeze quickly in the

wintertime due to the great difference between ocean temperature and air temperature (Wadhams, 2000). Polynyas are non-linear openings in sea ice that have not re-frozen. Leads and polynyas are the sites of heat exchange between the ocean and the atmosphere; heat is lost from the ocean through polynyas in the winter months, while heat is absorbed through them by the ocean in the spring and summer months. The presence of leads and polynyas in an ice covered area indicates that the ice there is not under pressure. This is important to note when attempting to identify regions of ice that are experiencing pressure.

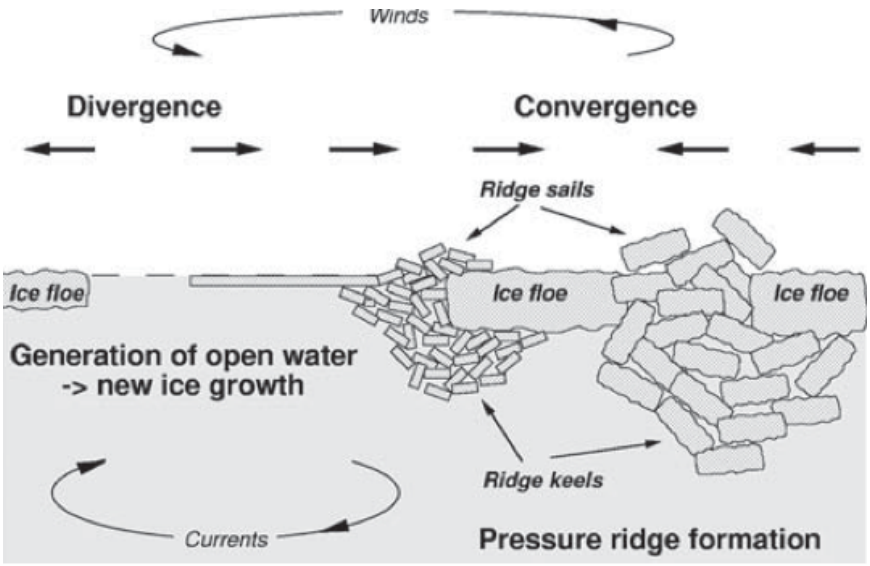

Figure 1.1: Convergent and Divergent Ice Processes (Haas, 2010)

1.2.2.2 Convergence, Pressured Ice and the Formation of Ridges

Convergent forces act to increase the ice concentration and thickness through ridging. They are the key forces that interact to put the ice under pressure causing it to ridge and are the focus of this study. Convergent forces are illustrated alongside divergent ones in Figure 1.1. These forces include currents, tides, winds and swell. Factors such as ice concentration, ice floe size and ice thickness interact with these forces, which determines the level of pressure the ice experiences. The impacts of these interdependent forces and

factors can be amplified by the presence of land or ice masses that provide resistance to the ice (Kubat et al., 2008; Kubat et al., 2011). Ice that is enclosed by land features or by land-fast ice is more likely to experience pressure as it is forced through a bottleneck (Kubat et al., 2008). Once pressure drivers have been released, the speed of pressure dissipation is highly dependent on the area of the convergence (Kubat et al., 2008). Small fields of pressure may be relieved relatively quickly but larger fields, that span several hundred kilometres, can take hours to dissipate (Kubat et al., 2008). In these cases, the release of pressure does not occur all at once; large chunks of ice will slowly break away from the ice edge, while the pressure may remain in the middle of the pack for much longer, especially if geography and bottleneck is a factor (Kubat et al., 2008).

Figure 1.2: Sea ice ridges in the Hudson Strait, January 2014 (Mussells, 2014)

When convergent forces, as well as shear forces, put the ice under pressure they can cause ridges when ice is crushed together and pushed both above the waterline (Weeks, 2010). As the ice is pushed together, blocks break off and are accumulated above and

below the water line (Timco et al., 1997). The stack of ice above the surface is called the sail and below is called the keel. Over time, the blocks freeze together and become consolidated. Keels are usually 4 times as deep as their corresponding sails are high and can reach 50m in depth, though more typically their depth is approximately 10-25 m (Wadhams, 2000). Sail height can be used as an indicator of the ridge thickness (Zakharov et al., 2014). Depending on the situation, ridges take different forms. In the case of shearing, with mobile ice moving past land-fast ice, the ridges formed are very strait and usually made up of ice that is finely ground (Parmerter and Coon, 1972). Whereas when two mobile ice floes are forced together, the ridge is usually made up of larger ice blocks (Parmerter and Coon, 1972).

Ridging commonly occurs in places where leads or polynyas have opened up and re-frozen since the ice in these locations are thinner and weaker than the surrounding ice (Wadhams, 2000). They also frequently form where mobile ice comes into contact with static, land-fast ice and shearing forces occur (Overland and Pease, 1988). For example, sea ice from the Arctic Ocean is pushed up against the northern edge of the Canadian Arctic Archipelago and Greenland and forms some of the thickest sea ice ridges in the world (Melling, 2002). Dynamic ice ridging is an important factor for thickening MYI and ridges account for an estimated 40% of the ice mass in ocean areas or up to 60% in coastal areas (Wadhams, 2000). This thicker ice is more likely to survive the summer melt season. Ridge nomenclature follows that of ice; first year ridges are those that have not yet survived a summer melt season, while multi-year ridges have and are assumed to be more consolidated than first year ridges (Ekeberg et al., 2015; Dalane et al., 2015). Ridges dynamically thicken sea ice and affect sea-atmosphere interactions, as well as the drag experienced by the ice in the air and water, thus altering ice motion (Kwok, 2014).

Pressured ice and ridges can be very hazardous to vessels. In some areas with seasonal ice cover and no icebergs, ridges and pressured ice can represent the greatest load experienced by a vessel or offshore structure (Timco et al., 2000). Their keels can

interfere with shallow water underwater pipelines (Barrette, 2011). In this vein, studies of ridging typically focus on the strength and measurements of the individual ridges and load it may place on vessels or offshore structures. There are few studies on the distribution of ridges in an area of ice and those that exist were carried out using laser profiles but these have limited coverage over time and space (Weeks, 2010; Kwok, 2014).

1.3 Study Area: The Hudson Strait

The Hudson Strait is, along with Hudson Bay and Foxe Basin, part of the Hudson Bay Complex that serves as a passage from both Hudson Bay and the Canadian Arctic Archipelago (via Fury and Hecla Strait) to the Atlantic Ocean (Figure 1.2). The Hudson Strait runs northwest for 400 km from its eastern entrance, and has an average width of 150 km (Straneo and Saucier, 2008b). The strait is U-shaped in profile, with steep sides, and ranges from 300 to 900 m in depth (Saucier et al., 2004; Drinkwater, 1986). Important drivers in the Hudson Strait system are the strong tidal currents (tidal ranges are up to 12m in Ungava Bay), local and regional atmospheric forcing, and ocean currents in Baffin Bay, the Labrador Sea, and the Arctic Ocean (Saucier et al., 2004; Drinkwater, 1986). Air masses over the Canadian Arctic Archipelago are important determinants of the climate over the Hudson Strait (Drinkwater, 1986). A strong low sea level pressure area centered over the Davis Strait is governs the movement of air masses and the cyclonic patterns it creates drives the north, northwest winds over the Strait. These winds bring the colder, drier air masses down from the Canadian Arctic Archipelago that have such a strong influence on temperatures in the region (Drinkwater, 1986).

Currents in the strait run in opposite directions. The Baffin Island current runs east to west along the northern half of the strait bringing saltier water from the Labrador Sea, while fresher water from Hudson Bay and Foxe Basin leave the strait along the southern

half (Straneo and Saucier, 2008a). The net volume of flow is out eastwards from the strait towards the Atlantic Ocean (Straneo and Saucier, 2008b). The eastern entrance to the strait is therefore very turbulent as strong tides meet with tides and island (Straneo and Saucier, 2008a). There are also significant amounts of fresh water runoff enter the strait from rivers flowing in Ungava Bay (Drinkwater, 1986).

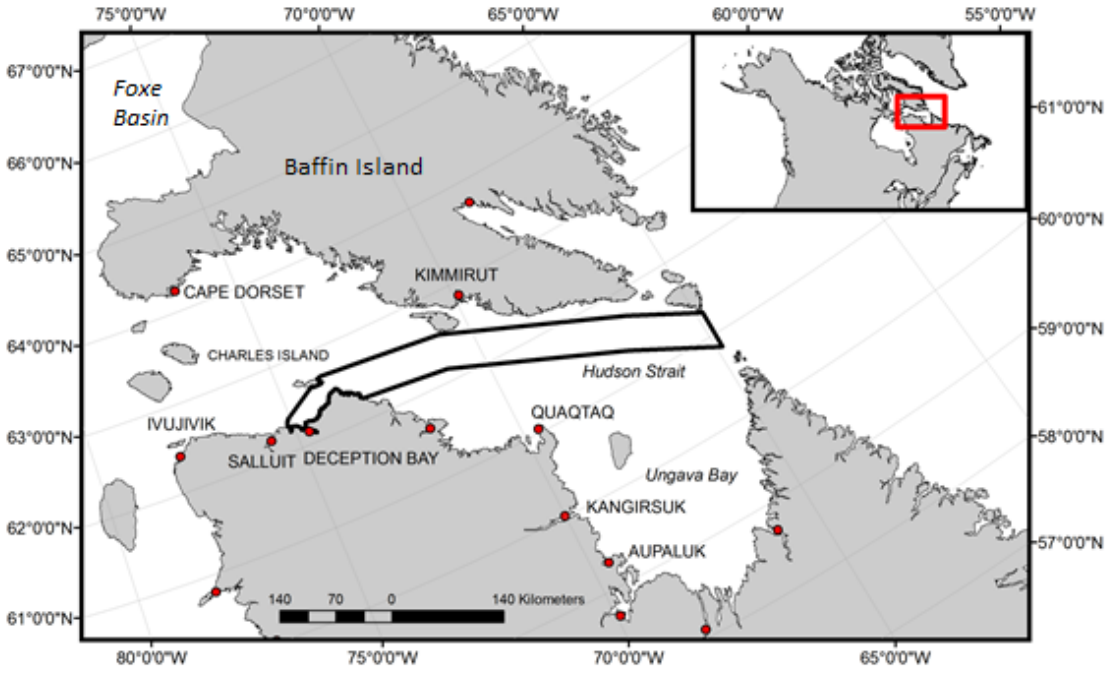

Figure 1.2: Map of the Hudson Strait

1.4 Seasonal Patterns of Sea Ice in the Hudson Strait

1.4.1 Freeze-up and Winter

The Hudson Strait is seasonally ice covered, for approximately 8 months per year. First intrusions of ice originate from the Foxe Channel in late October, early November (Drinkwater 1986; Houser and Gough, 2003). *In situ* ice formation begins in the western portion of the strait in late November, beginning with land-fast ice forming along the coast, especially the islands along the southern coast of Baffin Island (Houser and Gough, 2003; Drinkwater, 1986).The formation of ice begins in the western portion of the strait and then continues eastwards (Crane, 1978). Even when fully covered, the ice in the strait

is highly mobile, except for the wide band of land-fast ice along the coast of Baffin Island, and in the bays of Ungava Bay (Drinkwater, 1986). This ice can reach 110cm to 160cm in thickness (Drinkwater, 1986).

For the period 1971 to 1999, the length of the ice coverage season ranged from 205 to 272 days for the middle and eastern portions of the strait and 212 to 280 days in the western portion (Houser and Gough, 2003). During the winter, leads typically form along the southern coast of Baffin Island as a result of prevailing winds from the northwest (Catchpole and Faurer, 1983). These winds push the ice into Ungava Bay and there it becomes heavily ridged; typically this ice is some of the last remaining in the strait during the melt season (CIS, 2011).

1.4.2 Melt Onset and Advanced Melt

The seasonal shift from ice cover to open water is relatively quick in the Hudson Bay and Hudson Strait; for the period 1985-2009, the average elapsed time from 90% to 10% coverage was 7.8 weeks (Galbraith and Larouche, 2011). Typically, ice retreat begins between late May and early June. First, the land-fast ice detaches from the coast, becoming part of the mobile pack ice (Campbell, 1958). By late July, ice remains only in Ungava Bay and the western portion of the Strait, which is influenced by the ongoing presence of pack ice in Foxe Basin (Houser and Gough, 2003). Houser and Gough (2003) observed that there is no set direction for ice retreat, unlike the formation of the ice. For the period 1971-1999, open water conditions occurred as early as late June and as late as mid-August (Houser and Gough, 2003).

1.4.3 Inter-annual Variability

Houser and Gough (2003) examined the inter-annual variability of ice formation and breakup dates in the Hudson Strait for the period of 1971 to 1999. They found there to be an autocorrelation of one year for the length of the ice covered season; years with longer

ice-covered seasons were likely to be followed by another relatively long ice-covered season, and vice versa (Houser and Gough, 2003). This so-called thermal memory occurs because a later ice break-up date reduces the length of time available for ocean heating by solar radiation absorption and the resulting cooler than average ocean temperatures allow for earlier ice formation (Houser and Gough, 2003). The residuals of this autocorrelation were found to be significantly correlated to the surface temperatures during the open-water season; warmer summer temperatures enhanced solar radiation absorption and reduced the influence of a shorter open water season (Houser and Gough, 2003).

1.4.4 Recent Changes to Seasonal Ice Patterns in the Hudson Strait

The Hudson Bay System, including the Hudson Strait, is expected to experience climatic changes in the future. Air temperatures in the Hudson Bay system for 2041 to 2070 are projected to be 0.8°C warmer in the summer and 10°C warmer in the winter, with an average warming of 3.9°C (Joly et al., 2010). This change will be amplified as a result of the decreased surface albedo that will result from earlier ice breakup and later ice formation. Gagnon and Gough (2005) analyzed multiple climate change models for the Hudson Bay System and found that for all models the open-water season was projected to lengthen as a result of either later freeze-up dates, earlier break-up dates, or both.

Evidence of climate change has already been observed in the Hudson Bay System. Total summer sea ice cover in Hudson Strait decreased by 14.2% decade^{-1} between 1968 and 2010 (Derksen et al., 2012). Tivy et al. (2011) found there to be a significant decrease (at a 99% confidence level) of 5.0±1.0 10^2 km^2 of ice coverage for all ice types in the Hudson Strait for the period from 1968 to 2008. Ice breakup in the Hudson Strait occurred 5.6 days decade^{-1} earlier between 1971 and 2009 (Galbraith and Larouche, 2011). Markus et al. (2009) found a similar rate of melt onset occurring 5.3 days decade^{-1} earlier for the entire Hudson Bay System. When Galbraith and Larouche (2011) used 1990 as the initial year, and shortened the study period to 1990-2009, the trend towards

earlier breakup dates was enhanced, except in the case of Hudson Bay where the trend lost its statistical significance. No trend was observed when the change was calculated from 1971-1990 in all regions (Galbraith and Larouche, 2011). This supports observations by Houser and Gough (2003) who did not identify statistically significant trends in ice formation and breakup dates in the Hudson Strait from 1971-1999, but did so when the years were limited to 1990-1999. However, this study period is too short to make conclusions about warming trends in the region.

1.5 Shipping Patterns and Context in the Hudson Strait

The Hudson Strait is the site of a diverse number of shipping operations. These include cargo ships from the Port of Churchill, community re-supply ships, tourism vessels, and ships associated with ongoing resource extraction exploration and projects. Vessel volumes in the Hudson Strait from 1990 to present were extracted from the Vessel Traffic Reporting Arctic Canada Traffic Zone (NORDREG zone) based on work by Pizzolato et al. (2014). These numbers are accumulated by the individual vessel name and so multiple visits to the region by the same vessel will only appear as one voyage. In 2013, a total of 14 different vessels reported their presence in the Strait. This included 6 tugs/barges, 3 bulk carriers, 3 general cargo ships, 1 tanker and 1 government vessel or ice-breaker. Since 1990, the year when the greatest number of individual ships reported their presence in the Hudson Strait was 2010, with a total of 31 ships. The different types of ships operating in the Hudson Strait are discussed below.

Cargo ships leaving the Port of Churchill, Manitoba must head through the Hudson Strait to reach eastern Canada or foreign markets and further destinations. The port is the only operating deep-water port in the Hudson Bay/Hudson Strait complex. It is privately owned and operated by OmniTRAX (Stewart and Lockhart, 2005). Grain has been the most commonly exported good through this port ever since the first shipment left in 1931 (Stewart and Lockhart, 2005). In recent years, the amount of grain passing through the

port has grown from 640,000 tonnes in 2013 to an expected 750,000 tonnes in 2014 (Graham, 2014). The Hudson Strait is part of the Arctic Bridge shipping route between Churchill, Manitoba and Murmansk, Russia, a route that is predicted to become more popular with changing sea ice conditions (Stephenson et al., 2011).

Community re-supply ships, or sealifts, also make use of the Hudson Strait. Remote communities in Nunavut and northern Quebec depend on sealifts for bringing in fuel and dry goods for the year. Currently, the summer sealift in the eastern Arctic is performed by Nunavut Eastern Arctic Shipping Inc. (NEAS, 2014). The ships are loaded in the southern Quebec before heading northwards (Stewart and Lockhart, 2005; NEAS, 2014). The ships visit some communities as many as three times during the summer season. NEAS services communities located directly in the Hudson Strait. These are Cape Dorset and Kimmirut, on the coast of Baffin Island in Nunavut, and Ivujivik, Salluit, Kangiqsujuaq, Quaqtaq, Kangirsuk, Aupaluk, Tasiujaq, Kuujjuaq, Kangiqsualujjuaq on the Quebec coast. NEAS ships also pass through the Strait to access communities located on the Nunavut mainland and northern Quebec. These include Arviat, Coral Harbour, Rankin Inlet, Whale Cove, Chesterfield Inlet, Baker Lake, Repulse Bay, Igloolik, Sanikiluaq in Nunavut and Akulivik, Puvirnituq, Inukjuak, Umiujaq, Kuujjuarapik, Whapmagoostui in Quebec (NEAS, 2014).

The Hudson Strait was once a very popular site for cruise tourism, many of which set off from Kuujjuaq, QC in Ungava Bay (Stewart et al., 2010). Recently, declining ice extents in the Northwest Passage have shifted tours northwards where there are better chances to see Arctic wildlife, icebergs, and glaciers (Stewart et al., 2010). However, Cape Dorset, located at the western entrance to the Hudson Strait, remains an important tourist destination as self-proclaimed hub for Inuit art and port of call for cruise ships and smaller pleasure craft (i.e. private yachts) (Stewart et al, 2010).

Finally, ongoing resource extraction activities are also responsible for ship traffic in the Hudson Strait and make up all of the winter ship traffic in the region. Currently, the Raglan nickel mine in Deception Bay, QC is the only operating mine on the shores of the Hudson Strait. An ice-strengthened ship services the mine year-round. However, exploration work in the region is ongoing and growing; there are several mining ventures that are expected to begin operations in the near future. These operations are expected to make use of the Hudson Strait. The Mary River iron ore mine on Baffin Island, for example, shipped its first load of ore this year out of Milne Inlet on the northern coast of Baffin Island (CBC, 2015). Plans are such that as the mine expands and a railway is built, the iron ore will be transported by rail to Foxe Basin and then shipped year-round to foreign markets by way of the Hudson Strait (Baffinland, 2012; Nunatsiaq News, September 13, 2013). Mining is in fact a burgeoning sector in the region and many projects in the region are at the advanced stages of exploration. This factor has already increased, and will continue to increase, ship traffic in the Hudson Strait. These projects include the Meliadine gold development project that currently uses the Rankin Inlet sealift in order to import fuel, equipment and dry goods for its exploratory activities (Agnico Eagle, 2013); the Kiggavik uranium ore project west of the community Baker Lake, which includes the provisions for building a dock facility near the community in order to import supplies by ship (AREVA, 2011); and finally, the Tuktu and Roche Bay iron ore projects, near Hall Beach NU, where the mining companies hope to export the ore directly to international markets by ship by way of the Hudson Strait once the mines are operational (CBC, May 14 2014).

The vast majority of the shipping operations described above occur during the summer open water shipping season, when the Hudson Strait is ice-free (from July to October). A small percentage of the activity does occur in the winter. These winter shipping operations are the focus of this study. This work is important as government and industry are anticipating the amount of winter shipping in the Hudson Strait to increase in the future with the expansion and implementation of resource extraction projects and ongoing resource exploration.

1.6 Organization of Thesis

Chapter 2investigates where and when pressured ice is forming ridges in the Hudson Strait. Chapter 3 investigates how the pressured ice and ridges are affecting winter shipping in the region. These chapters are followed by a concluding chapter than includes a summary of the findings, a discussion of the contributions and limitations of the research and directions for future work in this area.

REFERENCES

Agnico Eagle (2013). Meliadine.*Advanced Exploration Projects*. Retrieved from: http://www.agnicoeagle.com/en/Exploration/Advanced-Projects/Meliadine/Pages/default.aspx

AREVA (2011).Tier 2 Volume 2; Project Description and Assessment Basis.*Kiggavik Project; Environmental Impact Statement*.Retrieved from: http://kiggavik.ca/wp-content/uploads/2013/04/Volume-2-Project-Description-and-Assessment-Basis_sm.pdf

Baffinland (February 2012). Mary River Project; Final Environmental Impact Statement. Baffinland Iron Mines Corporation

Barrette, P. (2011).Offshore pipeline protection against gouging by ice: An overview. CRST, 69, 3–20. http://dx.doi.org/10.1016/j.coldregions.2011.06.007.

Campbell, N. J. (1958) The oceanography of Hudson Strait. *Oceanography and Limnology*, 12:1-60.

Canadian Ice Service (2011), Sea Ice Climatic Atlas: Northern CanadianWaters 1981–2010, 995 pp., Ottawa.

Catchpole, A. J. W. and M. A. Faurer (1983).Summer sea ice severity in Hudson Strait, 1751–1870.*Climatic Change*, 5:115-139.

CBC (May 14, 2014). Chinese company joins Roche Bay iron ore project. *CBCNews*. Retrieved from: http://www.cbc.ca/news/canada/north/chinese-company-joins-roche-bay-iron-ore-project-1.2642364

CBC (August 11, 2015). Baffinland's Mary River mine ships first load of iron ore. *CBC News*. Retrieved from: http://www.cbc.ca/news/canada/north/baffinland-s-mary-river-mine-ships-first-load-of-iron-ore-1.3186459

Crane, R. G. (1978). Seasonal variations of sea ice extent in the Davis Strait–Labrador Sea area and relationship with synoptic-scale atmospheric circulation. *Arctic*, Vol. 31, 1978, pp. 434-447.

Curry, J.A., Schramm, J.L., Ebert, E. (1995). Sea Ice-Albedo Climate Feedback Mechanism.*J. Climate*. 8: 240-247, doi: http://dx.doi.org/10.1175/1520-0442(1995)008<0240:SIACFM>2.0.CO;2

Dalane, O., Aksnes, V., Løset, S. (2015). A moored Arctic floater in first-year sea ice ridges.*J. Offhsore Mech. Eng.* 137(1) doi: 10.1115/1.4028814

Derksen, C., S. L. Smith; M. Sharp; L. Brown; S. Howell; L. Copland; D. R. Mueller; Y. Gauthier; C. Fletcher; A. Tivy; M. Bernier; J. Bourgeois; R. Brown; C. R. Burn; C. Duguay; P. Kushner; A. Langlois; A. G. Lewkowicz; A. Royer; A. Walker. 2012. Variability and Change in the Canadian Cryosphere. *Climatic Change*. DOI: 10.1007/s10584-012-0470-0.

Drinkwater, K.F. (1986).Physical oceanography of Hudson Strait and Ungava Bay. In Martini EP (ed) Canadian Inland Seas, *Oceanogr Ser 44* Elsevier New York pp 237–261

Eicken, H. (2003). From the microscopic to the macroscopic to the regional scale: Growth, microstructure and properties of sea ice. In D.N. Thomas and G.S. Dieckman (Eds.)*Sea Ice: An Introduction to its Physics, Chemistry, Biology, and Geology*. Backwell Science Ltd., 22-81

Ekeberg, O.-C., Høyland, K., Hansen, E. (2015) Ice ridge keel geometry and shape derived from one year of upward looking sonar data in the Fram Strait. *Cold Regions Science and Technology*. 109: 78-89

Fetterer, F. and N. Untersteiner (1998).Observations of melt ponds on Arctic sea ice.*J.Geophys. Res*. 103 C11, 24,821-24,835

Gagnon, A.S., W.A. Gough (2005). Climate change scenarios for the Hudson Bay region: An intermodal comparison. *Climatic Change*. 69: 269-297

Galbraith, P.S., P. Larouche (2011). Sea-surface temperature in Hudson Bay and Hudson Strait in relation to to air temperature and ice cover breakup, 1985-2009. *Journal of Marine Systems*. 87 (2011) 66–78. doi:10.1016/j.jmarsys.2011.03.002.

Graham, Ian. (April 14 2014). Changes could make Churchill shipping more efficient. *Thompson Citizen*.Retrieved from: http://www.thompsoncitizen.net/news/nickel-belt/changes-could-make-churchill-shipping-more-efficient-1.1365111

Haas, C. (2010): Dynamics versus Thermodynamics: The Sea Ice Thickness Distribution , Sea ice / Ed. by David N. Thomas and Gerhard S. Dieckmann Ames, Iowa : Blackwell, ISBN: 978-1-4051-8580-6 , 113-151Houser, C., W.A. Gough (2003). Variations in sea ice in the Hudson Strait. *Polar Geography*. 27(1) 1-14

Joly, S., Senneville, S., Caya, D., Saucier, F.J. (2011). Sensitivity of Hudson Bay Sea ice and ocean climate to atmospheric temperature forcing.*Clim Dyn* 36:1835-1849

Kubat, I. and Sudom, D. (2008). "Ship Safety and Performance in Pressured Ice Zones: Captains' Responses to Questionnaire" Technical Report CHC-TR-059/ TP14847

Kubat, I., D. Watson, M. Sayed (2011).Characterization of Pressured Ice Threat to Shipping. Proceedings of the 21st International Conference on Port and Ocean Engineering under Arctic Conditions July 10-14, 2011; Montréal, Canada

Kubat, I., M. Hossein Babaei, M. Sayed (2012). Quantifying Ice Pressure Conditions and Predicting the Risk of Ship Besetting. *Paper No. ICETECH12-130-R0*

Kubat, I., M. Sayed, M. H. Babaei (2013).Analysis of Besetting Incidents in Frobisher Bay During 2012 Shipping Season.Proceedings of the 22nd International Conference on Port and Ocean Engineering under Arctic Conditions.June 9-13, 2013, Espoo, Finland.

Maykut, G.A. (1986) The surface heat and mass balance. In N. Untersteiner (ed.) *The Geophysics of Sea Ice*. NATO ASI Ser., Ser. B Phys., Vol. 146. New York: Plenum, pp. 395-464

Melling, H. (2002), Sea ice of the northern Canadian Arctic Archipelago, *J. Geophys. Res.*, 107(C11), 3181, doi:10.1029/2001JC001102.NEAS (Nunavut Eastern Arctic Shipping) (2014).Shipping Schedule.*Nunavut Eastern Arctic Shipping Inc*. Retrievedfrom: http://www.neas.ca/schedule.cfm

Nunatsiaq News (September 13, 2013). Nunavut's Mary River sets off shipping boom at Valleyfield port. *Nunatsiaq Online*. Retrieved from: http://www.nunatsiaqonline.ca/stories/article/65674nunavuts_mary_river_sets_off_shipping_boom_at_valleyfield_port/

Overland, J.E., Pease, C.H. (1988). Modeling ice dynamics of coastal seas. *J. Geophys. Res.*, 93(C12) 15619-15637

Parmerter, R.R., Coon, M.D. (1972). Model of pressure ridge formation in sea ice.*Journal of Geophysical Research.*77(33) 6565-6575

Pizzolato, L., Howell, S.E.L., Derksen, C., Dawson, J., Copland, L. (2014). Changing sea ice conditions and marine transportation activity in the Canadian Arctic between 1990 and 2013.*Clim Change*. 123(2) 161-173

Saucier, F.J., Senneville, S., Prinsenberg, S., Roy, F., Smith, G., Gachon, P., Caya, D., Laprise,R., (2004). Modelling the sea ice-ocean seasonal cycle in Hudson Bay, Foxe Basin andHudson Strait.*Climate Dyn*. 23, 303–326.

Serreze, M.C. and R.G. Barry (2005).The Arctic Climate System. Cambridge University Press: Cambridge

Stephenson, S.R., Smith, L.C., Agnew, J.A. (2011). Divergent long-term trajectories of human access to the Arctic.*Nature Climate Change,* 1 156-160 doi:10.1038/nclimate1120

Stern, H. L. and M. P. Heide-Jorgensen (2003).“Trends and variability of sea ice in Baffin Bay and Davis Strait, 1953–2001,” *Polar Res*, 22, 2003, pp. 11-18.

Stewart, D.B., and Lockhart, W.L. 2005. An overview of the Hudson Bay marine ecosystem.Can. Tech. Rep. Fish.Aquat. Sci. 2586: vi + 487 p.

Stewart, E.J., A. Tivy, S.E.L. Howell, J. Dawson, D. Draper (2010). Cruise Tourism and Sea Ice in Canada’s Hudson Bay Region. *Arctic*.63(1) 57-66

Straneo, F., Saucier, F.J., 2008a.The Arctic-subarctic exchange through Hudson Strait. In: Dickson, R., Meincke, J., Rhines, P. (Eds.), Arctic–Subarctic ocean fluxes. Springer Science, pp. 249–261. Ch.10.

Straneo, F., Saucier, F.J. (2008b).The outflow from Hudson Strait and its contribution to the Labrador Current. Deep Sea-Research I, I 55, 926–946

Timco, G.W., Croasdale, K., Wright, B. An overview of first year sea ice ridges (2000)Technical report HYD-TR-047, 157 p.

Timco, G.W., Burden, R.P. An analysis of the shapes of sea ice ridges (1997) *Cold Regions Science and Technology*, 25, pp. 65-77

Tivy, A., S.E. Howell, B. Alt, S. McCourt, R. Chagnon, G. Crocker, T. Carrieres, J.J. Yackel (2011). Trends and variability in summer sea ice cover in the Canadian Arctic based on the Canadian Ice Service Digitial Archive, 1960-2008 and 1968-2008. *J Geophysl Res, Oceans*. 116, C3, DOI: 10.1029/2009JC005855

Wadhams, P. (2000). Ice in the Ocean. Amsterdam: Gordon and Breach Science Publishers

Weeks, W. F. (2010).On sea ice.Univ. of Alaska Press (664 pp.).

Xue, C., X. Wen, Q. Dong, X. Wang (2011). Tracking the dynamic sea ice process with RADARSAT-2 Imagery.Proceedings of the Twenty-first (2011) International Offshore and Polar Engineering Conference. Maui, Hawaiim USA, June 19-24, 2011

Zakharov I., Bobby P., Power D., Warren S., (2014). Monitoring extreme ice features using multi-resolution RADARSAT-2 data. IGARSS-2014, Quebec City, Canada, July 13-18.

CHAPTER 2: OBSERVATIONS OF PRESSURED SEA ICE AND RIDGING IN THE HUDSON STRAIT FROM RADARSAT: IMPLICATIONS FOR SHIPPING

ABSTRACT

Ridges in sea ice and the convergent forces that form them are a serious hazard to ships traveling in the Arctic. There have been few studies on ridge distribution at a basin level in the Canadian Arctic. This is an important knowledge gap that needs to be filled to ensure safe and efficient shipping in the region. The Hudson Strait connects Hudson Bay and the north Atlantic and is the site of ongoing winter shipping where vessels encounter pressured ice conditions and ridging. In this study, RADARSAT-1 and -2 ScanSAR Wide images were used to manually identify ridges in a winter shipping corridor in the Hudson Strait, for the period 1997 to 2012. The values were standardized by the number of images used for each year. Ridging patterns were analyzed temporally and spatially. Ridge count peaked in the month of March. There was no significant linear trend in the number of ridges identified on either a monthly or annual scale, but there was a high amount of variability from year to year. Spatially, there were distinct patterns of ridging that occur in the eastern and western sectors of the strait, including the region between Charles Island and the coastline and at the eastern entrance to the Hudson Strait. NCEP reanalysis data was used to compare seasonal sea level pressure (SLP) anomalies and wind patterns to high and low ridge density seasons. Some consistent wind and SLP patterns were associated with low ridge density years, which were frequently associated large high pressure SLP anomalies over the eastern Canadian Arctic. This method could be used when developing future winter shipping routes and provides information for ship operators in the Hudson Strait.

HIGHLIGHTS

- Pressured sea ice and ridges are hazardous to vessels in the Arctic
- Satellite images are used to study ridge density in the Hudson Strait
- No significant temporal trends of more or less ridging over a 15 year period
- Clear spatial patterns of ridging at eastern and western ends of the strait.
- Greater understanding of how pressured ice is formed and how we can project ridging is needed to ensure safe winter shipping in the Arctic.

KEYWORDS: *Arctic shipping, pressured ice, ridges, RADARSAT, ice hazards*

2.1 INTRODUCTION

Shipping in the Canadian Arctic has increased significantly since 2007 (Pizzolato et al., 2014) and is projected to become more viable in the future (Stephenson et al., 2013; Smith and Stephenson, 2013). While some of the interest in Arctic shipping can be attributed to the decline in sea ice, tourism, community re-supply needs, the increasing activity around resource exploration and extraction are also important drivers (Brigham, 2011). The Hudson Strait is an excellent example of where all these driving factors are at play. It is an important passage between the North Atlantic Ocean and the Hudson Bay that makes up a section of the Arctic Bridge shipping route between Churchill, Manitoba and Murmansk, Russia. Cargo vessels transport goods from the privately operated Port of Churchill though the Strait to destinations in eastern Canada and foreign markets (Stewart and Lockheart, 2005). The Strait is also the site of as many as three re-supply trips during the summer months to the communities that line the coast of the strait and Hudson Bay (NEAS, 2014) and is host to a number of regular cruise ship routes. Finally, there is the Raglan nickel mine in northern Quebec that is owned and operated by Xstrata Nickel and which has been serviced year-round by an ice strengthened vessel through the Hudson Strait since 1998. It is this vessel that has experienced the hazards of pressured ice throughout the winter months. Resource exploration continues in the region, including proposed mines in mainland Nunavut, and could lead to even greater year-round ship traffic meaning a likely increase in probability that ships will encounter hazardous ice conditions such as pressured and ridged ice.

When ice converges and comes under pressure, it can raft or form ridges (Marchenko, 2008; Timco et al., 1997; Bradford, 1972).Rafting occurs when one sheet of ice slides over another, whereas ridges form once ice has become too thick to raft (Weeks and Kovacs, 1970). Sea ice under pressure and the ridges in the ice that pressure causes represent some of the most hazardous navigational conditions that ships can encounter while operating in the Arctic region.

The build-up of pressure is usually as a result of convergent forces from winds, currents or tides (Kubat et al., 2012). For example, the ice breaker *Louis S St Laurent*, which escorted the tanker *Manhattan* through the Northwest Passage in 1969, encountered pressured ice twice as frequently when wind speeds averaged 21-30 knots than 0-10 knots, and it was observed that greater wind speeds brought greater intensity of pressured ice (Bradford, 1972). These forces can be enhanced by bottleneck areas such as when ice is pushed between an island and coastline (Kubat et al., 2012). As the floes come together, blocks of ice break off and are piled up above and below the water line, forming what is called a sail and a keel respectively (Marchenko, 2008; Weeks, 2010). Ridges can occur anywhere sea ice is mobileand it is estimated that about 40-50% of the entire Arctic sea ice cover is ridged (Leppäranta, 2005; Wadhams, 2000). Ridge age is described in the same way as sea ice age. First year ridges, which are the focus of this study, are those that have not survived the summer melt season and that re-form annually; they are typically less consolidated than multiyear ridges and often have sharp sails that are still visibly made up of blocks of ice (Strub-Klein and Sudom, 2012).

Sea ice ridges are an important consideration for shipping, as well as offshore structures (Obert and Brown, 2011). Ridges can represent the greatest load experienced by a vessel or structure, though the ice has to be mobile enough for them to form (Vakulenko, Bolshev, 2015; Gorbunova and Shkhinek, 2015; Timco, 2000).Despite the hazard that pressured ice and ridges pose to vessels, it is surprising that there are only a very limited number of studies examining ice under pressure as it relates to shipping in the Canadian Arctic (see Bradford, 1972; Xue et al.,2011; Kubat et al., 2012; Kubat et al., 2013). Most of these studies have focused on individual ridge geometry and ridge dimensions for engineering purposes; few have examined the distribution of ridges within a geographic area over a period of time (Kwok, 2014). This is a knowledge gap that has been identified within the shipping community as ship captains and operators, when interviewed, have described the need for pressured ice forecasts and for increased availability of information regarding pressured ice distribution (Kubat and Sudom, 2008; Timco et al. 2005).

Currently, there are very few studies focused on the distribution and prevalence of pressured ice in the Canadian Arctic and little is known about the factors that lead to ridging making it extremely difficult to predict where and when ridging may occur until vessels make visual or physical contact with the ice. Generating better understanding of pressured ice and filling this important knowledge gap is urgent considering the predicted increases in Arctic shipping. The Hudson Strait is the site of year-round shipping with a highly mobile winter ice coverage that is prone to ridging.

The objective of this work is to examine ridging patterns in a winter shipping corridor in the Hudson Strait from 1997 to 2012. . An ice climatology of the region was created to understand regional ice patterns. Ridge density patterns were analyzed spatially across the strait and temporally through the 15 year time period. Factors affecting ridge formation, including sea level pressure (SLP), winds and air temperatures were also investigated

2.2 Study Area

The Hudson Strait serves as a passage between Hudson Bay and the Labrador Sea and is illustrated in Figure 2.1.The strait is approximately 400km long and has an average width of 150km. It ranges from 300 to 900m in depth (Saucier et al., 2004). The hydrology is heavily influenced by strong tidal currents (the tidal range in Ungava Bay can be as much as 12m), freshwater runoff, local and regional atmospheric forcing and ocean currents in the Baffin Bay, the Labrador Sea and the Arctic Ocean (Saucier et al., 2004). Currents flow through the strait in opposite directions: the Baffin Island current flows in from Baffin Bay from east to west along the northern coast of the strait while fresher waters from Hudson Bay travel west to east along the southern coast (Drinkwater, 1988). Overall, there is a net export of water through the Hudson Strait from west to east and out into the North Atlantic (Straneo and Saucier, 2008a).

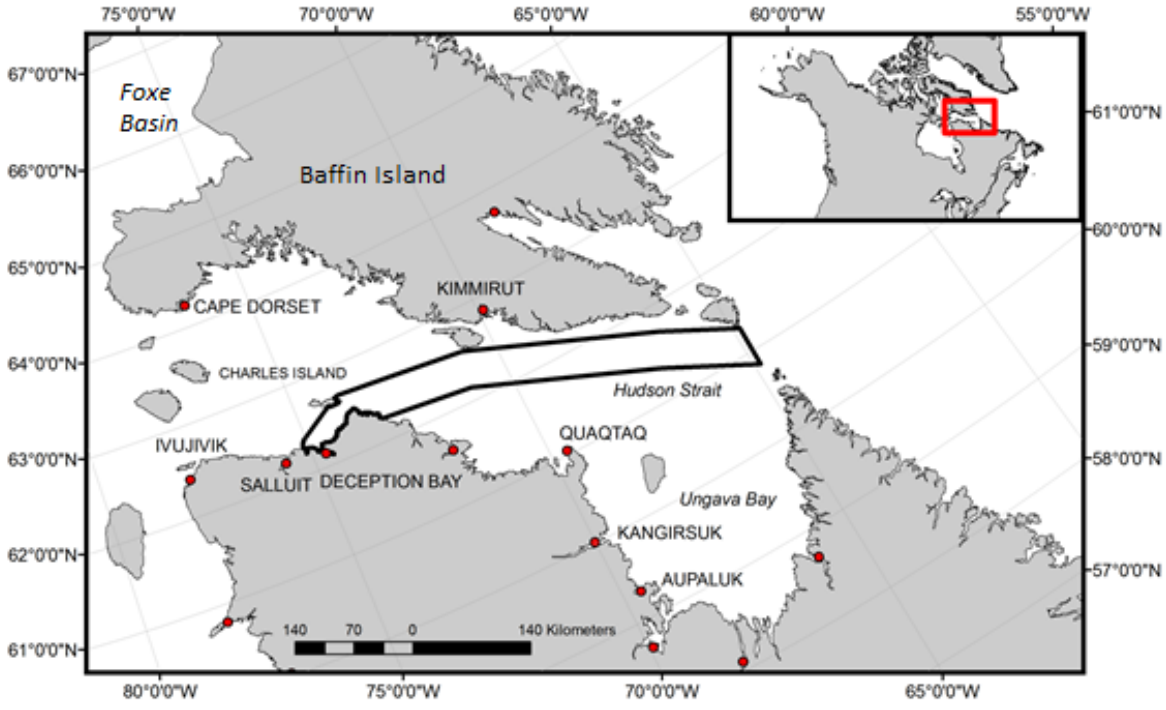

Figure 2.1: Map of the Hudson Strait and surrounding region. The winter shipping corridor examined in this study is outlined in black

During the winter months, from January to April, the strait is covered in 9-10 tenths of ice (Markham, 1986; CIS, 2011).Ice formation begins in the western portion of the strait, which is also the site of ice intrusions from Foxe Basin and the rest of the Arctic, and then spreads eastwards (Crane, 1978). Except for land-fast ice along the coasts, the ice in the Hudson Strait remains mobile all winter; leads open and close frequently and the ice can become heavily ridged by March (Saucier et al., 2004).Markham (1986) observed 6-14 ridges $km^{-1,}$ and an average of 3 ridges km^{-1}, although the spatial coverage of the study was limited. There is a recurring polynya, or area of open water, along the south coast of Baffin Island that persists throughout the winter (CIS, 2011).Ice breakup follows a reverse pattern to ice formation, beginning with the breakup of land-fast ice along the coast, then the movement of the ice out the eastern opening of the strait (Houser and Gough, 2003). The last ice to remain in the strait is in western sector of the strait, where ice continues to intrude from Foxe Basin, and in Ungava Bay, where ice accumulates throughout the winter and becomes highly ridged and rubbled (Houser and Gough, 2003; CIS, 2011).

2.2.1 Selection of Corridor and Timing

The Hudson Strait has been used for year-round ship access to the Raglan Mine in Deception Bay since 1998. During these voyages vessels follow a similar track through the strait (P. Bourbonnais, pers. comm., June 11, 2014).For this study, a shipping corridor through the Hudson Strait was selected based on previous trips by the vessel (P. Bourbonnais, pers. comm., June 11, 2014). The corridor is 40 km wide and 300 km long and can be seen outlined in Figure 2.1. For this paper, this corridor will be considered the winter shipping season shipping lane. The timeframe for this study was chosen as the December to May, inclusive. This is when there is more than 5 tenths ice coverage in the strait based on a sea ice climatology from 1981-2010, which can be seen in Figure 2.3.

2.3 Data and Methods

2.3.1. RADARSAT Imagery

RADARSAT-1 and -2 SAR imagery was used in this study to identify the spatial and temporal distribution of sea ice ridges. SAR imagery is useful for monitoring hazardous ice conditions because it is not dependent on solar illumination and therefore are not limited by the polar night. Additionally, microwaves are able to penetrate clouds, and are independent of weather conditions. SAR imagery has been widely used for the identification of pressure ridges (see Vesecky et al., 1990; Melling, 1998; Scheuchl et al., 2004; Kwok et al., 2006; Kwok, 2014). In SAR images, ridges appear as bright white, linear features that are easily discernible from level ice. In a study using remote sensing and an in situ field validation campaign, Johnston and Flett (2001) assessed the possibility of using RADARSAT ScanSAR Wide imagery for detecting deformed ice. Despite the difference in scale between sea ice ridge (typically 3.5-4m wide) and ScanSAR Wide resolution (100m), Johnston and Flett (2001) concluded that deformed ice could successfully be identified in the RADARSAT images, but that the measurement of the length and width individual ridges could be troublesome. This conclusion is in agreement with the results of Melling (1998) and Johnston (2001) who used on-ice field data to validate ridge observation in RADARSAT images. These lower resolution images are advantageous in that they provide larger spatial and temporal coverage (Johnston and Flett, 2001). There have been some attempts to automate ridge detection in SAR images. For example, Vesecky et al. (1990) used backscatter intensity thresholds and linear feature detection algorithms in order to isolate ridges in airborne SAR images with some success. However, given the relatively small geographic area of this study, and the inaccuracies associated with automated detection, manual identification of ridges was used.

RADARSAT-1 and -2ScanSAR wide images (200 m pixel^{-1})at HH (horizontal transmission, horizontal reception) polarization of the Hudson Strait for the period 1997 to 2012 were acquired from the Canadian Ice Service for the months December to May.

Both RADARSAT -1 and -2 operate in the C-band of the electromagnetic spectrum, with centre frequencies of 5.3 GHz and 5.405 GHz respectively. The annual number of images covering the study corridor is presented in Figure 2.2.For each season between 1997 and 2011, there was an average of 53 images season. The number of images ranged from a minimum of 33 images in 1998-1999 to a maximum of 58 images in 2000-2001 and 2007-2008. However, in 2011-2012 there was a sharp rise in the number of images of available that covered the study region, with 212 images available in 2011-2012 season. It is not known why there might have been such a large increase in the number of images available, except perhaps it was an increase in acquisitions in anticipation of the decommissioning of RADARSAT-1 (CIS, pers. communication, May 21, 2015).

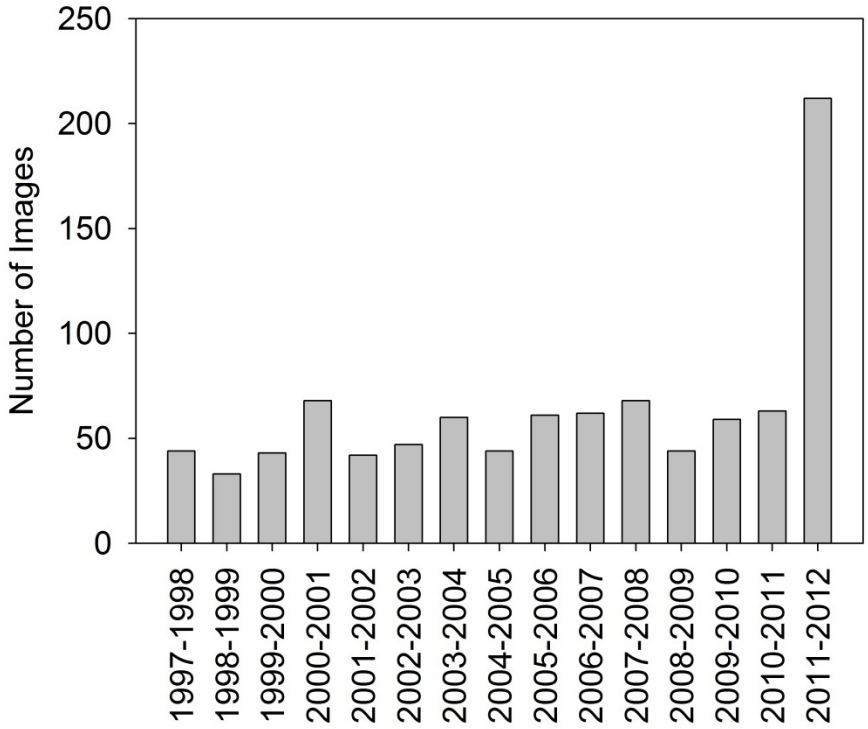

Figure 2.2: Total number of RADARSAT-1 and -2 images available covering the shipping corridor in Hudson Strait

2.3.2. CANADIAN ICE SERVICE DATA ARCHIVE (CISDA)

Sea ice concentration in the Hudson Strait was derived from the Canadian Ice Service Digital Archive (CISDA) (http://iceweb1.cis.ec.gc.ca/Archive/). The CISDA is a collection of CIS's daily operational ice charts, regional ice analysis charts, and weekly ice thickness and on-ice depth measurements. Weekly regional ice charts are available for the Hudson Bay region from 1971 until present. The operational ice charts are created by integrating information from satellite images, ship reports, operational model outputs, and ice forecaster knowledge (CIS, 2011). A complete description of the CISDA can be found in Tivy et al., (2011). The average area of ice covering the Hudson Strait each week for the period 1981-2010 was extracted and graphed to understand the typical ice formation patterns in the Strait. The dates of ice freeze-up (first date when more than 50% of the Strait was covered by ice) and breakup (first date when less than 50% of the Strait was covered by ice) were also derived for each year in order to assess trends the period of time the Hudson Strait was covered by ice in the winter.

2.3.3. RIDGE DETECTION

For each winter season, defined for this study as December 1st to May 31st, between 1997 and 2012, RADARSAT images were examined. In each image, ridges were identified visually and manually digitized. Ridges are identified in the images as linear features with high levels of backscatter. The ridges needed to be able least 3 pixels long to be identified. In areas where there were many ridges, it was more difficult to identify individual ridges but the utmost care was taken to ensure that as many individual ridges as possible were identified in these areas. As well, there the chance that the same ridges might have been counted in two different images over the same area. However, this is highly unlikely given the great mobility of the ice in the Hudson Strait; the patterns in the ice change drastically between images. The ridges were subsequently tallied on a monthly and a seasonal basis to calculate total annual ridge frequency for each winter season. There is some uncertainty associated with manual identification, as the ridge dimensions (3-4m wide) are much smaller than the resolution of the images. As well, in

areas of heavy ridging it is difficult to discern individual ridges when many have become consolidated. In these areas, some ridges may have been missed as they were too close to another ridge.

To understand the temporal distribution of ridging in Hudson Strait, the number of ridges identified in each winter season was calculated. Because the number of images available per season varied, the total ridge count was divided by the number of images available that winter in order to calculate standardized monthly and seasonal ridge count per image values. These values were analyzed to determine if the number of identified ridges per image has been decreasing or increasing between seasons. The annual average ridge counts were analyzed for trends using a linear regression analysis, both annual and monthly. The mean monthly ridge counts were also calculated.

Ridge densities were calculated in order to understand the spatial distribution of ridges in the study area corridor. A grid of 2500m by 2500m grid cells was overlaid on the study corridor. Coverage of the study corridor by the satellite images was variable as some areas were covered more frequently than others. In order to account for this, the number of times each grid cell was "viewed" by an SAR image was calculated for each winter season to be used to standardize the density values by dividing the density values by the number of viewings .For each of the winter seasons, all the ridges identified that season were intersected with the grid in order to segment the ridges by grid cell. The length of each ridge segment in each grid cell was calculated. All the segment lengths in each grid cell were added together, then divided by the grid cell area and then divided by the number of times that grid cell was viewed that season in order to get a standardized seasonal ridge density value. All of the identified ridges for each season were amalgamated to create an all seasons composite. The ridge density values (total length of ridge segments in m m^{-2}) were divided into four categories, <-0.5 standard deviations, -0.5-0.5 standard deviation, 0.5-1.5 standard deviation, and >1.5 standard deviation away from the mean values for the composite figure. The maps were examined for patterns in

the distribution of high and low ridge density areas.

2.3.4 NCEP Reanalysis Monthly Composites

Factors that might influence ridge formation in the Hudson Strait were investigated using the NCEP reanalysis data provided by NOAA/OAR/ESRL PSD, Boulder, Colorado on their website (http://www.esrl.noaa.gov/psd/data/gridded/data.ncep.reanalysis.html) (Kalnay et al., 1996). Monthly and seasonal composites were created of sea level pressure (SLP), meriodonal winds, zonal winds and vectors winds, all at the surface layer. Both the mean and climatological anomaly composites (1981-2010) were investigated. ridge density in the corridor.

2.4 Results and Discussion

2.4.1. Sea Ice Climatology and Trends of the Hudson Strait

The average weekly ice coverage in the Hudson Strait can be seen below in Figure 2.3. The spatial distribution of ice concentrations throughout the year is illustrated in 6 panels in Figure 2.4. Sea ice concentration is typically measured in tenths, which refers to the fraction of an area covered by ice. Ice formation begins in early November in Foxe Basin, the western sector of the Hudson Strait and along the coastlines, as visible in the first panel of Figure 2.4. By early December, the western half of the sector is covered by at least 5 tenths ice concentration or greater. Hudson Strait reaches full coverage of 9 tenths concentration by January 1st, when there is also a wide band of land-fast ice along the coast, especially along the islands and inlets of southern Baffin Island (Figure 2.4). The ice coverage begins to decrease in early May, as also illustrated in the 4th panel of Figure 2.4, when the land-fast ice begins to break away from the coast, as visible along the northern coast of the strait. Ice clears out of the northern half of the strait before the southern half; June 25th, there is only 1-3 tenths coverage along the southern shore of Baffin Island but there is up to 9 tenths concentration in Ungava Bay. This is the last

region to lose ice coverage as it becomes thick and rubbled due to prevailing winds and currents patterns, so the ice remains until early July (Markham, 1986).

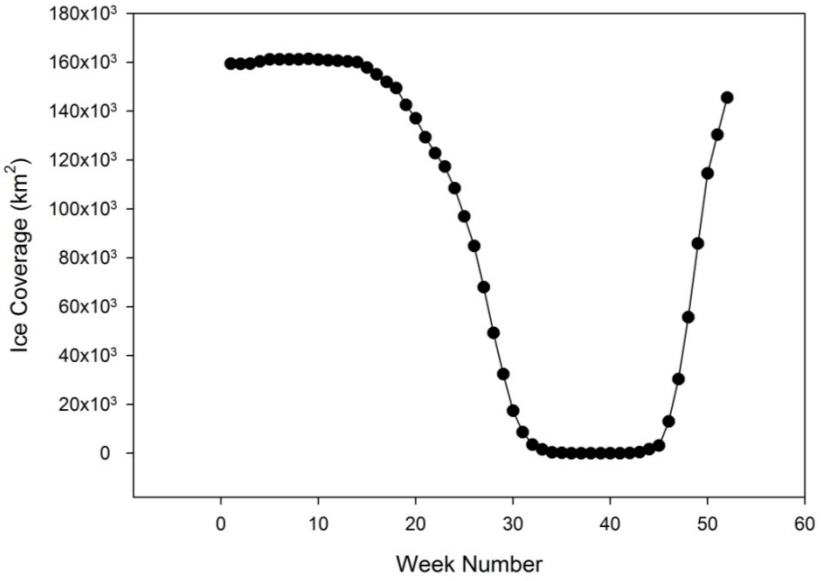

Figure 2.3: Annual Ice Coverage Cycle in the Hudson Strait, 1981-2010 (CIS, 2011)

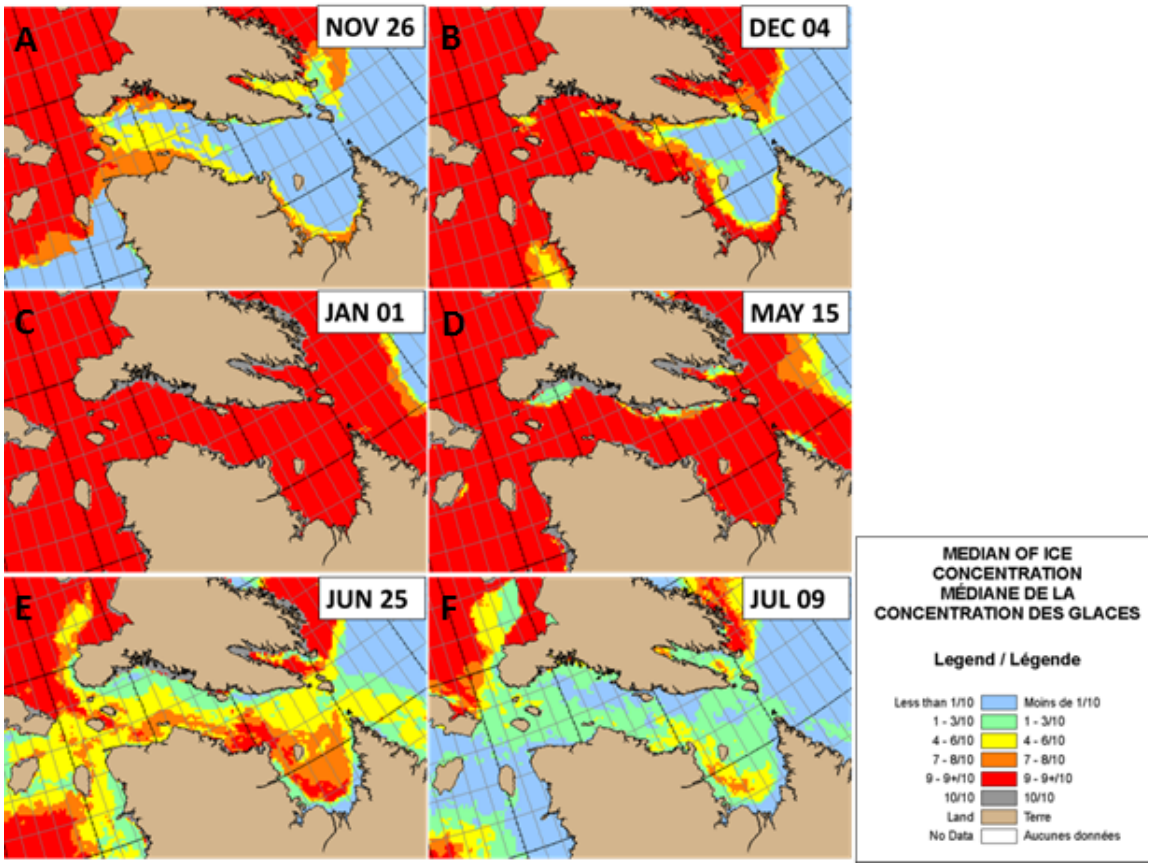

Figure 2.4: Median Ice Concentration in the Hudson Strait on November 26 (A), December 4 (B), January 1 (C), May 15 (D), June 25 (E) and July 9(F) based on a 30 year sea ice climatology 1981-2010(CIS, 2011).

There has been a declining trend in ice coverage in some of the winter months the Hudson Strait, associated with later freeze-up and earlier breakup, as seen in the 1981-2013 sea ice climatology broken down on a monthly scale(Figure 2.5)The decline is distinctly visible in the months of December and May. The decline is statistically significant at the 95% level in a linear regression analysis for all months (December p=0.001; March p=0.024; April p=0.08; May p= 0.01); except January and February, where the declining trend is significant at the 90% level (January p=0.074; February p=0.099). During these months, the ice has covered the full extent of the strait. This result is in agreement with later freeze-up and earlier breakup trends elsewhere in the Arctic as observed by Stroeve et al, (2014).

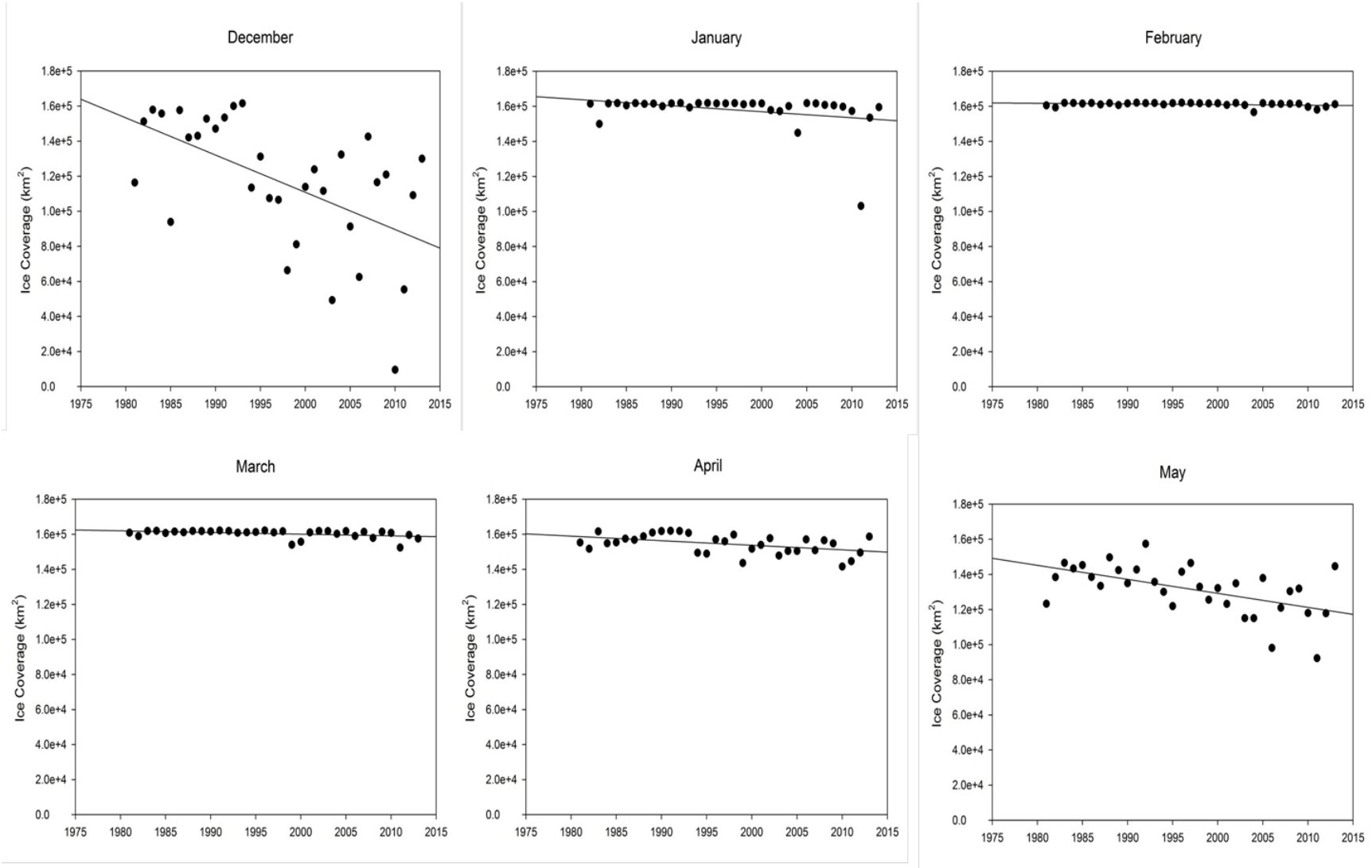

Figure 2.5: Mean December to May ice coverage in Hudson Strait from 1981-2013 (CIS, 2011).

Ice freeze-up and breakup dates during the study time period are listed in Table 2.1. All seasons have freeze-up dates that are equal to or later than the climatological mean, and all seasons, except the 2008-2009, have breakup dates that are on or before the climatological mean. This observation is in agreement with the declining trends in Figure 5.However the freeze-up and breakup dates within the study time period are relatively consistent, though 2008-2009 is notable for having a breakup date three weeks later than the study time period mean. As well, the 2010-2011 season had an extremely late freeze-up, as ice did not cover 50% of the region until the 3rd week of January.

Table 2.1: Freeze-up and Breakup dates for the Hudson Strait. Freeze-up is defined as when ice first covers 50% of the Strait; breakup is when ice first covers less than 50% of the Strait(CIS, 2011).

	Freeze-up Week Number	Breakup Week Number
1997-1998	50	26
1998-1999	51	25
1999-2000	51	25
2000-2001	49	25
2001-2002	50	26
2002-2003	50	25
2003-2004	52	26
2004-2005	49	25
2005-2006	51	22
2006-2007	52	26
2007-2008	49	26
2008-2009	50	28
2009-2010	50	24
2010-2011	55	24
2011-2012	52	25
Mean (1997-2012)	50.7	25.2
Climatology Mean (1981-2010)	49.2	26.9

2.4.2. Temporal Analysis of Ridge Counts in the Hudson Strait, 1997 to 2012

The annual standardized average ridge count for all seasons is displayed in Figure 2.6. The overall mean ridge count was 110. The 2006-2007winter season had the highest mean count at 231ridges identified per image. 2000-2001, 2001-2002, 2004-2005, 2005-2006 were also seasons with greater than average ridge. The 1998-1999 season displayed the least, with 39 ridges.2008-2009, 2009-2010, 2010-2011 are notable in that they were three winter seasons in a row with less than average ridge counts.2003-2004 was also striking for having a lower than average seasonal ridge count. The seasons were categorized as very low ridge density seasons (annual average less than 50 ridges per image), normal ridge density seasons (annual average 51 to 149 ridges per image) and high ridge density seasons (annual average more than 150 ridges per image). The extremely low ridge density seasons (1998-1999, 2003-2004, 2008-2009, 2009-2010, 2010-2011) and extremely high ridge density seasons (2000-2001, 2001-2002, 2004-2005, 2005-2006, 2006-2007) will be examined in greater detail in the discussion section. Indeed, there is a high inter-annual variability in the average number of identified ridges, but there is no trend towards more or less ridging based on annual average values of ridge counts on the scale of the entire shipping corridor. The latter is also the case at the monthly scale (Figure 2.7).

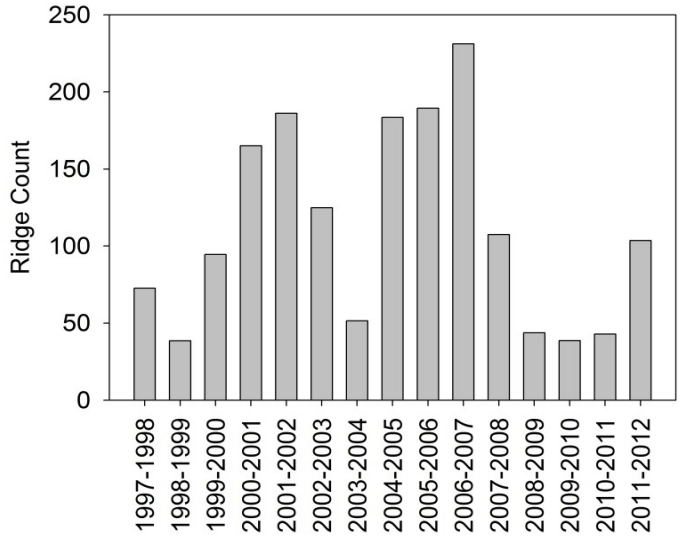

Figure 2.6: Mean Annual Standardized Ridge Count in Hudson Strait corridor, from 1997- 2012.

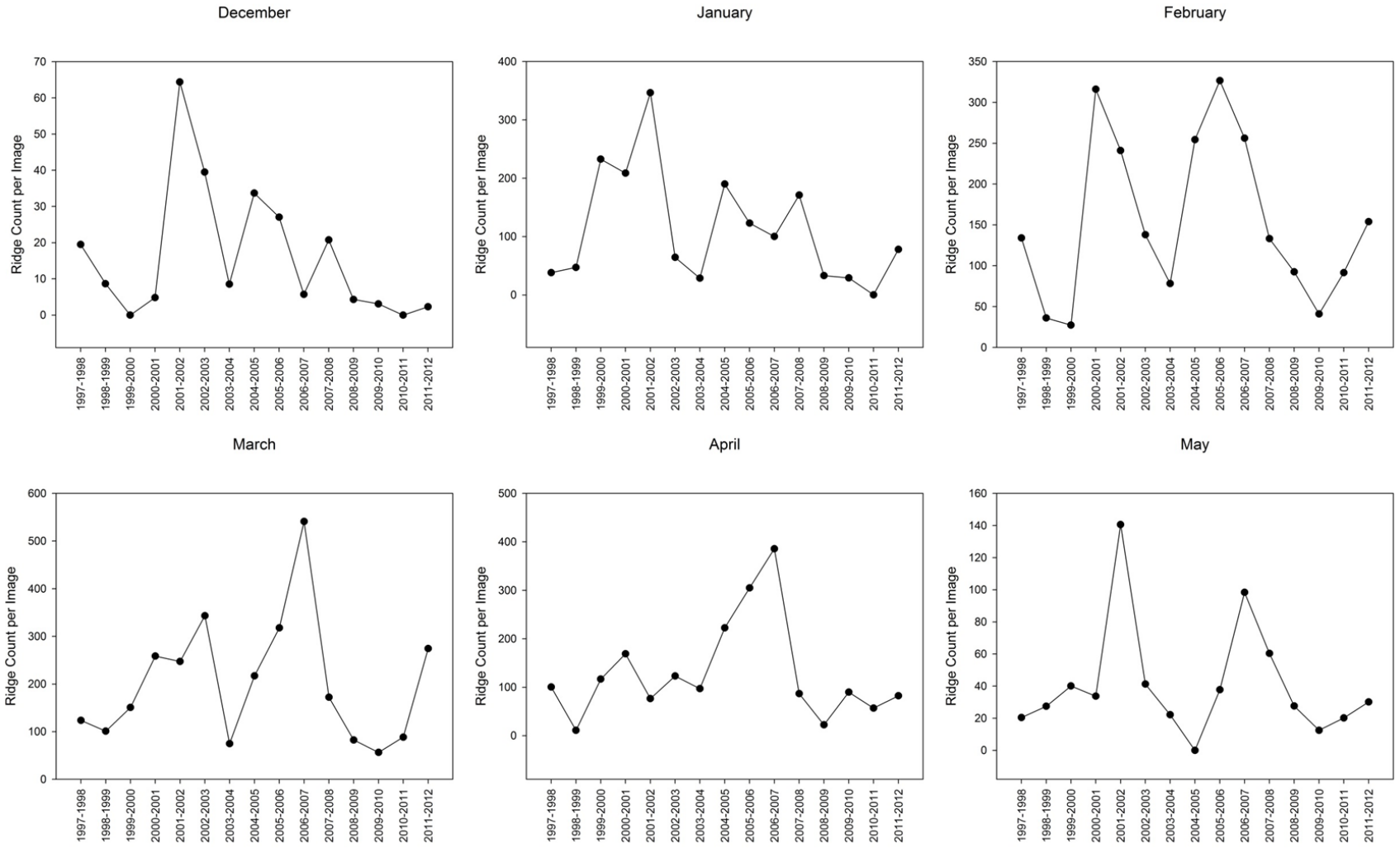

Figure 2.7: Monthly Standardized Ridge Counts for individual seasons within Hudson Strait corridor from 1997 - 2012.

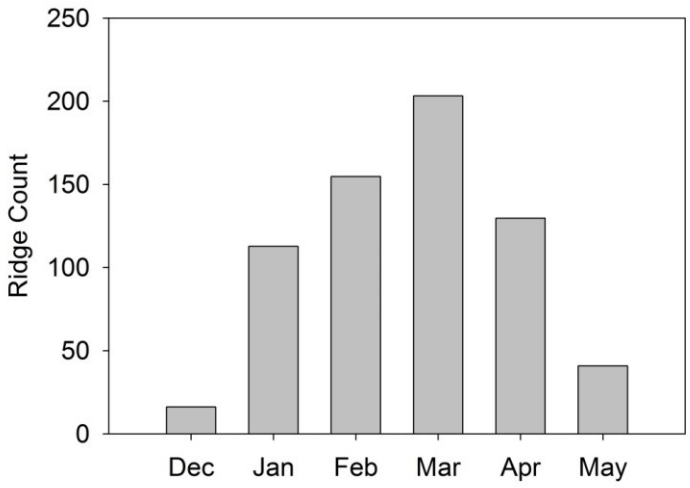

Figure 2.8:Mean Monthly Distribution of Standardized Ridge Count, within Hudson Strait corridor from 1997 - 2012.

Figure 2.8 illustrates that on a monthly basis, ridging was found to peak in March, with mean of 203 ridges that was followed by February (155), and April (130).The ridge count monthly distribution is shown for each individual season in Figure 9. Most of the seasons follow the average distribution, with ridge counts peaking in March. During 2003-2004 and 2008-2009, two extremely low ridge count seasons, there were almost identical ridge counts in February and March. The low ridging seasons of 2003-2004 and 2009-2010 are also notable in that ridge counts peaked later than average, in the month of April.2001-2002 and 2005-2006 are both heavily ridged seasons where the ridging peaks earlier, in January, and 2000-2001 is a heavily ridged season that where ridge counts peaked in February. 2006-2007 is a heavily ridged season where that peak occurs in March.

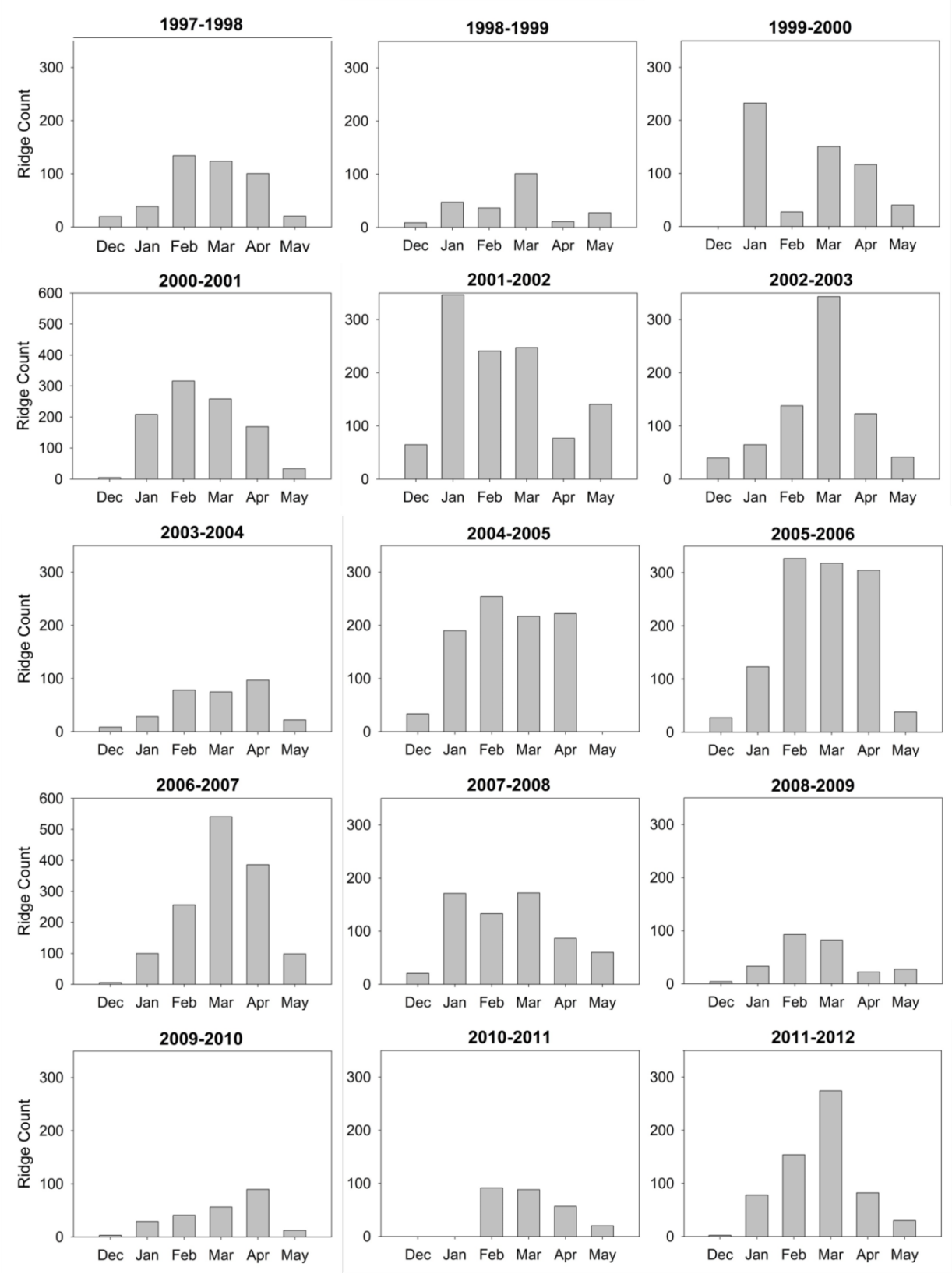

Figure 2.9: Annual distribution of ridges for individual winters, 1997-2012. Note, all graphs have the same y-axis, except 2000-2001 and 2006-2007

Figure 2.10 shows the development of the ice coverage in the Hudson Strait in both the low ridge density and the high ridge density seasons. It is notable that in the high ridge density seasons, the onset of ice formation is relatively consistent, where as in the low ridge density seasons, there is a gap of almost 8 weeks between when the 2008-2009 season reached full ice coverage and when the 2010-2011 season reached full coverage. In 2010-2011, the ice in the strait did not reach full coverage until Week 4. For this reason, it is not surprising that there were no ridges counted in December and January. However, this cannot be the sole explanation for less ridging, as in 2009-2010, the previous season, there was also less than average ridging but freeze-up occurred during week 49, which is typical. However, in 2009-2010, the ice coverage did not reach its full extent as quickly as other seasons; it reached 16,000km^2 in week 4 and broke up earlier than usual. 2008-2009, the first in a series of low ridge count seasons had more typical ice cycle, freezing up in week 49 and breaking up later than other seasons. The high ridge density seasons appear to have more consistent breakups in terms of timing as well as ice loss. In many of the low ridge density seasons the loss of ice in the spring time happens in steps, with dramatic losses and then slight recoveries.

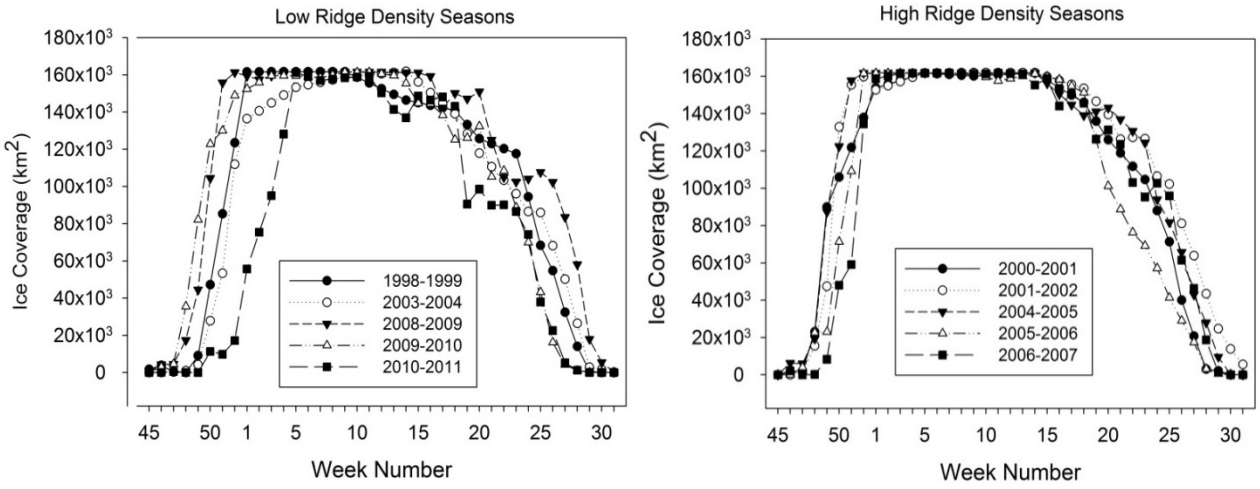

Figure 2.10: Ice coverage development in the Hudson Strait for low ridge density and high ridge density seasons

2.4.3. Spatial Distribution of Ridge Density in the Hudson Strait, 1997-2012

The spatial distribution of all the ridge densities from all seasons (1997-2012) is illustrated in Figure 2.11. Clusters of higher ridge densities are grouped in the western and eastern zones of the study area corridor. This includes along the coast east of Deception Bay, between the Quebec mainland and Charles Island, and at the east end of the shipping corridor, near the mouth of the Hudson Strait. Ridging along the coast is to be expected as this is where the mobile ice meets with the land-fast ice and shear zones are formed. These are areas of heavy ridging and pose navigational difficulties for vessels attempting to cross them (P. Bourbonnais, pers. communication). Ridging is also to be expected between Charles Island and the mainland, as ice typically travels from west to east in the Hudson Strait along with net volume of water (Straneo and Saucier, 2008b) and so the ice there is being forced into a bottleneck (Saucier et al., 2004). Ridging in the east end of the Hudson Strait is likely as a result of the ice from Ungava Bay moving north to meet the ice moving through the strait from west to east, where it converges and forms ridges and pressured ice(Saucier et al., 2004). The lack of ridging in the middle of the corridor, along the southern coast of Baffin Island is also to be expected as there an identified polynya in that area that is typically open wall winter (CIS, 2011).

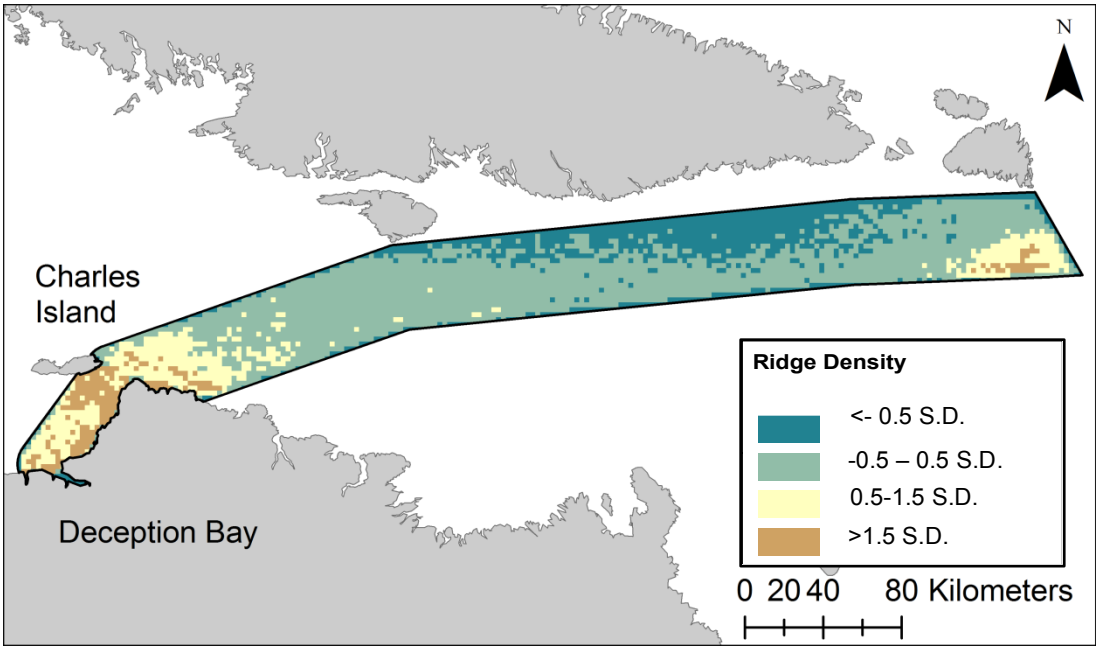

Figure 2.11: Mean ridge density spatial distribution along the corridor in the Hudson Strait, 1997 to 2012

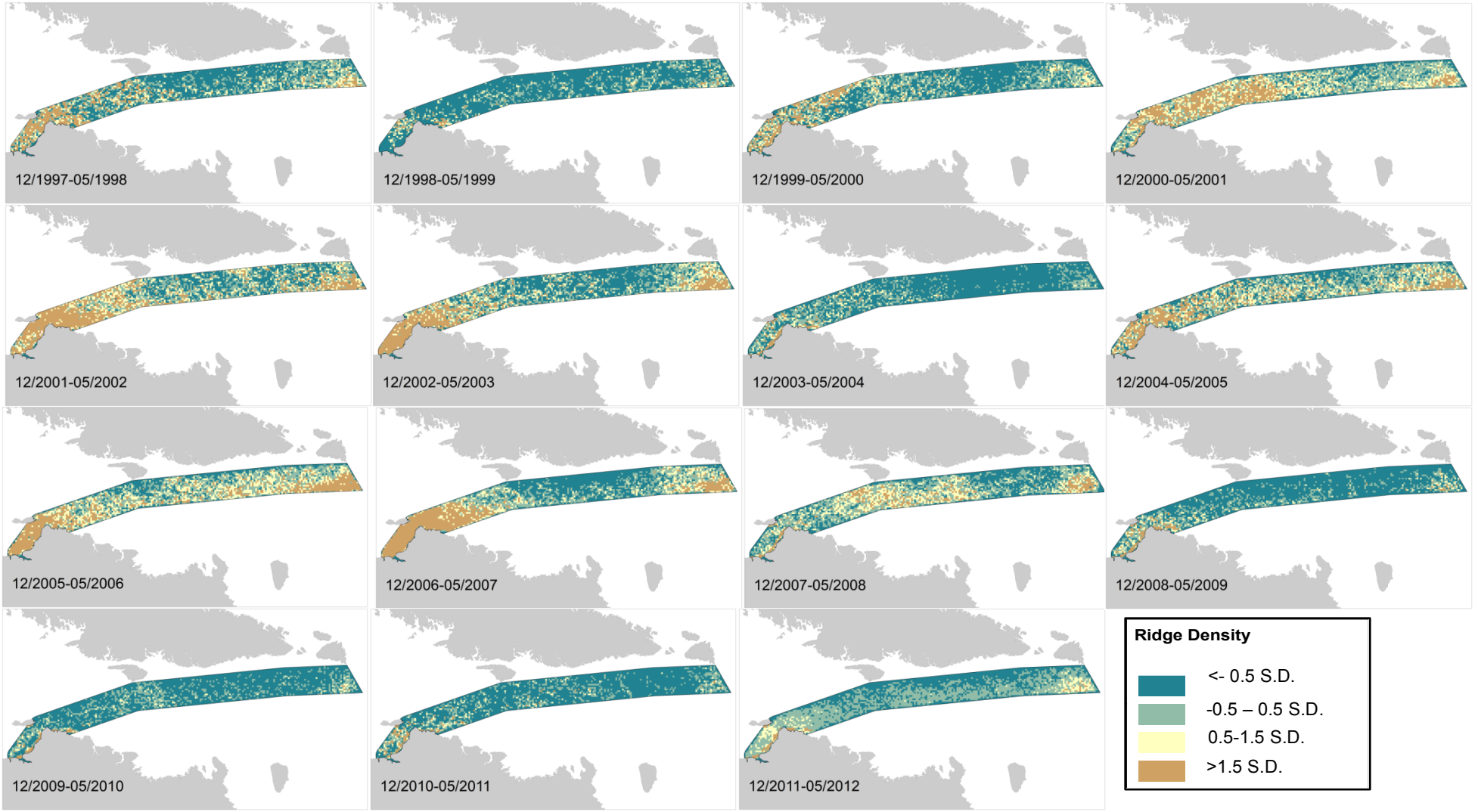

Figure 2.12:Mean annual ridge density distribution each season along the corridor in the Hudson Strait, 1997-2012

Figure 2.12 shows the spatial distribution of ridge density for each individual season from 1997-2012. During most seasons, ridging is concentrated in the eastern and western zones of the study corridor, as was seen in the all seasons composite in Figure 2.6. This pattern is seen in 2002-2003, 2005-2006, and 2006-2007. 2006-2007, identified as the season with the highest annual ridge count, had extensive amounts of ridging in the western zone of corridor. The seasons of 1998-1999 and 2003-2004 both had less ridging than other seasons, with little ridging in either the eastern or the western parts of the strait.2008-2009, 2009-2010, 2010-2011 were similarly seasons with less than average ridge densities. Unlike the others, 1998-1999, which was also a season with anomalously low ridging, had almost no ridging along the coast near Deception Bay, while the other low ridging seasons continued to show that ridge distribution pattern. 2000-2001, 2001-2002 and 2007-2008 were anomalous in that the majority of the areas with higher ridge density occurred in the central-western zone of the corridor, not in the western or eastern zones of the corridor as the other seasons.

2.4.4 Atmospheric Circulation and Ridging in the Hudson Strait

Winds are an important driving factor in the creation of pressured ice and ridges, and geostrophic winds have been found to explain most sea ice motion on short time scales (Kubat et al., 2012; Thorndike and Colony, 1982). Typically, winds move from areas of high pressure the areas of low pressures whereby the ice moves in parallel to the sea level pressure isobars (Thorndike and Colony, 1982).

A summary of the seasonal patterns in atmospheric circulation, as well as freeze-up and breakup characteristics, for each of the 15 seasons is illustrated in Table 2.2. Typically, the Hudson Strait is influenced by the large low pressure area over the North Atlantic, a strong high pressure area over Greenland and a large area of high pressure over the Canadian Arctic (Drinkwater, 1986). The area of low pressure over the North Atlantic is what drives the prevalent northwesterly winds over the Strait, which bring with them

cold, Arctic air (Drinkwater, 1986). However, anomalies in pressure patterns demonstrate the differences between seasons. Seasons with low ridge densities are characterized by wide high pressure anomalies over Hudson Strait, the Atlantic or mainland Nunavut. In Figure 12, 1998-1999, 2003-2004, 2009-2010 and 2010-2011 are all seasons where most of the ridging that does exist is focused along the land-fast ice on the northern coast of Quebec. In these years, except for 2009-2010, the wind anomalies were from the winds were from the W, SW through the Hudson Strait, facilitating the flow of ice through the Strait without hindrance except along the coast. The coastal ridging is expected as ice is constantly moving through the strait and coming into contact with static ice along the coastline. The SLP patterns in those 4 years would encourage that ice motion, as the winds push the ice from west to east through the Strait (Figure 2.13; Table 2.2). The only season that does not exhibit this pattern is 2008-2009 (Table 2.2), when a very large low pressure anomaly was present over SW Greenland and while a high pressure anomaly was found over mainland Nunavut (Figure 2.13). The large area of high pressure over the Strait likely facilitated the movement of sea ice through the Strait and prevented it from converging and becoming compacted. There is more ridging that is between Charles Island and the Quebec mainland, as well as at the eastern entrance to the Strait during 2008-2009 (Figure 2.12).

The SLP patterns for high ridge density seasons are more complicated. For example, in 2000-2001 and 2004-2005, there are large seasonal high pressure anomalies centred over the North Atlantic that extend over the Hudson Strait, similar to what was seen in lower ridge density seasons (Figure 2.13). . In 2004-2005 in particular, the anomalous winds were from the W, SW over the Hudson Strait but were from the SE over the Atlantic. This could have prevented some ice from leaving the strait, as it met with the SE winds in the Labrador Sea, causing the ridging in the eastern half of the corridor, seen in Figure 12.On the other hand, in 2000-2001 there were east wind anomalies directly over the strait, which would have created convergent forces as it met with the eastern flowing currents leading to ridging in the middle of the strait, as seen that year However, in 2001-2002 and 2006-2007, there were large seasonal low pressure anomalies centered over the

Labrador Sea, with small high pressure anomalies over the Canadian Arctic (Figure 2.13; Table 2.2). Winds flowed from the low pressure in the east to the regions of high pressure in the west, and this westward force on the ice would meet the eastward force on the ice caused by the currents flowing from the west, creating convergence and ridging. In 2006-2007, the low pressure anomaly over the North Atlantic was very strong (Figure 2.13) which would cause the stronger east winds visible in the eastern section of the corridor and could explain the very heavy ridging seen that year in Figure 2.12 as the ice acted upon by these winds met the ice being pushed by the west winds in the western half of the corridor. That season there were also anomalously high wind speeds through the strait, which could have increased the forces acting on the ice and very heavy ridging between Charles Island and the coast of Quebec. This particular distribution could be a result of the strong westerly winds that forced the ice into the bottleneck caused by the island. 2005-2006 was unique in that there was a large high pressure anomaly over Greenland and the Canadian Arctic and low pressure anomaly over Quebec. The seasonal SLP anomalies for three notable high density ridge seasons (2006-2007, 2005-2006, and 2000-2001) and three notable low ridge density seasons (2008-2009, 2003-2004, 1998-1999) are presented in Figure 2.12.

Table 2.2: Seasonal atmospheric circulation patterns and ice coverage over the Hudson Strait, 1997-2012. Seasons marked in bold were high ridge density seasons (annual average more than 150 ridges per image). Seasons marked in italics were low ridge density seasons (annual average less than 50 ridges per image).

Season	Ridge Density and Distribution	Seasonal Sea Level Pressure Anomaly	Ice Coverage	Zonal winds (E/W)	Meridonal winds (N/S)	Zonal winds
1997-1998	Average density, concentrated in East and West of corridor.	Strong positive anomaly over Northern Quebec, extends all over the HS.	Average freeze-up; breakup one week later than average	Positive anomaly over Davis Strait, negative anomaly over Northern Quebec	Strong positive anomaly over Davis Strait and HS.	Winds W, SW through HS
1998-	*Low ridge density*	*High pressure anomaly over*	*Freeze-up one*	*Small negative anomaly over*	*Positive anomaly over Hudson Bay,*	*Winds SW*

1999		*Baffin Island, extends over HS, Hudson Bay and North Atlantic*	*week late; breakup average*	*Northern Quebec*	*negative anomaly over Davis Strait*	*through HS*
1999-2000	Low to medium ridge density; concentrated in western half of corridor.	Strong negative anomaly over NU, extends through HS. Strong positive anomaly over northeastern Atlantic	Average freeze-up; average breakup	No anomalies over HS. Strong positive anomaly over north Atlantic.	Positive anomaly over Atlantic, smaller positive anomaly over the HS	Winds W,SW through the Strait
2000-2001	**High ridge density; concentrated in middle of corridor**	**Strong high pressure anomaly over SE Greenland.**	**Freeze-up two weeks early; average breakup**	**Negative anomaly over eastern Atlantic, extends over HS.**	**Small positive anomaly over HS**	**Winds from E, SW through the strait.**
2001-2002	**High ridge density; concentrated in west and east of corridor.**	**Large low pressure anomaly over North Atlantic, med-high anomaly centred over Ontario**	**Average freeze-up; breakup one week late**	**Small negative anomaly over Quebec, small positive anomaly over entrance to HS**	**Strong negative anomaly over eastern entrance to HS**	**Winds from the E, SE and E over HS**
2002-2003	High ridge density; concentrated in east and west of corridor	Very strong negative anomaly centred over Iceland, extends over Hudson Bay system	Average freeze-up; average breakup	Positive anomaly (W) over the eastern half of HS	Negative anomalies over NU and eastern entrance of HS.	Winds SW through HS
2003-2004	*Low ridge density*	*Low pressure anomaly over Labrador Strait, Large high pressure anomaly over mainland NU.*	*Freeze-up 2 weeks late; breakup one week late*	*Positive anomaly over the entrance to HS.*	*Strong negative anomaly over entrance to HS*	*Winds from W, SW over HS, strong E winds just east of the entrance to HS*
2004-2005	**High ridge density; concentrated in east and west of corridor,**	Large high pressure anomaly over SE Greenland, extends over HS	Freeze-up two weeks early; average breakup	No anomalies over HS	Positive anomaly over Davis Strait	Winds from W, SW over HS

	some ridging in centre					
2005-2006	**High ridge density, concentrated in east and west of corridor**	**High pressure anomaly over SE Greenland, extends through Canadian Arctic, low pressure over Ontario**	**Average freeze-up; breakup 3 weeks early**	**Negative anomaly over Davis Strait, second anomaly over Quebec**	**Very large negative anomaly over Hudson Bay, positive anomaly over Labrador Sea**	**Winds from W, SW over HS**
2006-2007	**Very high ridge density, concentrated in west, and some in east of corridor**	**Strong gradient between very large low pressure anomaly over Labrador Sea and high pressure over mainland Nunavut**	**Freeze-up 2 weeks late; breakup one week late**	**Small positive anomaly over strait**	**Very strong negative anomaly over HS**	**Wind from the NW over HS, positive anomalies (strong winds)**
2007-2008	Average ridge density, concentrated in centre of corridor	Very strong negative anomaly centred over Hudson Bay, positive anomaly over Labrador Sea	Freeze-up one week early; breakup one week late	No anomalies over the Strait	Strong positive anomaly over the Strait, negative anomalies both over NU and Davis Strait	Winds from SE , SW over the Strait
2008-2009	*Low ridge density*	*Strong low pressure anomaly over North Atlantic and over Hudson Bay, high pressure over mainland NU*	*Average freeze-up; breakup 3 weeks late*	*Positive anomaly over North Atlantic, extends over Strait*	*Negative anomalies centred over NU, and over DavisStrait*	*Winds from W. SW through the HS*
2009-2010	*Low ridge density*	*Large positive anomaly centred over Greenland, extends over Canadian Arctic. Low pressure anomaly centred over Atlantic*	*Average freeze-up; breakup one week early*	*Very strong negative anomaly over the North Atlantic*	*Strong negative anomaly over Quebec*	*Winds from E, NE over Strait*
2010-2011	*Very low ridge density*	*High pressure anomaly centred over Davis Strait, low pressure anomaly over Canadian Arctic*	*Freeze-up 5 weeks late;breakup one week early*	*Positive anomaly over HS, negative anomaly centred over Labrador Sea*	*Positive anomaly over Davis Strait, negative anomalies over Hudson Bay and North Atlantic*	*Winds from W, SW over the HS*

2011-2012	Average ridge density, concentrated in west and east of corridor	Strong negative anomaly over Baffin Island and NU,, extends over HS, positive anomaly over North Atlantic	Freeze-up two weeks late; average breakup	Positive anomaly over North Atlantic, extends over HS	Positive anomaly over SE Greenland	Winds from SW

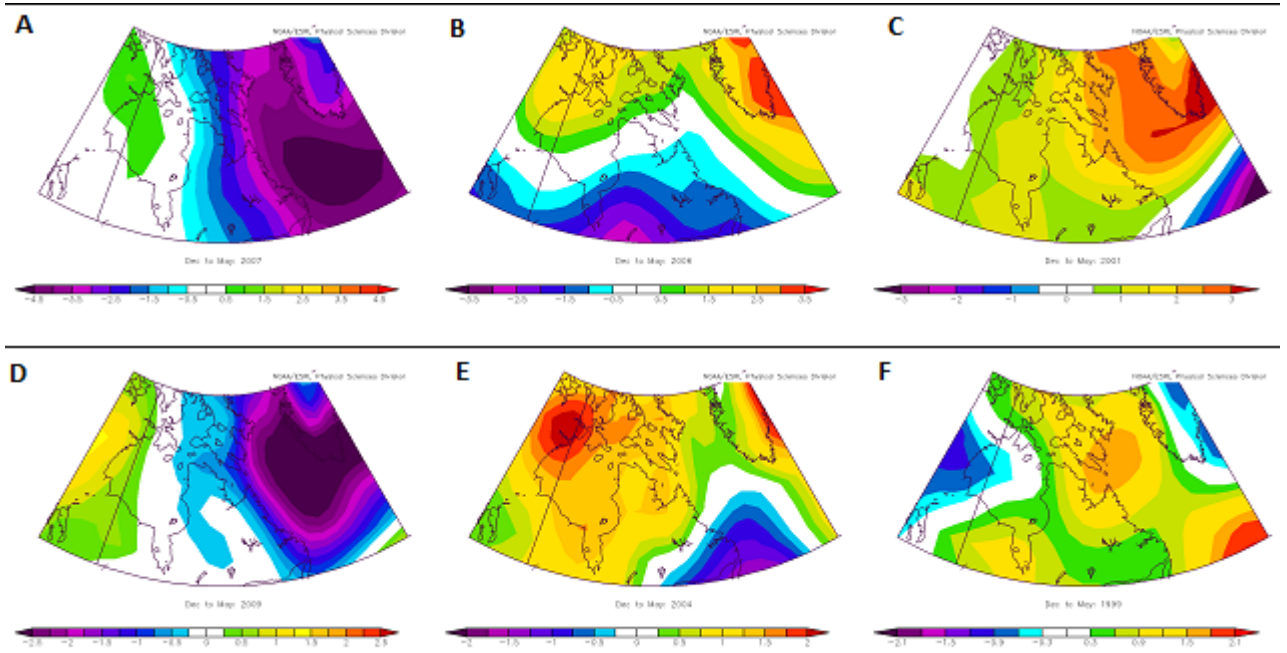

Figure 2.13: Seasonal SLP anomalies for high ridge density seasons 2006-2007 (A), 2005-2006 (B), and 2000-2001 (C) and seasonal SLP anomalies for low ridge density seasons (2008-2009 (D), 2003-2004 (E), 1998-1999(F))

2.4.5 Implications for Winter Shipping in the Hudson Strait

Currently, the Hudson Strait is being used year-round by an ice strengthened vessel for servicing a mine in northern Quebec. The strait may be the site of increasing winter shipping as proposed resource development projects move forward. Besetments caused by pressured sea ice and heavy ridging can be very costly to the vessels traveling through the strait, both economically and environmentally.

This study has demonstrated that there are relatively consistent patterns in ridge density distribution spatially in the strait, as well as there being peak ridge periods throughout the winter. The ridging peak in March indicates that ship captains should prepare for the increased likelihood of besetment and slower voyage times during the month of March in the shipping corridor. As well, there were distinct spatial patterns in the distribution of high ridge density areas found in this study. There is the prevalence of ridges along the land-fast ice near Deception Bay, where the contact between the land-fast ice and the mobile ice of the strait forms a shear zone. This area is almost always heavily ridged in each of the studied seasons. This area would need to be approached with caution by ship captains. A high density of ridging that occurs between Charles Island and the mainland of Quebec also consistently appears in many of the years studied. It is an example of a bottleneck area, where the ice is being pushed between the island and the mainland on its way eastwards through the strait. Areas of high density ridging would be expected elsewhere in the Strait where prevailing winds and currents are pushing ice through a narrower gap. Coastal geography can be used to predict potential areas of high sea ice pressure and ridge density. Finally, the high ridge density at the entrance of the strait in some seasons is also notable for vessels entering the strait. This isn't present every season, and it will take further research to understand why some seasons more ridges appear than others. Freeze-up and breakup dates in the Strait were relatively consistent throughout the study time period, with a few outliers (the extremely late ice breakup in 2008-2009, and the extremely late freeze-up in 2010-2011). This is also important

information for ship operators, who can expect significant ice within the strait by week and that ice coverage to continue until at least week 25.

2.5. CONCLUSIONS

Pressured sea ice and ridges are extremely hazardous for ship operators and as a result, better understanding of the temporal and spatial extent of ridging is needed in order to improve the safety of winter shipping. Ships traveling through the Hudson Strait during the winter months often encountered ridged ice and pressure. The observational method used in this study provides an understanding of the temporal and spatial frequency and distribution of ridging using RADARSAT images.

Based on the standardized ridge count, there is no significant change over time from the 1997-1998 and 2011-2012 winter seasons in the amount of ridges that were identified. The standardized ridge counts varied greatly from season to season. However, there were notable patterns in the distribution of high ridge density areas, with ridging peaking in the eastern and western zones of the shipping corridor. These distributions can be explained by the presence of shear zones between the mobile ice and the land-fast ice, where ridging and pressure can occur, as well as bottlenecking, where the ice is forced to converge while being pushed between two land masses. Differences exist in the development of ice coverage between high ridge density and low ridge density seasons, where low ridge density seasons show later and more variable freeze-up and breakup dates. Additionally, there were some connections between ridge density and seasonal SLP anomalies, such as high pressure anomalies over the North Atlantic, which could explain the differences in ridge densities and counts.

Understanding patterns in basin-level ridge distribution is highly important for improving winter shipping navigation. This information can be used by ship operators to predict

where an when ridges and hazardous ice conditions may be encountered in the Hudson Strait. This method could be used elsewhere in the Canadian Arctic to understand ridging patterns in preparation for the development of new winter shipping routes. This work could be built upon by attempting to automate the ridge identification process, which would greatly increase the speed at which the analysis could be performed. As well, understanding the conditions that cause ridging is also key, and so correlations between ridging patterns and sea level pressure, air temperature and currents should be undertaken. This could aide in predicting where and when ridging might occur in the future, as well as understanding where ships have become beset in the past.

REFERENCES

Bradford, D. (1972). Sea ice pressures observed on the second "Manhattan" voyage.*Arctic.*25(1) 34-39

Brigham L (2011) Marine protection in the Arctic cannot wait. Nature 478(7368):157,

10.1038/478157a.

Canadian Ice Service (CIS) (2011). Sea Ice Climatic Atlas: Northern Canadian Waters

Canadian Ice Service (2011), Sea Ice Climatic Atlas: Northern CanadianWaters 1981–2010, 995 pp., Ottawa.

Crane, R. G. (1978). Seasonal variations of sea ice extent in the Davis Strait–Labrador Sea area and relationship with synoptic-scale atmospheric circulation. *Arctic,* Vol. 31, 1978, pp. 434-447CIS, 2011

Drinkwater (1986). Physical Oceanography of Hudson Strait and Ungava Bay. In I. P.Martini (Ed.), Canadian Inland Seas (pages of chapter). New York: Elsevier Science Ltd.

Gorbunova, K., Shkhinek, K. (2015). Engineering properties of sea ice ridges in the Barents Sea in 2012-2014 years for Evaluation of ice loads on offshore structures. *Applied Mechanics and Materials.*(725-726) 263-269

Houser, C., W.A. Gough (2003). Variations in sea ice in the Hudson Strait. *Polar Geography*. 27(1) 1-14

Johnston, M. (2001). Validation of RADARSAT imagery using in situ measurements from first year ridged ice. Proceedings of the 16th International Conference on Port and Ocean Engineering under Arctic Conditions POAC'01 August 12-17 2001, Ottawa, Ontario, Canada.

Johnston, M. and D. Flett. (2001). First year ridges in RADARSAT ScanSARimagery:influence of incidence angle and feature orientation. Proc. of 4th Int. Symp.On Remote Sensing, Int. Glac.Soc., 4 – 8 June 2001, College Park, U.S.A.,

Kalnay, E. et al, (1996): The NCEP/NCAR Reanalysis 40-year Project. *Bull. Amer. Meteor. Soc*., 77, 437-471.

Kubat, I. and Sudom, D. (2008). "Ship Safety and Performance in Pressured Ice Zones: Captains' Responses to Questionnaire" Technical Report CHC-TR-059/ TP14847

Kubat, I., M. Hossein Babaei, M. Sayed (2012). Quantifying Ice Pressure Conditions and Predicting the Risk of Ship Besetting. Paper No. ICETECH12-130-R0

Kubat, I., M. Sayed, M. H. Babaei (2013).Analysis of Besetting Incidents in Frobisher Bay During 2012 Shipping Season.Proceedings of the 22nd International Conference on Port and Ocean Engineering under Arctic Conditions.June 9-13, 2013, Espoo, Finland.

Kwok, R. (2014). Declassified high-resolution visible imagery for Arctic sea ice investigations: An overview.*Remote Sensing of Environment*. 142:44-56

Kwok, R., G. F. Cunningham, H. J. Zwally, and D. Yi (2006): ICESat over Arctic sea ice: Interpretation of altimetric and reflectivity profiles, J. Geophys. Res., 111, C06006, doi:10.1029/2005JC003175

Leppäranta, M. (2005).The drift of sea ice. New York: Springer-Verlag (266 pp.).

Marchenko, A.V (2008). Thermodynamic consolidation and melting of sea ice ridges. *Cold Regions Science and Technology*. (52) 278-301

Markham, W.E. (1986). The ice cover. In: Martini, I.P., ed. *Canadian inland seas*. Amsterdam: Elsevier. 101 – 116.

Melling, H. (1998). Detection features in first-year pack by synthetic aperture radar (SAR). *Int. J. Remote Sensing.*19(6) 1223-1249

NEAS (Nunavut Eastern Arctic Shipping) (2014).Shipping Schedule.*Nunavut EasternArctic Shipping Inc.* Retrieved from: http://www.neas.ca/schedule.cfm

Obert, K.M., Brown, T.G. (2011). Ice ridge keel characteristics and distribution in the Northumberland Strait.*Cold Regions Science and Technology*. 66(2011) 53-64

Pizzolato, L., Howell, S.E.L., Derksen, C., Dawson, J., Copland, L. (2014). Changing sea ice conditions and marine transportation activity in the Canadian Arctic between 1990 and 2013.*Clim Change.* 123(2) 161-173

Saucier, F.J., Senneville, S., Prinsenberg, S., Roy, F., Smith, G., Gachon, P., Caya, D., Laprise,R., (2004). Modelling the sea ice-ocean seasonal cycle in Hudson Bay, Foxe Basin and Hudson Strait.*Climate Dyn*. 23, 303–326.

Scheuchl, B, Flett, D, Caves, R and, Cumming, I (2004).“Potential of RADARSAT-2 data for operational sea ice monitoring,” *Can. J. Remote Sensing.*30(3) 448–461.

Smith, L. C. and Stephenson, S. R. (2013). New Trans-Arctic shipping routes navigable

by mid-century, *Proc. Nat. Acad. Sci.,* 110, E1191–E1195, doi:10.1073/pnas.12142121

Stephenson, S. R., Smith, L. C., Brigham, L. W., and Agnew, J. A. (2013). Projected 21st-century changes to Arctic marine access*, Clim. Change*, 118, 885–899, doi:10.1007/s10584-012-0685-0, 2013.

Stewart, D.B., and Lockhart, W.L. 2005. An overview of the Hudson Bay marine ecosystem. Can. Tech. Rep. Fish. Aquat. Sci. 2586: vi + 487 p.

Straneo, F., Saucier, F.J., (2008a).The Arctic-subarctic exchange through Hudson Strait. In: Dickson, R., Meincke, J., Rhines, P. (Eds.), Arctic–Subarctic ocean fluxes. Springer Science, pp. 249–261. Ch. 10.

Straneo, F, Saucier, F. (2008b).The outflow from Hudson Strait and its contribution to the Labrador Current.*Deep Sea Research 1*. 55(8) 926-946

Stroeve, J. C., T. Markus, L. Boisvert, J. Miller, and A. Barrett (2014), Changes in Arctic melt season and implications for sea ice loss, Geophys. Res. Lett. , 41 1216 –1225, doi:10.1002/2013GL058951

Strub-Klein, L., Sudom, D. (2012).A comprehensive analysis of the morphology of first-year sea ice ridges.*Cold Regions Science and Technology*.82: 94-109

Thorndike, A.S., Colony, R. (1982). Sea ice motion in response to geostrophic winds *J. Geophys Res.* 87(C8) 5845-5852., doi: 10.1029/JC087iC08p05845

Timco, G.W., Burden, R.P. (1997) An analysis of the shapes of sea ice ridges. *Cold Regions*. 25(1) 65-77

Timco, G.W., Croasdale, K., Wright, B. (2000) An overview of first year sea ice ridges Technical report HYD-TR-047, 157 p.

Timco, G.W., Gorman, R., Falkingham, J. and O'Connell, B. (2005) Scoping Study: Ice Information Requirements for Marine Transportation of Natural Gas from the High Arctic, Technical Report CHC-TR-029, February 2005

Tivy, A., S.E. Howell, B. Alt, S. McCourt, R. Chagnon, G. Crocker, T. Carrieres, J.J. Yackel (2011). Trends and variability in summer sea ice cover in the Canadian Arctic based on the Canadian Ice Service Digitial Archive, 1960-2008 and 1968-2008. *J Geophysl Res, Oceans.* 116, C3, DOI: 10.1029/2009JC005855

Vakulenko, A.M., Bolshev, A.S. (2014). Loads from ice ridge keels—analytical vs. numerical.*Applied Mechanics and Materials* (725-726) 229-234

Vesecky, J.F., M.P. Smith, R. Samadani (1990). Extraction of lead and ridge characteristics from SAR images of sea ice. IEEE Transactions on Geoscience and remote sensing. 28(4) 740-744

Wadhams, P. (2000). Ice in the ocean. London: Gordon and Breach Science Publ. s(351 pp.).

Weeks, W. F. (2010).On sea ice. Univ. of Alaska Press (664 pp.).

Weeks, W. F., and A. Kovacs (1970), On pressure ridges, CREEL Rep. IR505, Cold Reg. Res. and Eng. Lab., 59 pp., Hanover, N. H.

Xue, C., X. Wen, Q. Dong, X. Wang (2011). Tracking the dynamic sea ice process with RADARSAT-2 Imagery.Proceedings of the Twenty-first (2011) International Offshore and Polar Engineering Conference. Maui, Hawaiim USA, June 19-24, 2011

CHAPTER 3: WINTER BESETTING EVENTS IN THE HUDSON STRAIT AND THEIR RELATIONSHIP TO PRESSURED AND RIDGED ICE

ABSTRACT

Pressured sea ice and sea ice ridges are serious navigational hazards for vessels traveling in the Arctic. These conditions can cause vessels to become beset, which is a significant risk to the environment and operational revenues considering time lost, fuel burned, and possible ship damage. There have been few studies so far on the ship-scale implications of encountering hazardous ridged ice in the Canadian Arctic. Ridged ice is highly prevalent in the Hudson Strait region, which connects Hudson Bay and the Atlantic Ocean and where there is currently year-round shipping to service a mine in the region. In this study, logbooks from the *MV Arctic,* a regularly transiting ship, were obtained for its winter voyages (January, February, and March) from 2005-2014. The logs notes include vessel location and whether or not the ship was beset at that particular point. Ship routes were digitized geospatially and besetting events were noted. The location and timing of the besetting events were investigated cluster analysis. Results indicated that regular besetment occured in the area between Charles Island and the coast of Quebec, as well as the eastern entrance to the Hudson Strait. The ship was more likely to become beset in February and March than in January. The timing and location of besetting events was compared to of identified ridge densities in the Hudson Strait. ere The ship often became in areas and times of year associated with high ridge densities. These results demonstrate the use of ridges as predictors of where and when vessels may become beset or encounter difficulties. This is important information for ship captains and for the development of new shipping routes.

HIGHLIGHTS

- Pressured sea ice and ridges are hazardous to vessels in the Arctic
- Ship logs were used to track winter shipping in the Hudson Strait
- Besetting events were compared to previously identified ridging patterns
- Clear correlation between presence of ridges and locations of besetting events

KEYWORDS: *Arctic shipping, pressured ice, ridges, RADARSAT, ice hazards*

3.1 Introduction

Hazardous ice conditions can have serious implications for ship safety and voyage efficiency in the Arctic. Pressured and ridged sea ice is difficult for vessels to navigate and can cause them to become beset for hours to days and thus can be extremely costly for ship operators (Kubat and Sudom, 2008; Kubat et al., 2009; Kubat et al., 2012). Pressured ice occurs where ice is mobile and is impacted by convergent forces such as winds, tides and currents that build up pressure within the ice and lead to the formation of ridges. Bottlenecks, choke points, and shear zones, which are created when mobile ice moves alongside land-fast ice, can also enhance the build-up of pressure in sea ice. Becoming beset in pressured and ridged ice is dangerous and can lead to operational delays; in extreme situations it can be the cause of environmental impacts related to increased ship-based emissions and fuel and/or cargo spills. Understanding how vessels interact with these hazardous ice conditions is important for predicting where and when delays may occur and can allow captains to plan for these hazards accordingly.

Figure 3.1: The *MV Arctic (Fednav, 2010)*

The ice-strengthened vessel the *MV Arctic* makes two winter trips as part of its year-round servicing of the Raglan mine in Northern Quebec located midway through the Hudson Strait (Figure 3.1).While transiting the strait in the wintertime, the vessel frequently encounters pressured and ridged ice (P. Bourbonnais, personal communication, January 28, 2014). The *MV Arctic* is not the only vessel that regularly

makes use of the Hudson Strait; it is the site of a diverse number of shipping operations, though all other industries make use of the Strait in the summertime only. For example, cargo ships loaded at the Port of Churchill pass through the Hudson Strait to reach domestic and foreign markets (Stewart and Lockhart, 2005). The Hudson Strait is also used for cruise tourism as well as community re-supply with 2-3 voyages being made each summer to bring supplies to the communities along the coast of the Hudson Strait and Hudson Bay (Stewart et al., 2010; NEAS, 2014). Finally, in addition to the Raglan mine, there are several other mines in the planning stages of development on mainland Nunavut that would be serviced by ship year-round if and when they are implemented (Agnico Eagle, 2013; AREVA, 2011). As well, the long term plan for the Mary River mine on Baffin Island is to transport ore to foreign markets via the Hudson Strait through the winter months (Baffinland, 2012).

Most attempts to model pressure and ridge formation have been carried out at scales of a few kilometres and, while these attempts have yielding important information, the reality is that ships experience pressure at a scale of only a few metres, thus the models that have been created are not always useful to ship operators or for predicting ship-scale pressured ice events (Kubat et al., 2012). Comparisons between modelled sea ice pressure predictions and actual besetting events, such as those undertaken in Kubat et al. (2011) and Kubat et al. (2012), are necessary to understand the impacts of pressure and ridging at a ship scale. However, there is a pressing need for more observational information about pressured ice and ridges in the Canadian Arctic including their prevalence and related impacts on shipping. This paper addresses this knowledge gap by examining ship besetting events and their relationship to pressured and ridged ice conditions over 9 years of data. Specifically, the actual impacts of ridged ice leading to besetment on the ice strengthened vessel, the *MV Arctic* are examined using previously identified ridging patterns in the Hudson Strait from 2005 to 2014.

3.1.1 Pressured Ice and Winter Shipping

Pressured ice occurs when ice comes under pressure due to convergent forces including winds, tides, and currents (Kubat et al., 2012). Shearing is another important mechanism that causes pressure, as mobile ice moves along an immobile surface such as land or land-fast ice, or even offshore structures (Parmerter and Coon, 1972). As the pressure within the ice builds up, pieces of ice slide over one another in a process called `rafting` (Marchenko, 2008; Timco et al., 1997; Bradford, 1972). At a certain thickness, the ice no longer rafts but instead forms ridges (Weeks and Kovacs, 1970). During the formation of a ridge, blocks of ice pile up above the surface of the ice, forming a sail, and below the surface of the ice, forming a keel (Marchenko, 2008; Weeks, 2010). The keel can be 4-5 times deeper than the sail is high (Weeks, 2010). In the case of shearing forces, the ridges are usually very straight and made of up very well ground up ice, where as in pressured ice, the ridges that are formed are made up of larger blocks of ice (Parmerter and Coon, 1972). As ridges age and survive the summer melt season, they smooth and individual blocks are no longer visible (Kwok, 2014). After surviving their first summer, ridges are considered to be fully consolidated (Ekeberg et al., 2015). Ridges can therefore be used as an indicator of present or past areas of pressured ice (Kubat and Sudom, 2008). Ridges are an important dynamic mechanism that thickens sea ice, especially first year ice (Wadhams, 2000). They also alter the ways in which the ice interacts with the air and ocean, changing aerodynamic and hydrodynamic drag which in turn alters ice drift as well as heat exchange between the atmosphere and the ocean (Kwok, 2014). Pressured ice and the formation of ridges is still a growing area of research in the Arctic. For example, understanding sail and keel geometry of a ridge can only be fully grasped through drilling but in the past 40 years of research only about 300-400 ridges have been sampled (Strub-Klein and Sudom, 2012).

Pressured ice and ridges are a severe danger facing winter shipping vessels in the Arctic. Ridges can represent the greatest load encountered by an offshore structure or vessel, and in shallower waters their keels can interfere with underwater pipelines (Barrrette,

2011).The frequency of ridges in an area can be a proxy for the ice's strength and thus an indicator to mariners of navigation challenges (Hibler, 1975). However, in general, pressured ice is extremely difficult to detect until a ship physically encounters it. In a study examining accident data from winter shipping in Finnish waters, results indicated that most accidents take place in consolidated ice (when ice completely covered the area). Among all accidents that occurring during voyages undertaken independently, (i.e. without icebreaker assistance), ridges were present at the site of 20% of the incidents (Valdez and Banda et al., 2015). There is a growing acknowledgement of the navigational issues associated with pressured ice and the need for more information about this type of ice hazard is becoming increasingly urgent. In a survey of captains and ship operators, Kubat and Sudom (2008) found that those questioned frequently requested information on ridges in order to help them predict where they might experience pressured ice or tougher conditions. They also requested information on ridge concentrations, ridge height, type of ice and ice concentration (Kubat and Sudom, 2008). While data on water currents, waves, storms, winds, air temperatures are already well provided, information on ridging is not available for decision-making (Kubat and Sudom, 2008). Currently, the ice charts available to captains in the Canadian Arctic present ice type, distribution and concentration but have no information about ridges and only a little about sea ice dynamics.

3.1.2 Study Area: The Hudson Strait

The Hudson Strait is an important link between Hudson Bay and the Atlantic Ocean (Figure 3.2). The strait is 400km long and an average of 150km wide. It is heavily influenced by freshwater runoff, strong tides, currents and atmospheric forcing that contribute to an increased prevalence of pressured ice and ridging in the region (Saucier et al., 2004). Currents in the strait flow in opposite directions as saltier water from the Atlantic Ocean flows westwards along the southern shore of Baffin Island and fresher water from Hudson Bay flows eastwards along the northern shore of Quebec (Drinkwater, 1988). Overall there is a net outflow of water through the eastern opening of

the strait and the region is also highly influenced by tides; the tidal range in Ungava Bay is up to 12m (Straneo and Saucier, 2008).

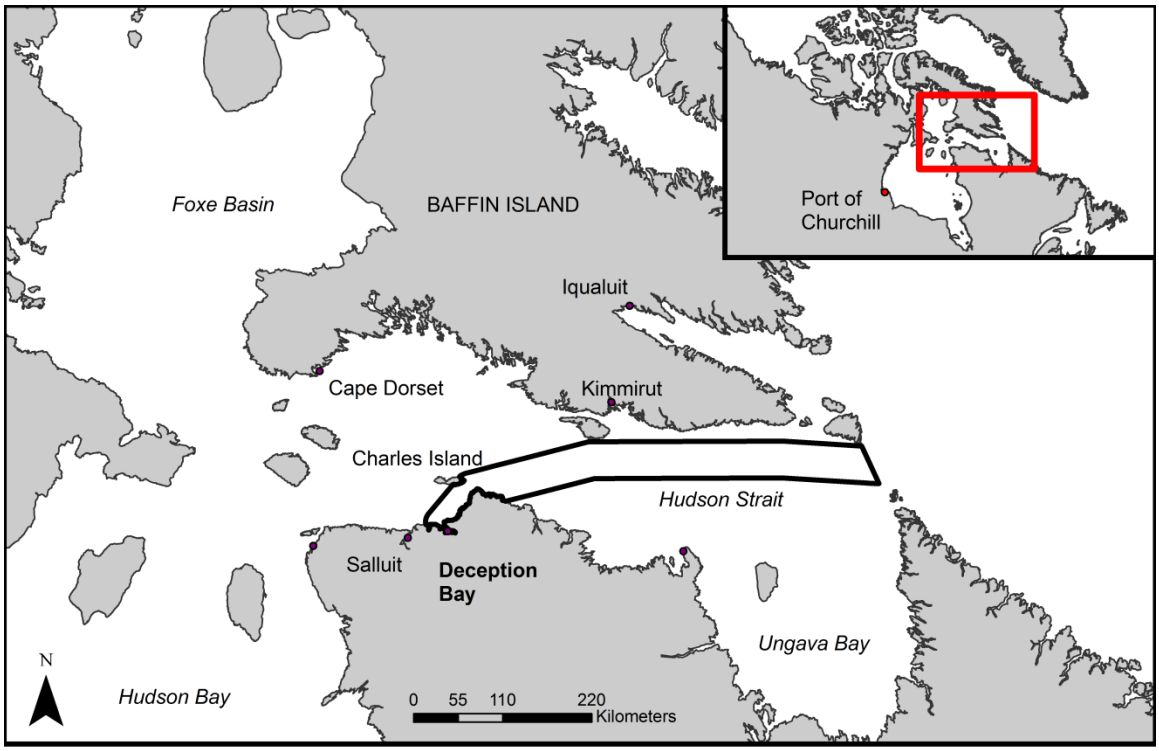

Figure 3.2: Map of Hudson Strait

The Hudson Strait is ice covered for approximately 8 months of the year. Ice formation begins in the western half of the strait in mid to late November, and spreads to the east (Crane, 1978). Land-fast ice first appears along the coast and ice formation continues in the centre until the entire strait is covered. From January to April there is 9-10 tenths ice coverage throughout the strait. In the winter, all of the ice, except for the land-fast ice along the coasts, is highly mobile. Leads, or areas of open water, are created as ice floes move apart, while ridges form as ice floes are forced together (Saucier et al., 2004). There is a recurring polynya along the southern coast of Baffin Island which remains mostly ice free throughout the entire winter, while along the northern coast of Quebec ice piles up and becomes heavily ridged and rubbled in and around Ungava Bay (Houser and Gough, 2003; CIS, 2011). Ice begins to leave the Hudson Strait in early May. By June 25th there is only 1-3 tenths coverage along the northern half of the strait, although there

is still 9-10 tenths coverage in Ungava Bay (CIS, 2011). The Strait is typically ice-free by mid-July each year (CIS, 2011).

The Hudson Strait is the site of ongoing and year-round shipping, including cargo, tourism, community re-supply and operations associated with resource extraction and development. The Strait is an integral part of the Arctic Bridge shipping route, between Churchill, Manitoba and Murmansk, Russia. Community re-supply vessels make at least two trips through the Strait to serve the communities along the coast of Quebec and Nunavut every summer (NEAS, 2014). Grain and other cargo are loaded at the Port of Churchill for shipments to markets in Eastern Canada and abroad (Stewart and Lockhart, 2005) also in the summer. There are also several proposed mines on mainland Nunavut that would bring vessels through the Hudson Strait to bring supplies and export ore when and if they are implemented (Agnico Eagle, 2013; AREVA, 2011) In the winter there is much less ship traffic with the only voyages made by the vessel *MV Arctic,* which services the Raglan Nickel mineoperated by Glencore Xstrata, in Deception Bay, Quebec. The *MV Arctic* is an ice strengthened vessel with a Polar Class 4 rating, which means it is safe for year-round shipping in thick first year ice that may include some multiyear ice (IACS, 2011). It can transport Ore, Bulk goods and Oil (OBO classification) and has been servicing the Raglan Mine since 1998. The vessel carries ore south from Deception Bay to Quebec City and transports supplies and fuel from Quebec City north to the mine (Têtu et al 2015). It makes two trips to the mine during the winter season between the months of January and March. The ship regularly encounters pressured ice and ridges throughout the strait during these winter voyages. According to the operators of the *MV Arctic*, the ship also encounter a very strong shear zone where the mobile ice of the strait comes into contact with the land-fast ice of Deception Bay. This shear zone frequently poses difficulties for the vessel as it attempts to enter and exit the bay but encounters strong pressure gradients and heavy ridging.

3.2 Data and Methods

Ship logs for the vessel *MV Arctic* were acquired for its winter voyages with permission from the ship operator (January, February and March) between 2005 and 2014. For each

winter season, the vessel typically makes two trips to the Raglan mine, therefore there are 4 winter voyages per year, two westwards and two eastwards. The ship logs contain written reports of the vessel location every 2 hours during the voyage, as well as a noontime location. The ship logs also include notes when the vessel becomes beset, the ongoing maintenance and other operations taking place, weather conditions, and observed ice coverage. "Beset" is when the vessel cannot make forward progress due to the ice conditions. Ship log locations and ice condition notations within the Hudson Strait region were digitized. Points were categorized by voyage number, date and whether or not the vessel was beset in ice at the time of reporting. In total there were 33 voyages available from the log books; two were available in 2005, 3 in 2006, 3.5 in 2007, and 0.5 in 2008, while all other years had 4 voyages. Each individual point(s) where the vessel was beset was also identified. There were 154 identified individual besetting events that were identified ranged from 1-2 hours to several days in length, made up of several individual reported points. The voyages are summarized in Table 3.1.

Table 3.1: Summary of voyages available in MV Arctic logbooks and average voyage times through the Hudson Strait

Year	Number of voyages	Average voyage length
2005	2	4.8 days
2006	3	3.4 days
2007	3.5	5.4 days
2008	0.5	4.9 days
2009	4	4.9 days
2010	4	2.9 days
2011	4	4.8 days
2012	4	3.7 days
2013	4	6.0 days
2014	4	7.2 days

For each unique voyage, the percentage of time that the vessel spent beset in the Hudson Strait was calculated. This was compared on a monthly and annual basis to understand temporal patterns of besetting events in the Hudson Strait.

To investigate the spatial distribution in besetting events, grouping and cluster analysis was performed. Grouping analysis provided a spatial summary of the data and enabled voyage and besetting data to be categorized by date. All the ship point locations classified by month (January, February, March) and by whether or the ship was beset that point. These results were then displayed on a map of the Hudson Strait. This information was used to understand not only where the vessel was getting beset but also what time of year the vessel was getting beset. Cluster analysis was used to determine where in the Hudson Strait there were statistically significant groupings of besetting events. Cluster analysis identifies significant hot and cold spots based on weighted factors. Specifically, hot spots are statistically significant clusters of higher values while cold spots are statistically significant clusters of lower values. In this case, a binary approach was used, with the value 1 being given to points where the vessel was beset and 0 being assigned to points where the vessel was not beset. Hot spot analysis examines each point in relation to its neighbours. In this case, a 15km fixed distance was chosen to define ‘neighbours’ as that was found to be the longest the ship moved during a single besetting incident (made up of many points) as a result of tides and currents. The Getis Ord Gi* statistic was calculated which compares the sum of besetting binary values of a single point and its neighbours within the 15km radius to the expected local sum based on the values for all points in the analysis (ArcGIS Help, 2013). When the local sum is significantly higher or lower than the expected sum, then that is considered a hot spot or cold spot, respectively (ArcGIS Help, 2013).

The overwhelming clustering of besetting events at the shear zone that exists where the mobile ice the Hudson Strait meets the land-fast ice of Deception Bay created an inflated average number of 1 values required for a significant cluster. Therefore, the cluster

analysis was also run on data where the besetting events in the shear zone had been eliminated. The number and location of besetting events for the years 2005 to 2012 were then compared to the results presented in Chapter 2 which identified ridges within the Hudson Strait winter shipping corridor using RADARSAT-1 and -2 ScanSAR Wide imagery. The annual spatial distribution of ridge density in the corridor from Chapter 2 was then compared to where and when the *MV Arctic* became beset those years in order to determine the impacts of ridged ice on an ice strengthened vessel.

3.3 Results and Discussion

3.3.1 Temporal Trends in Vessel Besetting Events in the Hudson Strait, 2005-2014

Table 3.2 shows a summary of each of the individual voyages, the month they spanned, voyage time, time spent beset and percentage of voyage spent beset. The mean voyage time through the Hudson Strait is 110 hours and the mean time the ship spends beset per voyage is 60 hours (i.e. 41% of average voyage time). The longest voyage, in February of 2014 was 366 hours and the shortest complete voyage was in January 2011 at 28 hours. The voyage with the greatest total time beset was in February 2014 when the vessel was beset for 302 hours or 82.5% of the voyage time. During voyages in January 2009, January 2010, and January 2011 the ship never became beset.

Table 3.2: Summary of Voyages and Besetting Event Durations

Voyage Name	Month of Voyage	Total Hours in Hudson Strait	Hours Beset	Percentage Time Beset
2005_1_E	Feb	109:32	33:32	30.6
2005_2_W	Mar	119:23	50:23	42.2
2006_1_W	Jan	32:00	3:00	9.4
2006_2_E	Mar	135:17	101:12	74.8
2006_3_W	Mar	79:30	21:20	26.8
2007_1_W ** partial voyage	Jan	10:00	0:00	0
2007_2_E	Jan	230:00	169:54	73.9
2007_3_W	Feb	90:00	39:00	43.3

2007_4_E	Mar	128:00	61:47	48.3
2008_1_E partial voyage**	Mar	118:00	84:00	71.2
2009_1_W	Jan	66:00	0:00	0
2009_2_E	Jan	56:00	15:00	26.8
2009_3_W	Feb	44:00	4:00	9.1
2009_3_E	Mar	302:00	202:00	66.9
2010_1_E	Jan	42:00	0:00	0
2010_2_W	Jan	40:00	4:00	10
2010_3_E	Feb	100:00	72:00	72
2010_4_W	Feb	92:00	36:00	39.1
2011_1_E	Jan	28:00	0:00	0
2011_2_W	Jan	36:00	0:00	0
2011_3_E	Feb	79:00	44:00	55.7
2011_4_w	Mar	70:00	29:00	41.4
2012_1_E	Jan	76:00	36:00	47.4
2012_2_W	Jan	35:00	6:00	17.1
2012_3_E	Feb	136:00	80:00	58.8
2012_4_W	Mar	112:00	66:00	58.9
2013_1_E	Jan	53:15	14:15	26.8
2013_2_W	Jan	136:00	84:00	61.8
2013_3_E	Feb	220:00	157:00	71.4
2013_4_W	Mar	170:00	100:00	58.8
2014_1_E	Jan	104:00	58:00	55.8
2014_2_W	Jan	58:00	10:00	17.2
2014_3_E	Feb	366:00	302:00	82.5
2014_4_W	Mar	160:00	88:00	55

The percentage of time during each voyage that the *MV Arctic* spent beset is shown in Figure 3.3. The mean was 41.9%. 2008, 2012, 2013 and 2014 are notable as the ship spent more than average time beset while in the Hudson Strait. The percentage time spent beset during voyages in 2009 and 2011, as well as 2010 were much less than average.

The year with highest percentage time spent beset was 2008, with a mean percentage of 72.8% and the lowest was in 2011, 24.3%.The mean monthly percentage time spent beset is illustrated in Figure 3.4. This is based on the month during which the majority of the voyage took place. Voyages in March had the greatest time spent beset at 54.4%, while in January they had the least (23.1%).

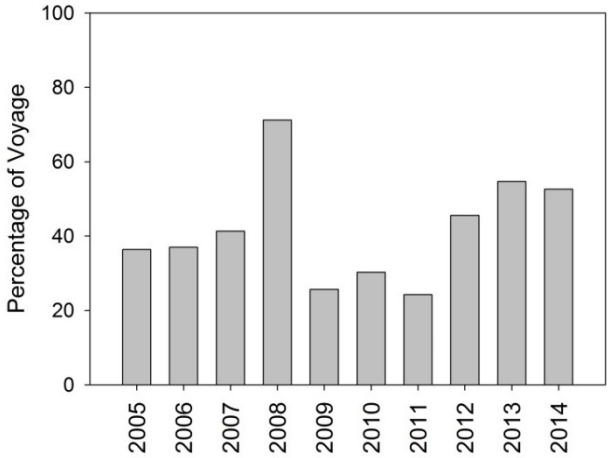

Figure 3.3: Mean Percentage of Voyage in the Hudson Strait Spent Beset, 2005-2014

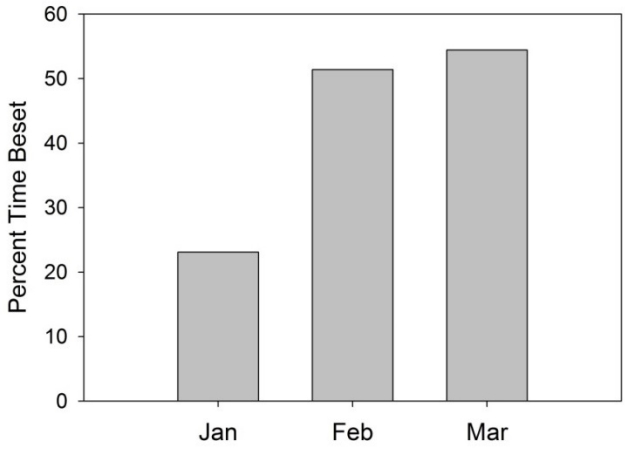

Figure 3.4: Mean percentage time spent beset on a monthly scale, 2005-2014

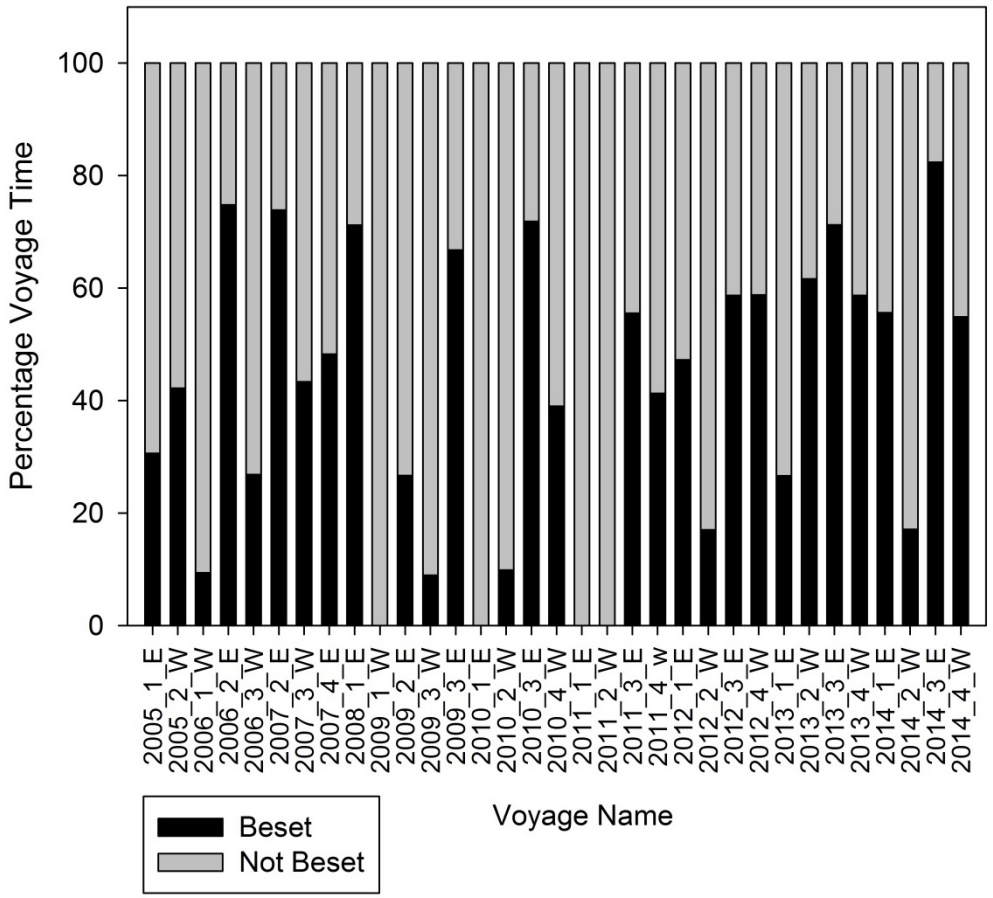

Figure 3.5: Percentage Time Beset by Individual Voyage, 2005-2014

The percentage of time spent beset for each individual voyage are shown in Figure 3.5. It is notable that for some voyages in 2009, 2010 and 2011 no time was spent beset. There is a large variability amount the times within years, which is expected as the January ice conditions are likely easier for navigation than March conditions, given that the ice is thinner then. A seasonal pattern can almost be seen in the earlier years. In 2007 for example, the first voyage of the year has the smallest percentage of time spent beset while the last voyage of the year has the most. However, not all years follow that trend. In 2009, the second voyage of the year was spent beset more than the third voyage, though the fourth voyage by far has the greatest time spent beset.

3.3.2 Spatial Variability in Vessel Besetting events in the Hudson Strait, 2005-2014

Figures 3.6 to 3.9 show typical fast (Figure 3.5 and 3.6) and typical slow (Figure 3.7 and 3.8) voyage routes through the Hudson Strait including RADARSAT images of the ice conditions that were available closest to the timing of the voyage. During the faster voyages, the route from the entrance of the Hudson Strait to Deception Bay is almost straight. There is also minimal sea ice present during those voyages. This is not the case for the slower voyages. In 2009 (Figure 3.7), it is obvious that the vessel became beset several times at the entrance to the Hudson Strait and was even moved by the tide. There is full ice coverage during the voyage and heavily ridged and rubbled ice can be seen at the entrance to the Hudson Strait. The besetting events in 2014 are less obvious, as it occurred in the shear zone, and so there is not much movement associated with it. That year, the vessel was beset in the shear zone for 10 days.

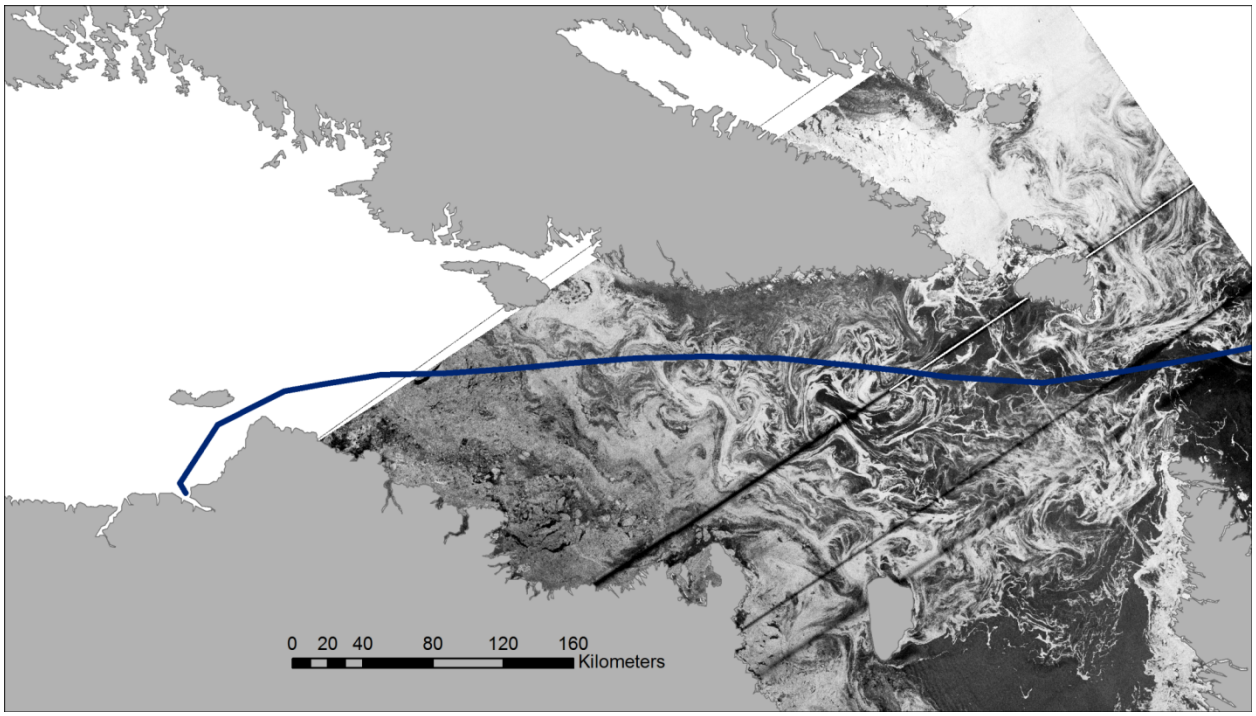

Figure 3.6: Fast Voyage January 5-6, 2010. RADARSAT 1 Image from December 26, 2009 (RADARSAT imagery © Canadian Space Agency).

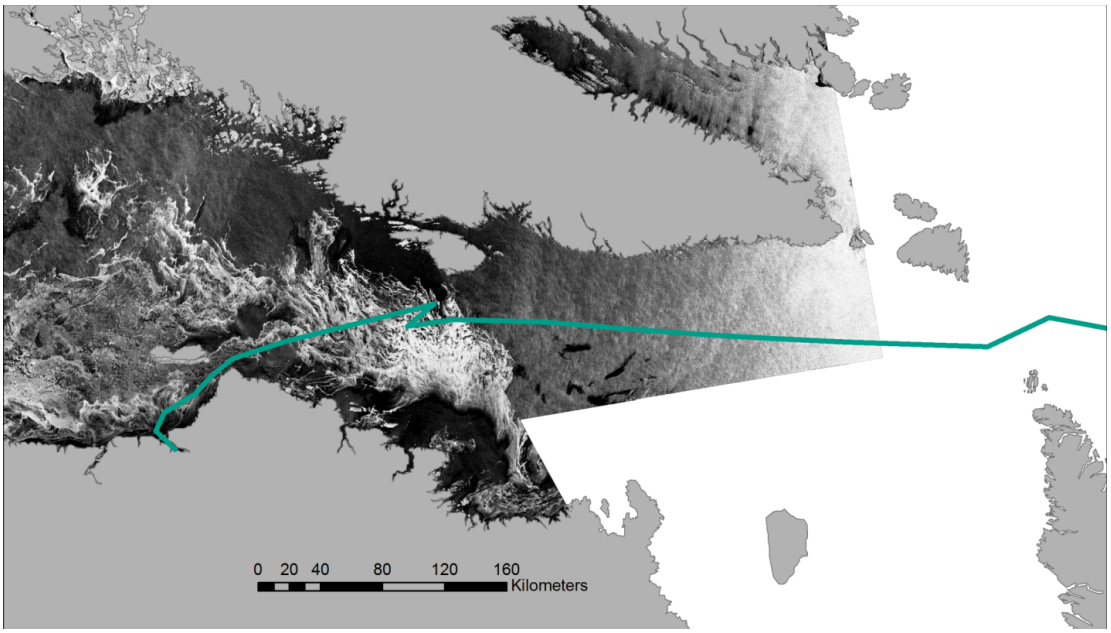

Figure 3.7: Fast Voyage January 7-9, 2011. RADARSAT 2 Image from January 1, 2011 (RADARSAT imagery © Canadian Space Agency).

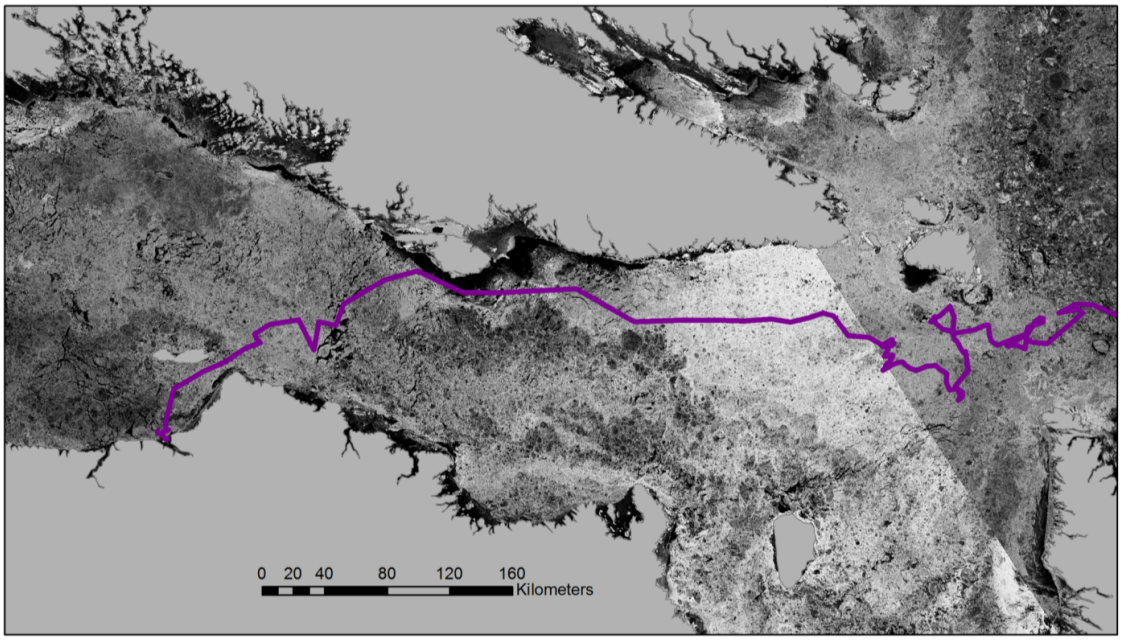

Figure 3.8: Slow voyage, March 18-30, 2009. RADARSAT2 image from March 28, 2009 (RADARSAT imagery © Canadian Space Agency).

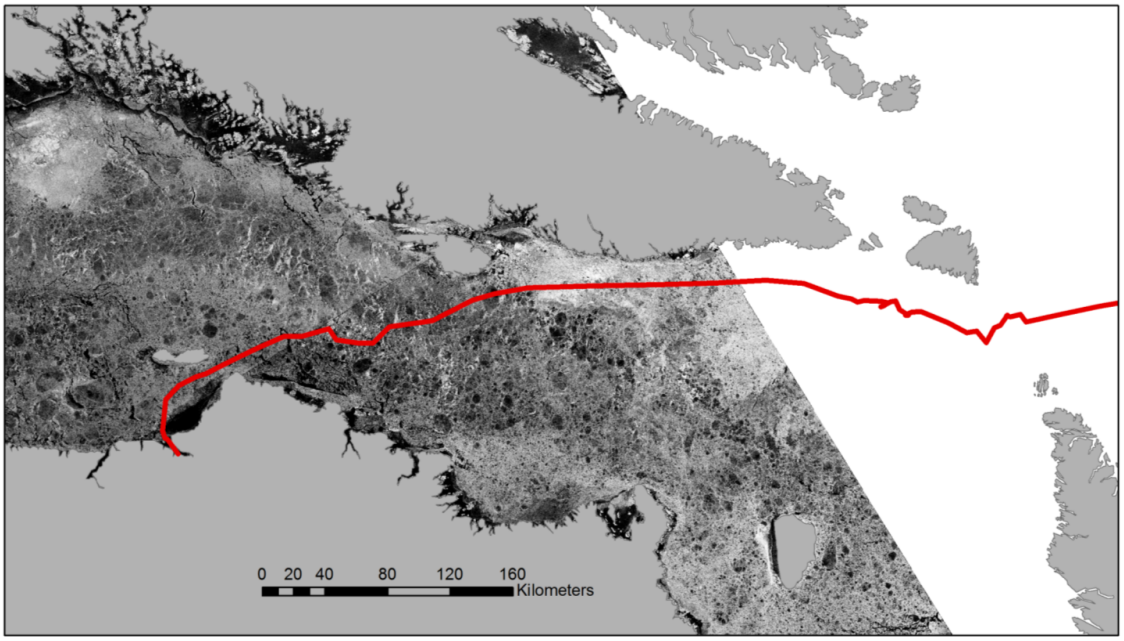

Figure 3.9: Slow voyage, February14-March 1, 2014. RADARSAT2 image from February 22, 2014 (RADARSAT imagery © Canadian Space Agency).

3.3.2.1 Grouping Analysis

Figure 3.10 illustrates the results of the grouping analysis by month. Red points denote where the vessel was beset, and the different point shapes correspond to the month of the besetting. Green points denote where the vessel was not beset, and again the point shapes correspond to the month that location was recorded. It is evident from Figure 3.10 that the besetting events for all three months are clustered in the eastern and western portions of the Strait and there are no besetting events in the middle of the Strait. As well, it can be seen that in January the ship follows a path closer to the middle of the strait while during March the ship follows a more northerly route closer to the shore of Baffin Island. This is likely because of the shrinking size of the polynya that is found along the coast of Baffin Island as the winter progresses (CIS, 2011).

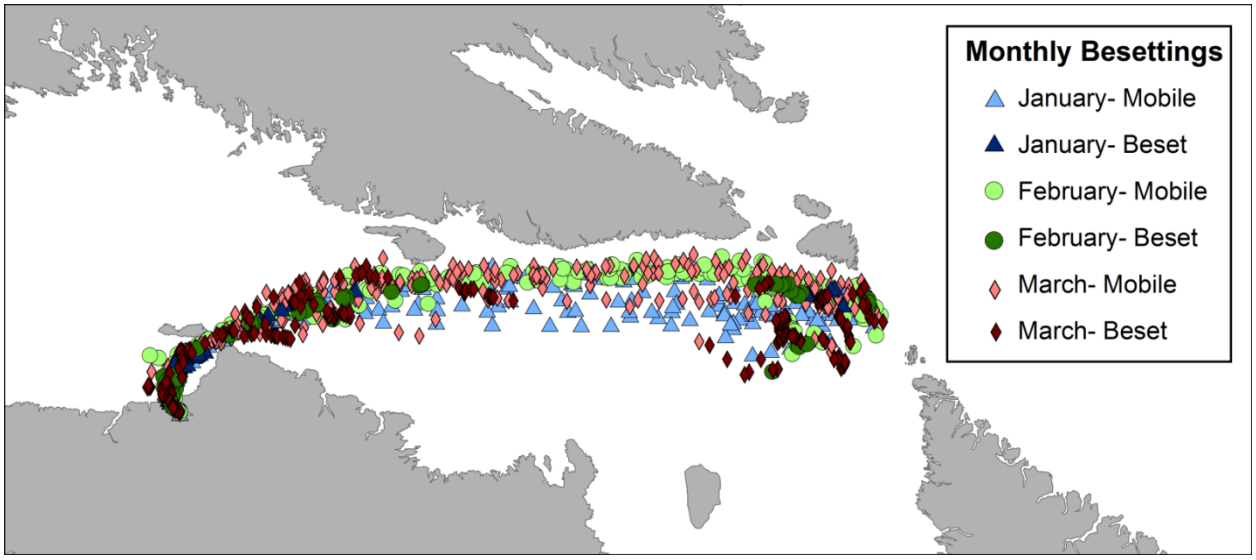

Figure 3.10: Grouping Analysis of Besetting Events for All Months in the Hudson Strait, 2005-2014

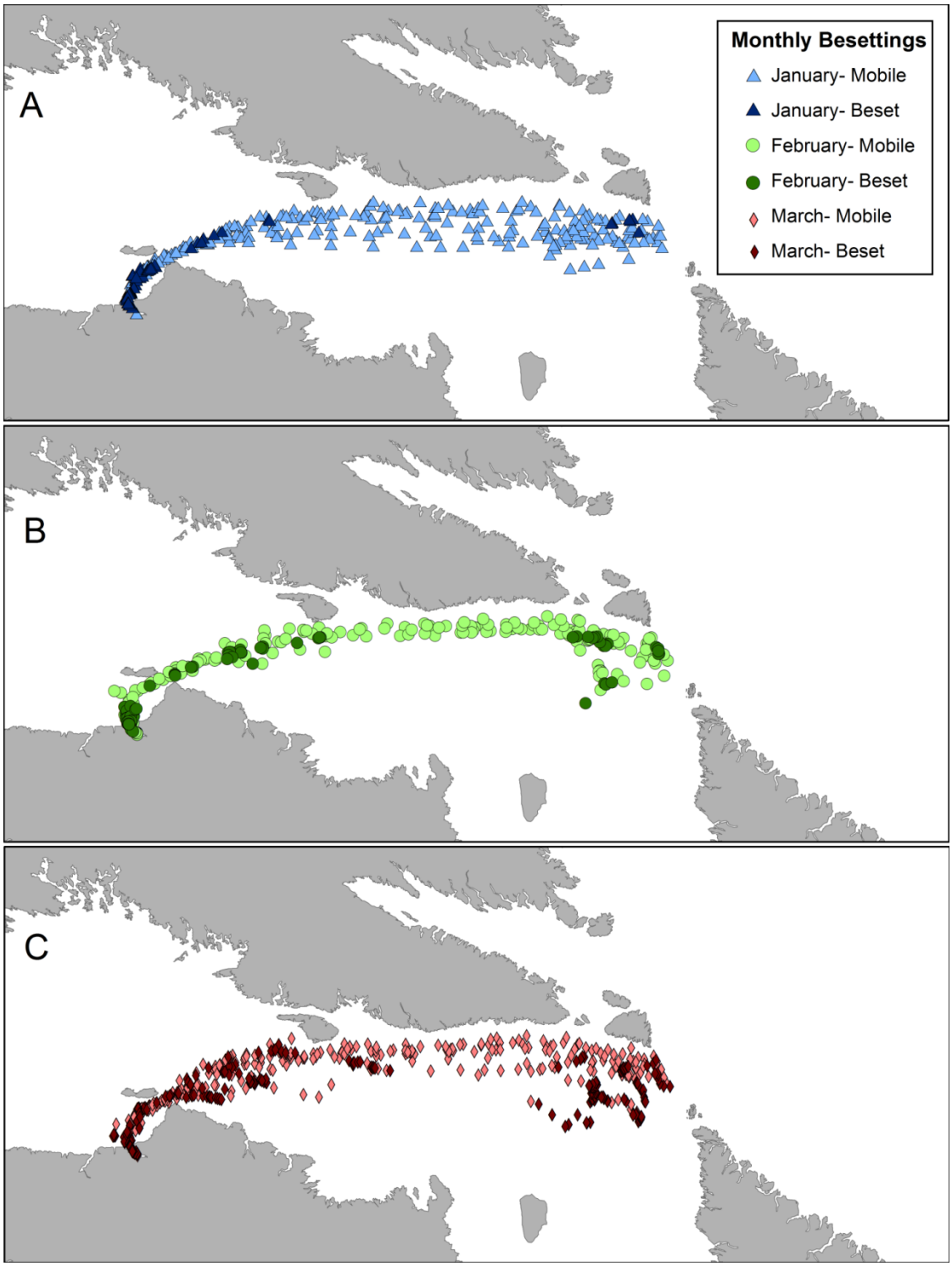

Figure 3.11: Monthly Besetting Events in the Hudson Strait, 2005-2014 (A – January, B- February, C- March)

Figure 3.11 displays a grouping analysis by month and the colour scheme is the same as Figure 3.10, with the green points representing locations where the vessel was not beset and the red points showing where the vessel was beset. In each of the months, there is the same clustering of besetting events at the opening of the Hudson Strait in the east and between Charles Island and Deception Bay in the west. There are notably fewer besetting events in January than in March and the besetting events in February and March spread further into the middle of the strait than in January. The points in January and February fall into a much narrower line than in March, perhaps indicative of harsher ice conditions during that month that force the vessel to take a more circuitous route to Deception Bay.

3.3.2.2 Cluster Analysis

Figure 3.12A illustrates where there are statistically significant clusters of besetting and non-besetting events. It is evident that the significant clustering of besetting events are the same as those areas identified in the grouping analysis: the entrance to the strait, as well as between Charles Island and Deception Bay. There is also a cluster to the east of Charles Island. For comparison, Figure 3.12B shows the results of the cluster analysis if the shear zone is not omitted. In this case, because the signal from the group of besetting events in the shear zone is so strong, no other significant besetment clusters are identified.

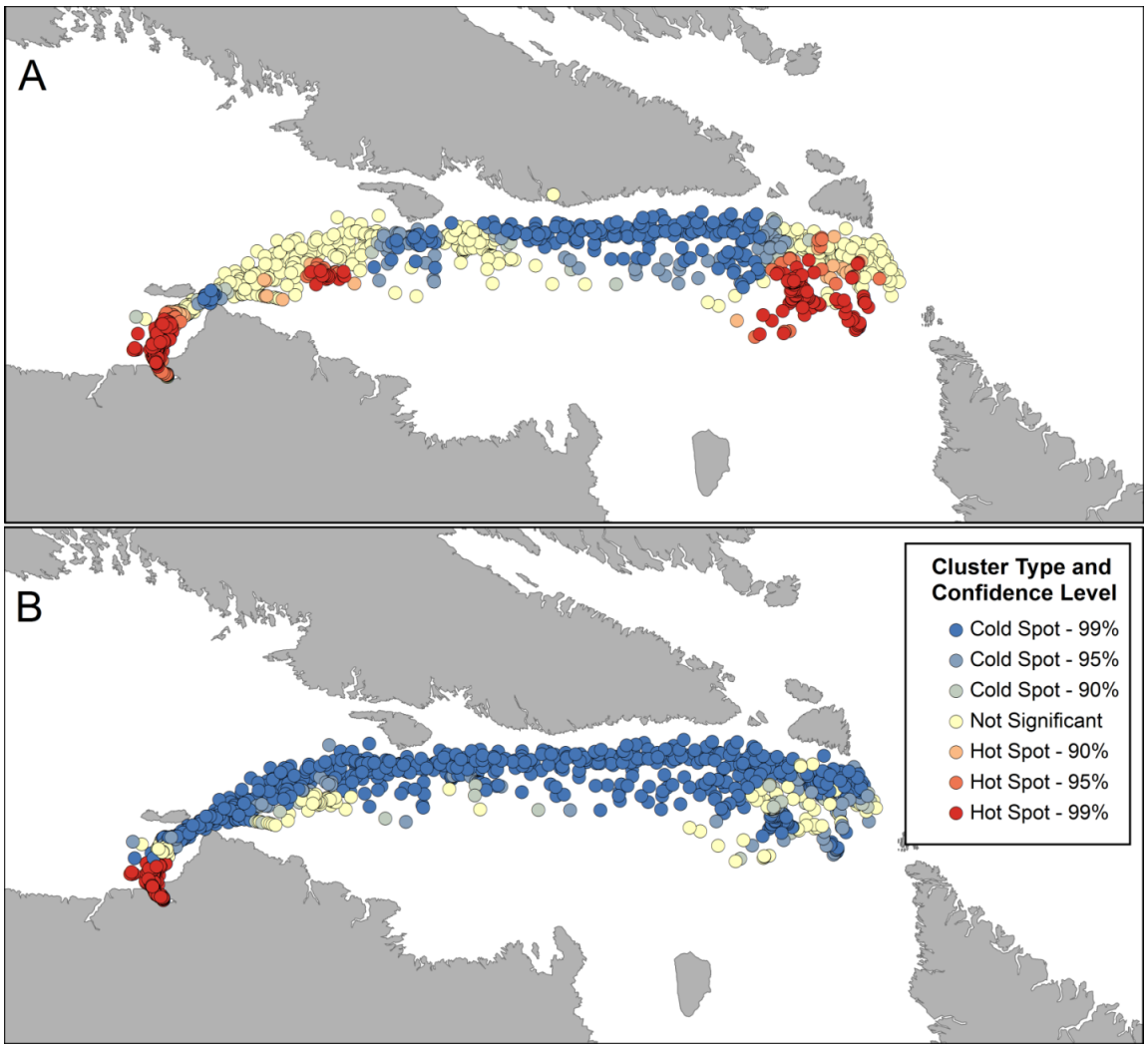

Figure 3.12: Cluster Analysis for All Years, 2005-2014; (A-Shear Zone Besetting Events Omitted; B- Shear Zone Besetting Events Included)

Figure 3.13 shows the results of the cluster analysis broken down by month as there are important differences between each of the months. In January, the largest cluster of besetting events is between Charles Island and Deception Bay, with a very small significant cluster at the eastern entrance to the strait. There is also a non-besetment cluster in that same area, while the points in the middle of the voyage are not significant clustering, indicating a mixture of besetting and non-besetting events. In February, there is also a large besetment cluster at the entrance to Deception Bay, as well as one to the east of Charles Island. In February there is a larger significant non-besetment in the

middle of the strait, where the vessel was consistently not beset. In March, there is a greater mix of besetting and non-besetting events than in the previous months, indicating a greater variability of ease that the ship traveled through the strait in different years. No clusters of besetting events between Deception Bay and Charles Island (although, the besetting events in the shear zone were omitted) were present, but there are some clusters east of Charles Island, as well as at the eastern entrance to the strait.

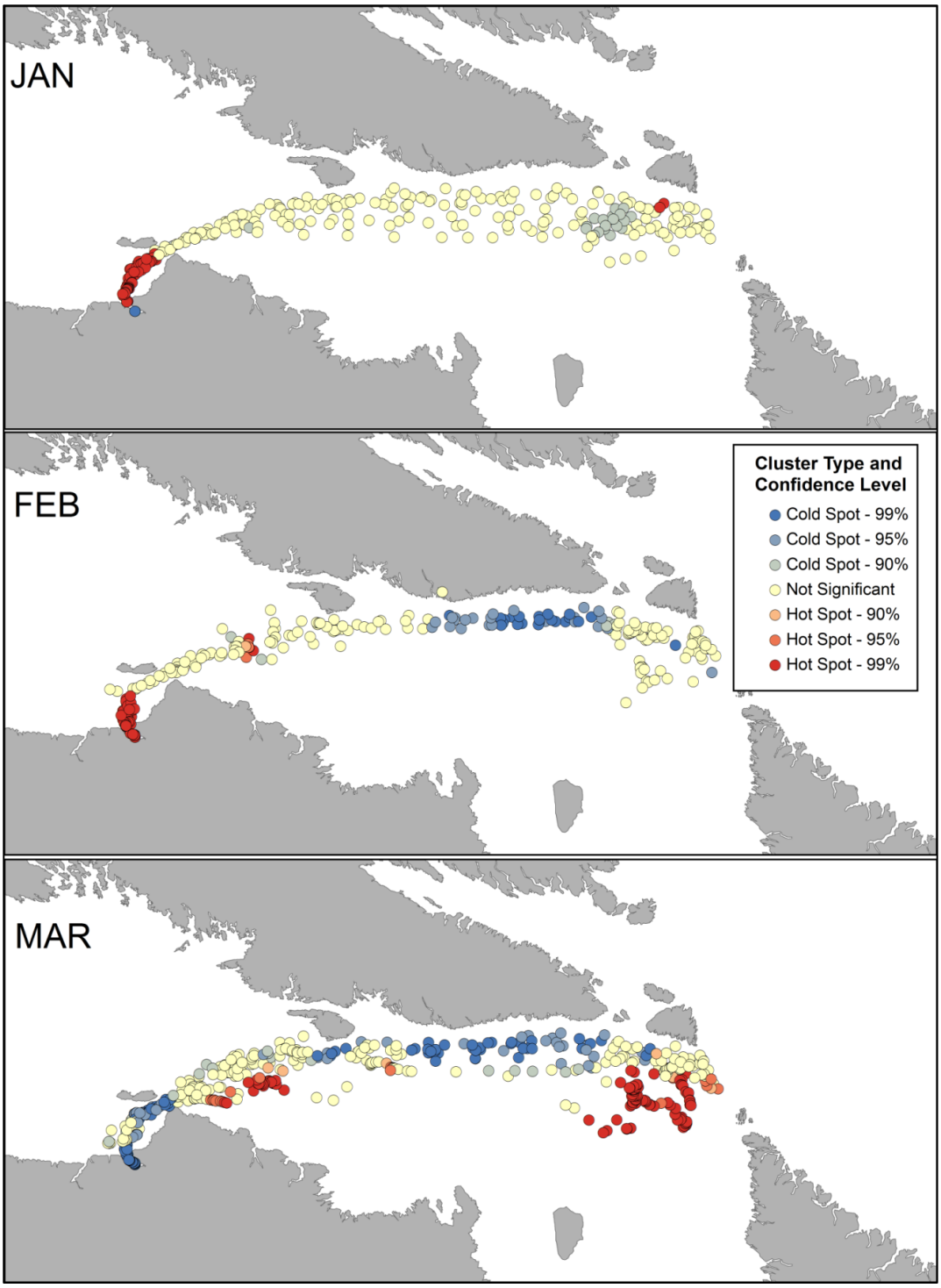

Figure 3.13: Cluster Analysis, Monthly, 2005-2014; Shear Zone Besetting Events Omitted

Figure 3.14 illustrates the results of the average besetting event duration for each location over the entire study period as summarized in a 5 km x 5 km grid. Figure 3.15 shows the standard deviations for each of these mean values. There is a wide range of mean besetting event durations over the entire corridor, with no clear pattern as to one area being the site of longer besetting events than another. However, the standard deviations do show a clear pattern. There is a much higher standard deviation in the shear zone, indicating that in this region the ship becomes beset for a highly variable amount of time. In the areas in the eastern half of the corridor, the besetting event lengths are more consistent.

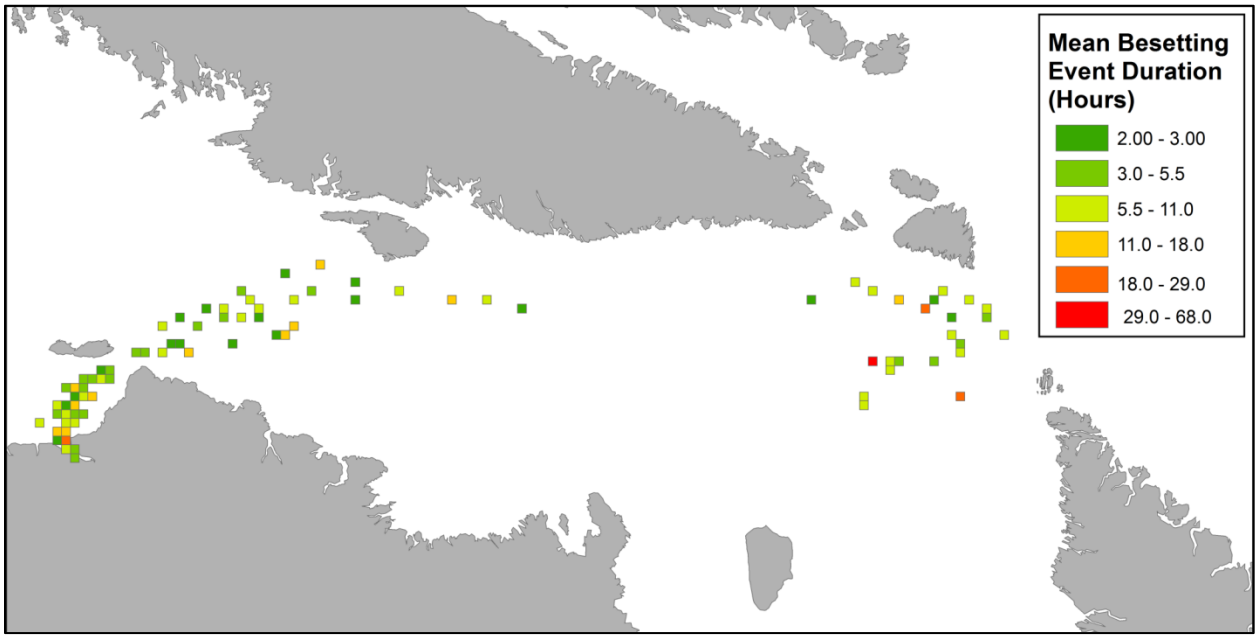

Figure 3.14: Mean Besetting Event Durations Summarized by 5km grids, 2005-2014

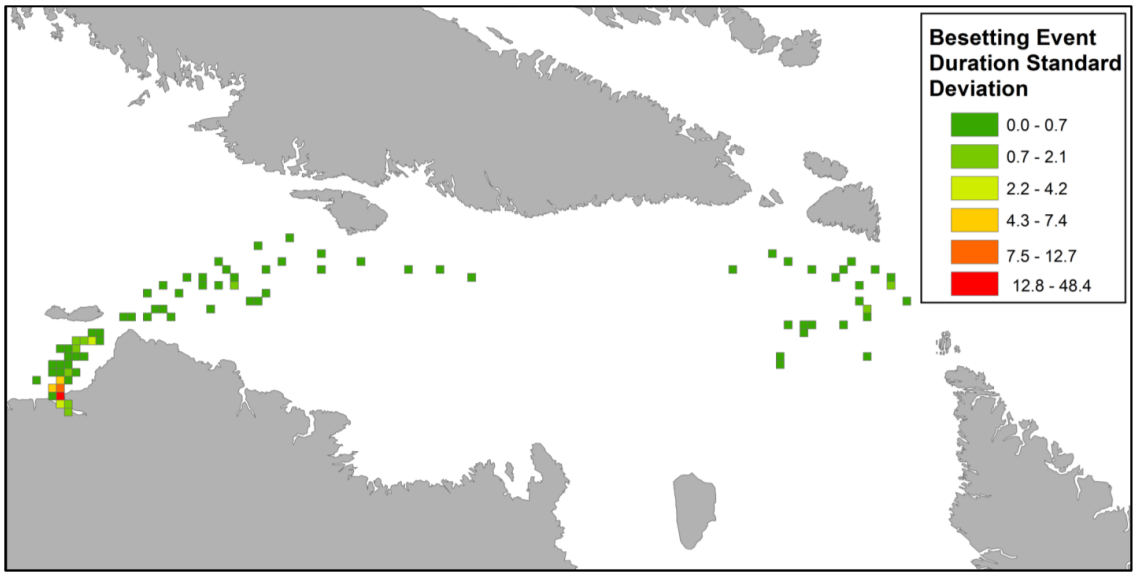

Figure 3.15: Besetting Event Durations Standard Deviations Summarized by 5km grids, 2005-2014

The boxplots in Figure 3.16 summarizes the besetting durations by month. February has the highest average besetting event duration but this is likely due to the anomalously long event when the ship was beset for 270 hours in the shear zone. As can be seen in Figure 3.12, February has the widest distribution of besetting lengths, while March has the greatest number of outliers. January has the shortest average besetting event length and the narrowest distribution of durations.

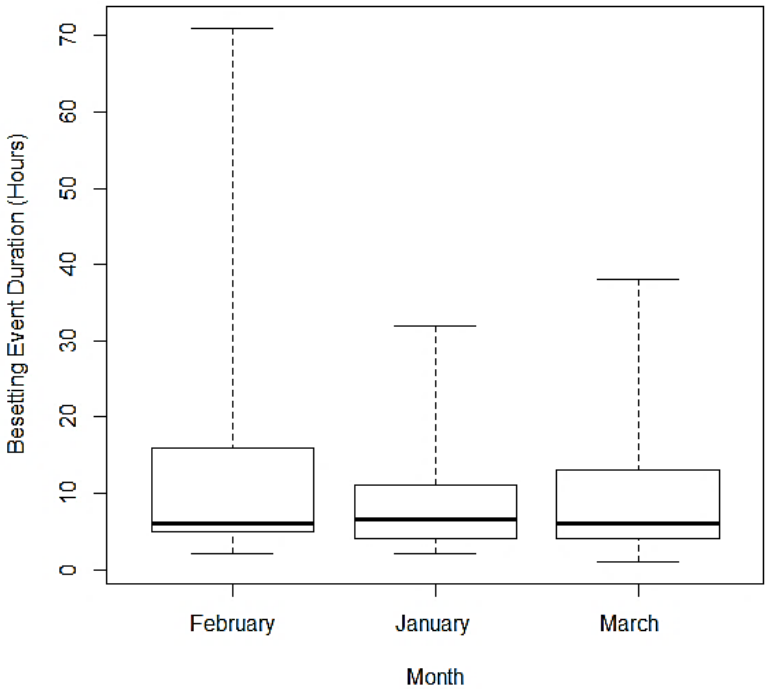

Figure 3.16: Distribution of Besetting Event Durations by Month, 2005-2014

3.4 Comparison between Besetting Events and Ridge Densities in the Hudson Strait, 2005-2012

The results of ridge counts and ridge densities within the winter shipping corridor in the Hudson Strait reported in Chapter 2 were compared with the patterns of besetting events endured by the *MV Arctic* in the Hudson Strait for the overlapping years of 2005 to 2012. Figure 3.17 illustrates the ridge counts from the winter shipping corridor in the Hudson Strait for the months of January, February and March as identified in Chapter 2. 2009, 2010 and 2011 are notable as years with lower ridge counts than most of the other years. In 2007, 2010 and 2012, March has the greatest number of ridges. In both 2006 and 2011, February and March have similar ridge counts and in 2005 and 2009, February has the highest ridge counts.

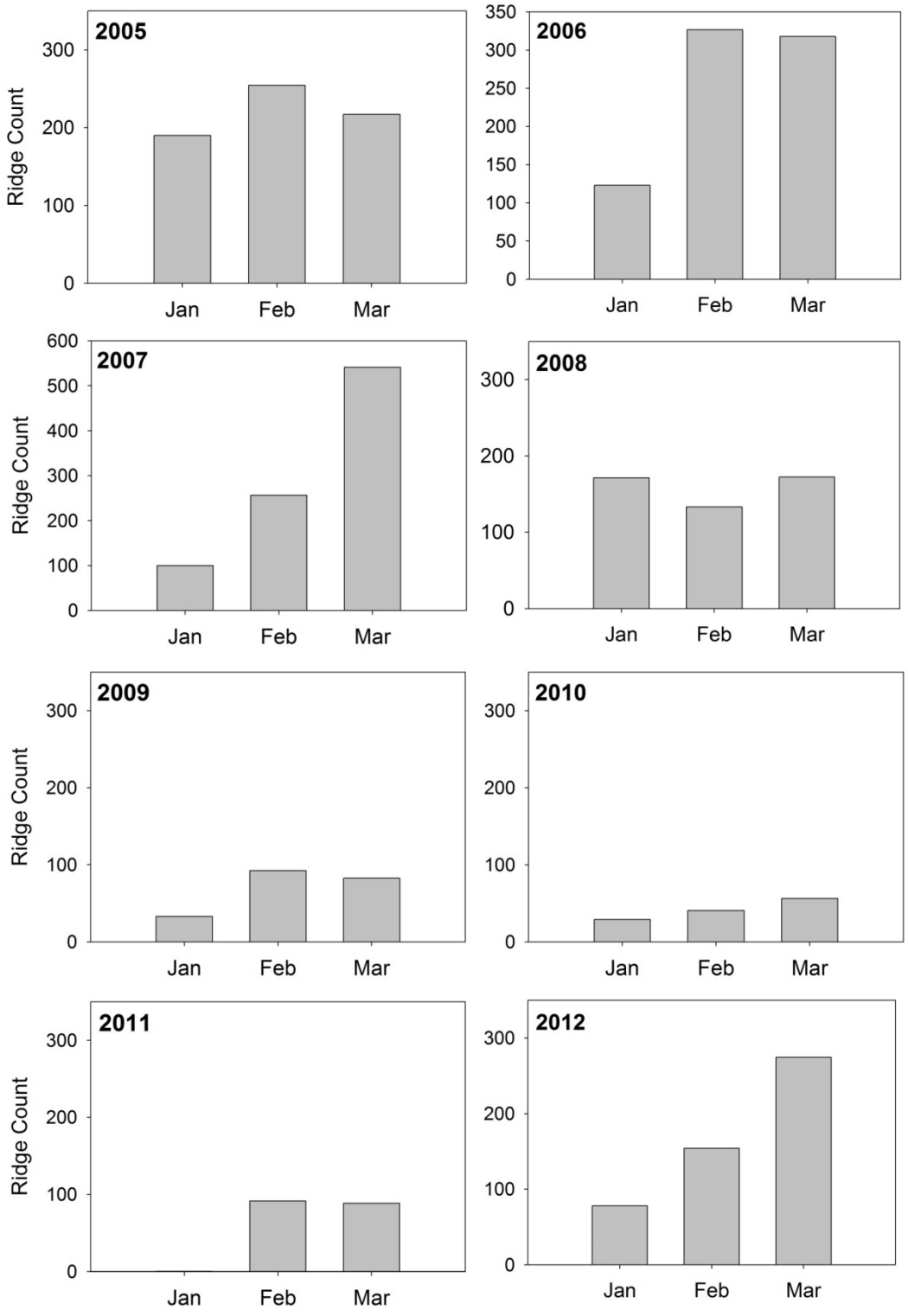

Figure 3.17: Ridge Counts in a corridor in the Hudson Strait from RADARSAT images, 2005-2012 (After Chapter 2)

In order to ease the comparison between voyage times and ridge counts, the voyages taken between 2005 and 2012 were classified as fast and slow, and are summarized in Tables 3.3 and 3.4. Slow voyages are defined as those where the vessel was beset more than 40% of the voyage time, whereas fast voyages are those when it was beset for less than 20% of the voyage time. It is evident that most of the faster voyages through the Strait occurred during the month of January, while March is typically when the vessel more than 50% of its time beset while in the Hudson Strait. Comparison of high besetting times of the year, March, and ridges counts, shows a good association between overall average monthly ridge counts and percentage times beset. A correlation between the monthly total time and monthly ridge count was found to be insignificant ($p=0.399$). However, when the values from March 2007 and March 2009 were removed, the correlation was significant ($r^2= 0.58$, $p=0.012$). These two months appear to be outliers. In March 2007 there was a very high ridge count number (541 ridges) but only an average number of besetting events. In March 2009, the vessel was beset at 112 different time intervals but there were only 82 ridges that month. This relationship is shown in Figure 3.14. It would appear that there are other factors at play during those two months. There was also a significant correlation between the number of individual besetting incidents and monthly ridge count ($p=0.07$).

Table 3.3: List of Slow Voyages through the Hudson Strait and Month of Voyage, based on Percentage Time Beset during Voyage

Slow Voyages (More than 40% of Voyage Time Beset)	**Month of Trip**
2005_2_W	Mar
2006_2_W	Mar
2007_2_E	Jan
2007_3_W	Feb
2007_4_E	Mar
2008_1_E** partial voyage	Mar
2009_3_E	Mar
2010_3_E	Feb
2011_3_E	Feb
2011_4_w	Mar
2012_1_E	Jan
2012_3_E	Feb
2012_4_W	Mar
2013_2_W	Jan
2013_3_E	Feb
2013_4_W	Mar
2014_1_E	Jan
2014_3_E	Feb
2014_4_W	Mar

Table 3.4: List of Fast Voyages through the Hudson Strait and Month of Voyage, based on Percentage Time Beset During Voyage

Fast Voyages(Less than 20% Voyage Time Beset)	**Month of Trip**
2006_1_W	Jan
2007_1_W** partial voyage	Jan
2009_1_W	Jan
2009_3_W	Feb
2010_1_E	Jan
2010_2_W	Jan
2011_1_E	Jan
2011_2_W	Jan
2012_2_W	Jan
2014_2_W	Jan

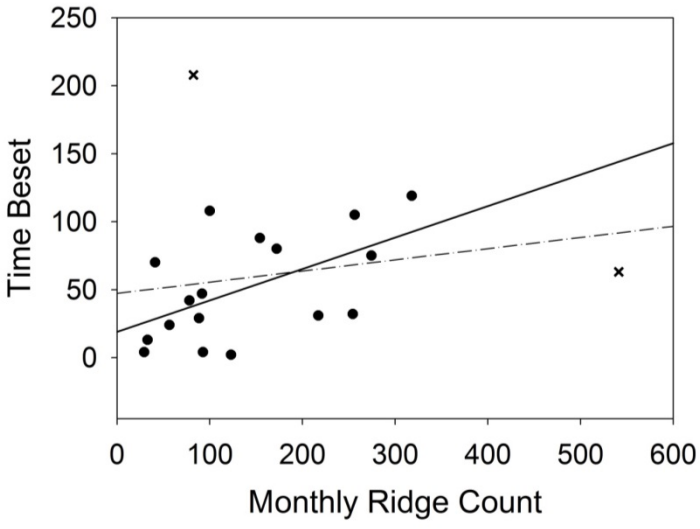

Figure 3.18: Correlation between Monthly Ridge Count and Time Beset. March 2007 and March 2009 are shown with an X. The dotted line shows the correlation including these two outliers. The solid line shows the correlation excluding the outliers.

Overall, months with higher ridge counts were typically associated with slower, longer voyages and low ridge count months and years were associated with faster voyages. Most of the faster voyages occurred during the month of January, which has the lowest sea ice ridge count compared to February and March. This is not surprising since the ice is thinner than in March, as it has not had all winter to thicken thermodynamically and dynamically. For example, there were two low besetting voyages in 2009, in January and February, two months that had lower than average ridge counts. In 2010, there were also two fast voyages, both in January, also expected as this was a low ridge count year. What is surprising is that later voyages in 2010 were not very fast and one was actually 72% beset, despite the overall low ridge counts that year. The following year, 2011, was another overall low ridge count year, and as expected both January voyages were faster than average. In that month in particular there were no ridges identified in the satellite images. Again, it is surprising that there was one voyage in February 2011 which was over 50% beset (it was 55% beset).

As for the highly ridged years, 2005 had high ridge counts all winter and the March voyage of the *MV Arctic* was beset for more than 40% of the time. Both 2006 and 2007 were also highly ridged years. In 2006, 1 out of 3 voyages was beset more than 40% of the time, and in 2007, 3 out of 4 voyages were beset more than 40% of the time. 2012 was last of the highly ridged years identified in Chapter 2 and again, 3 out of 4 voyages that year spent 40% of their time beset.

In order to compare the spatial distribution of ridges identified in Chapter 2, which are shown in Figure 3.19, and the locations of the besetting events of the MV Arctic, a grouping analysis was carried out on the *MV Arctic* locations on an annual scale from 2005-2012 and show in Figure 3.20. 2005 was a high ridge count year, notable ridging in the middle of the strait that is not seen in other years. Several besetting events also occurred in the middle of the strait that year, as seen in Figure 3.16. These are possible a result of those identified ridges. 2006 was another high ridge density year, with lots of

ridging at each end of the shipping corridor. The vessel did not encounter any issues at the eastern end of the strait but did become beset in the area between Charles Island and Deception Bay, as well as east of Charles Island, where there was an area of high ridge density that has extended beyond the typical area of bottlenecking. In 2007, there was much greater ridging than average, and that year 3 of 4 voyages were considered slow voyages. The identified ridging was concentrated in both the eastern and western portions of the corridor. Most besetting events occurred between Charles Island and Deception Bay in the western half of the corridor. However, some also occurred at the entrance to the strait, where there was a high concentration of ridges.

The winters of 2009, 2010 and 2011 were notable for having less than average ridge counts; Figure 3.19 shows the very low ridge densities that were identified in most areas of the shipping corridor in those years. The winter of 2009 had low overall ridge densities. However, the ship did endure quite a number of besetting incidents at the eastern entrance of the Hudson Strait, but annual ridge densities overall in that area were no higher than other years. Other than those March besetting events in the east, 2009 overall had a low frequency of besetting events. . The following year, 2010, was very similar with low ridge densities and low besetting event frequencies, except in the shear zone at the entrance to Deception Bay. In 2011, there were some besetting events near Charles Island, that align with the ridges that were identified in that region, but otherwise there were few ridges and few besetting incidents. The winter of 2012 had greater ridge densities than the previous 3 years, but not as much as 2006 or 2007. Ridging was concentrated in the western and eastern ends of the corridor, where most of the besetting events occurred as well. Some besetting events occurred in the middle of the corridor, where there was some ridging present, at least on an annual basis.

Overall, there are very strong overlap both temporally and spatially between observed ridging patterns in the Hudson Strait and where and when the *MV Arctic* became beset. In all years, the more difficult and besetting-prone journeys were later in the winter, in

February and March, when there was typically a greater number of ridges identified in the corridor. The vessel also frequently became beset between Charles Island and Deception, east of Charles Island and in the eastern entrance to the strait, all locations where there was often high ridge densities. These can be explained by the shear zone that exists at the entrance to Deception Strait, as well as by the bottleneck formed by Charles Island which causes pressure to build up between the island and the coast. As well, pressure ridges at the eastern entrance of the strait could be explained by the convergence of ice outflowing from the strait as the entrance is narrower than the rest of the Hudson Strait

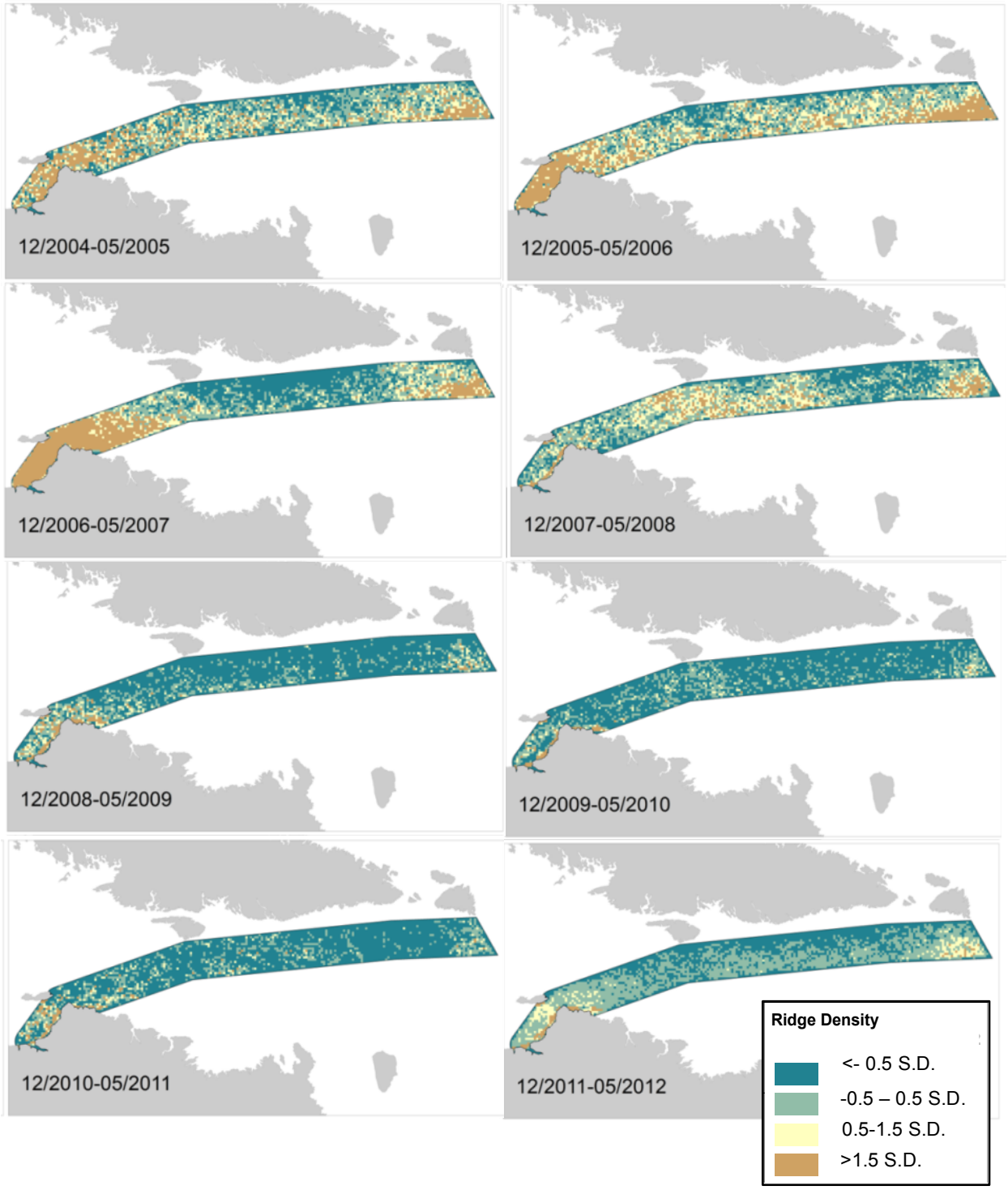

Figure 3.19: Ridge densities based on RADARSAT images from December to May in the Hudson Strait, 2005-2012

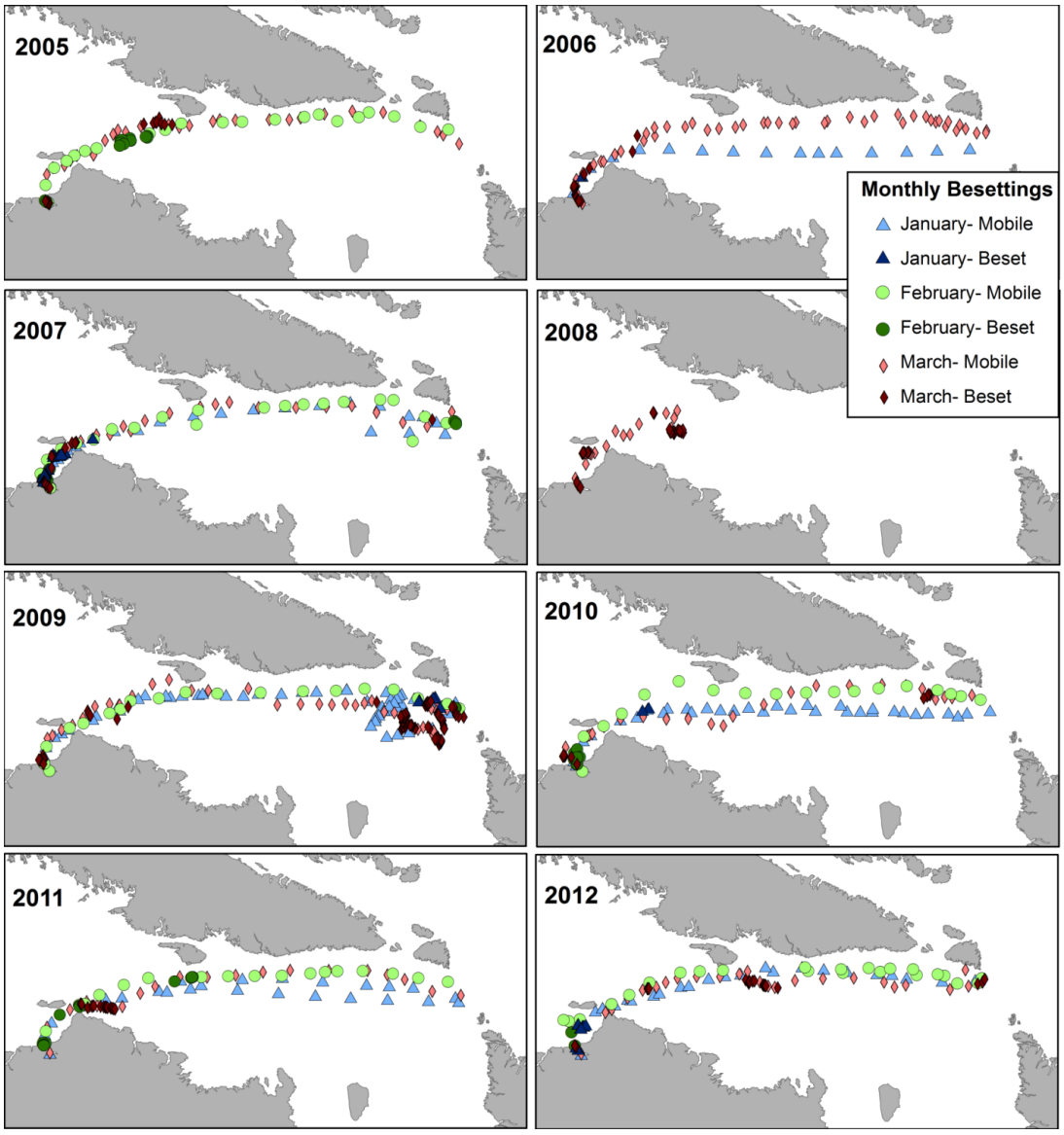

Figure 3.20: Annual grouping analysis for besetting events endured the MV Arctic in the Hudson Strait, 2005-2012

3.5 Conclusion

Pressured ice and ridges pose a serious threat to vessels traveling in ice infested waters. Most past studies have attempted to model ridging and pressure at a larger scale. More research is needed about the impacts of these conditions on an individual vessel to help captains predict where and when they might encounter pressured ice and how the ship might fare in particular ice conditions. The Hudson Strait is the site of winter shipping and is prone to the development of pressured ice and ridges as the ice moving through the Strait remains mobile all winter. The *MV Arctic* has used the Strait to access the Raglan mine year-round since 1998 and thus has a long history of encountering the ice hazards that result from the build-up of pressure and ridged ice.

Through the use of ship logs and previously identified ridges, this study attempted to understand how an ice strengthened vessel would be impacted by ridges and pressured ice in the Hudson Strait. The vessel was found to become beset in a few locations, at the entrance to Deception Bay, between Charles Island and the coast of Quebec and at the eastern entrance to the Strait. The vessel typically had the most difficulty navigating the strait in February and March, as the ice has only just formed in January and is thinner.

There was a very good correspondence between the incidence of ridges identified in Chapter 2 and the locations the besetting events. . This is important information for ship captains who can use the presence of ridges in order to predict where and when they might encounter difficult conditions and could become beset. When developing future shipping lanes, observations of ridging in the area could be used to determine the safest shipping routes before vessels attempt navigation. In the future, this approach to better predicting prevalence of pressured ice and ridges could be used to anticipate challenging areas for winter shipping. In the short term future, it may be advantageous to examine regions of the Canadian Arctic that are expected to experience increased winter ship traffic related to the now operational Mary River mine. Future studies of new shipping

lanes could focus on identifying areas and times of year when ridging occurs in order to develop safer shipping routes that avoid those hazardous conditions. .

REFERENCES

Agnico Eagle (2013). Meliadine.*Advanced Exploration Projects*. Retrieved from: http://www.agnicoeagle.com/en/Exploration/Advanced-Projects/Meliadine/Pages/default.aspx

ArcGIS Help (2013). How Hot Spot Analysis (Getis-Ord Gi*) works. ArcGIS Resources. Retrieved from: http://resources.arcgis.com/EN/HELP/MAIN/10.1/index.html#/How_Hot_Spot_Analysis_Getis_Ord_Gi_works/005p00000011000000/

AREVA (2011).Tier 2 Volume 2; Project Description and Assessment Basis.*Kiggavik Project; Environmental Impact Statement*. Retrieved from: http://kiggavik.ca/wp-content/uploads/2013/04/Volume-2-Project-Description-and-Assessment-Basis_sm.pdf

Baffinland (February 2012). Mary River Project; Final Environmental Impact Statement.Baffinland Iron Mines Corporation

Barrette, P. (2011). Offshore pipeline protection against gouging by ice: An overview. CRST, 69, 3–20. http://dx.doi.org/10.1016/j.coldregions.2011.06.007.

Bradford, D. (1972). Sea ice pressures observed on the second "Manhattan" voyage.*Arctic.*25(1) 34-39

Canadian Ice Service (2011), Sea Ice Climatic Atlas: Northern CanadianWaters 1981–2010, 995 pp., Ottawa.

Crane, R. G. (1978). Seasonal variations of sea ice extent in the Davis Strait–Labrador Sea area and relationship with synoptic-scale atmospheric circulation. *Arctic,* Vol. 31, 1978, pp. 434-447CIS, 2011

Drinkwater, K.F. (1988). On the mean and tidal currents in Hudson Strait.*Atmosphere-Ocean*. 26:255-266

Ekeberg, O.-C., Høyland, K., Hansen, E. (2015) Ice ridge keel geometry and shape derived from one year of upward looking sonar data in the Fram Strait. *Cold Regions Science and Technology*. 109: 78-89

Fednav (2005).Logbook.*MV Arctic*

Fednav (2006).Logbook.*MV Arctic*

Fednav (2007).Logbook.*MV Arctic*

Fednav (2008).Logbook.*MV Arctic*

Fednav (2009).Logbook.*MV Arctic*

Fednav (2010).Logbook.*MV Arctic*

Fednav (2011).Logbook.*MV Arctic*

Fednav (2012).Logbook.*MV Arctic*

Fednav (2013).Logbook.*MV Arctic*

Fednav (2014).Logbook.*MV Arctic*

Fednav (2010). Arctic. *Fleet*. Retrieved from: http://www.fednav.com/en/arctic

Hibler, W. D., III (1975).Characterization of cold-regions terrain using airborne laser profilometry. Journal of Glaciology, 15(73), 329–347.

Houser, C., W.A. Gough (2003). Variations in sea ice in the Hudson Strait. *Polar Geography*. 27(1) 1-14

International Association of Classification Societies (IACS) (2011).Requirements Concerning Polar Class. Retrieved from: http://www.iacs.org.uk/document/public/Publications/Unified_requirements/PDF/UR_I_pdf410.pdf

Kubat, I. and Sudom, D. (August 2008). Ship Safety and Performance in Pressured Ice Zones: Captains' Responses to Questionnaire. Canadian Hydraulics Centre. TP 14847E

Kubat, I., M. Hossein Babaei, M. Sayed (2012). Quantifying Ice Pressure Conditions and Predicting the Risk of Ship Besetting. Paper No. ICETECH12-130-R0

Kubat, I., M. Sayed, M. H. Babaei (2013).Analysis of Besetting Incidents in Frobisher Bay During 2012 Shipping Season.Proceedings of the 22nd International Conference on Port and Ocean Engineering under Arctic Conditions. June 9-13,2013, Espoo, Finland.

Kubat, I., Watson, D., Collins, A., Sayed, M. (2009).Modelling of ice pressure build-up in the Strait of Belle Isle and Northeast Coast of Newfound.Canadian Hydraulics Centre. CHC-TR-065

Kubat, I., Watson, D., Sayed, M. (2011).Characterization of Pressured Ice Threat to Shipping. POAC 11

Kwok, R. (2014). Declassified high-resolution visible imagery for Arctic sea ice investigations: An overview.*RemoteSensing of Environment*. 142:44-56

Marchenko, A.V (2008). Thermodynamic consolidation and melting of sea ice ridges. *Cold Regions Science and Technology*. (52) 278-301

NEAS (Nunavut Eastern Arctic Shipping) (2014).Shipping Schedule.*NunavutEasternArctic Shipping Inc.* Retrieved from: http://www.neas.ca/schedule.cfm

Parmerter, R.R., Coon, M., D. (1972).Model of Pressure Ridge Formation in Sea Ice. *Journal of Geophysical Research*. 77(33) 6565-6575

Saucier, F.J., Senneville, S., Prinsenberg, S., Roy, F., Smith, G., Gachon, P., Caya, D., Laprise,R., (2004). Modelling the sea ice-ocean seasonal cycle in Hudson Bay, Foxe Basin and Hudson Strait.*ClimateDyn*. 23, 303–326.

Stewart, D.B., and Lockhart, W.L. 2005. An overview of the Hudson Bay marine ecosystem.Can. Tech. Rep. Fish.Aquat. Sci. 2586: vi + 487 p.

Strub-Klein, L., &Sudom, D. (2012).A comprehensive analysis of the morphology of first-yearsea ice ridges. CRST, 82, 94–109. http://dx.doi.org/10.1016/j.coldregions.2012.05.014

Têtu, P-L., Pelletier, J.-F, Lasserre, F. (2015) The mining industry in Canada north of the 55th parallel: a maritime traffic generator?, *Polar Geography*, 38:2, 107-122, DOI: 10.1080/1088937X.2015.1028576

Timco, G.W., Burden, R.P. (1997) An analysis of the shapes of sea ice ridges. *Cold Regions*. 25(1) 65-77

Valdez Banda, O.A., Goerlandt, F., Montewka, J. Kujala, P. (2015). A risk analysis of winter navigation in Finnish sea area.*Accid. Anal Prev.* 79: 100-116, doi: 10.1016/j.aap.2015.03.024

Wadhams, P. (2000). Ice in the ocean. London: Gordon and Breach Science Publ.
s(351 pp.).

Weeks, W. F. (2010).On sea ice.Univ.of Alaska Press (664 pp.).

Weeks, W. F., and A. Kovacs (1970), On pressure ridges, CREEL Rep. IR505, Cold Reg. Res. and Eng. Lab., 59 pp., Hanover, N. H.

CHAPTER 4: CONTRIBUTIONS, LIMITATIONS AND RECOMMENDATIONS FOR FUTURE RESEARCH

4.1 Summary of Work and Conclusions

Pressured ice and ridges pose a dangerous risk to vessels traveling through ice infested waters. Pressured ice and ridges are difficult for even ice strengthened ships to navigate through and can cause them to become beset—stuck in the ice. More research is needed about these hazardous ice conditions in order to improve navigational decision-making and provide more information for captains and ship operators. This thesis addresses this knowledge gap by answering two questions: where and when are ridges occurring in the Hudson Strait and how ships transiting through the strait during the winter months are affected by this ridge and pressured ice.

In Chapter 2, ridge counts and ridge density distributions were determined using RADARSAT-1 and -2 images. A sea ice climatology for the Hudson Strait was created, which illustrated trends of later break up and earlier freeze-up dates in the region over the past 30 years. This is useful information for captains planning voyages through the Hudson Strait, especially in the shoulder seasons. Consistent patterns in the spatial distribution of ridges were identified, especially in the eastern and western regions of the winter shipping corridor where the ice was being forced through bottlenecks between islands and coasts. Linkages were between ridging patterns and sea level pressure and wind patterns were explored and found that low ridging seasons were associated with high SLP but high ridge seasons where associated with a combination of factors. Freeze-up dates were also associated with the level of ridging that occurred in the Strait. Freeze-up and breakup dates in the Hudson Strait were relatively consistent over the 15 year study period, which is useful information for captains operating during the shoulder seasons.

In Chapter 3, the impacts of pressured ice and ridges on vessel travel time and besetting events were investigated using data from the *MV Arctic's* ship logs. Where and when the ship became beset in the ice was determined from the vessel's reported location and notes

made in the *MV Arctic* ship log book. The vessel most frequently became beset in the shear zone formed where the mobile ice of the Hudson Strait met the land-fast ice in Deception Bay, It is also became beset in area between Charles Island and the northern coast of Quebec, as well as the eastern entrance to the Strait. The results of this analysis were compared to the ridge counts and densities identified in Chapter 2 finding that there is a significant correlation between ridge counts and besetting events.

4.2 CONTRIBUTIONS

Chapters 2 and 3 each make original contributions to the body of research on pressured ice and shipping in the Canadian Arctic, and combined they provide a comprehensive investigation on ridging and pressured ice in the Hudson Strait. Considering that vessel traffic in Arctic has increased in recent – including winter shipping related to resource development (see Pizzolato et al. 2014) –understanding in this area can facilitate safer and efficient ship navigation in the Hudson Strait.

Chapter 2 provides a characterization of ridging patterns over space and time within a winter shipping corridor in the Hudson Strait. The research provides a baseline ridge dataset for future studies. The research also addresses the current lack of knowledge on ridging distribution and pressured ice, and also establishes a new observational-based methodology for investigating sea ice dynamics in new winter Arctic shipping lanes. Currently, no detailed information about sea ice dynamics in the Hudson Strait is available and there has been a lack of research in general on the spatial distribution of ridging (and pressured ice) in a given area (Kwok, 2014). Previous work has modeled the factors leading to ice pressure events at a ship scale based on individual besetting events or a few besetting events over the course of one season (Kubat et al., 2008; Kubat et al., 2012; Kubat et al., 2013), but most work has focused on modelling pressure ridge formation and geometry (Parmerter and Coon, 1972;Hopkins, 1998; Amundrud at al., 2004; Gorbunova and Shkhinek, 2015; Ekeberg et al., 2015) and modelling ship voyages

(Montewka et al., 2015; Lasserre, 2015; Choi et al., 2015). There has also been some research into identifying ridges and tracking ice motion in satellite images (see Vesecky et al., 1988; Vesecky et al., 1990 Johnston, 2001; Johnston and Flett, 2001; Xue et al., 2011; Komarov and Barber, 2014; Kwok, 2014). In particular, what sets the research in Chapter two apart from previous works is that it covers a much longer spatiotemporal time period than any previous research and allows for comparison between ridging patterns between years. By covering a 15 year time period, there is the possibility of looking for changes over time, as well as to learn which ridging patterns and densities are typical for a given region and which are anomalous.

In addition to covering a long time span, the work in Chapter 2 makes important contributions to understanding the causes of pressure ridging by describing linkages between ridging patterns and sea level pressure, winds, and ice coverage over that 15 year period. Few previous papers have investigated the causes of ridging in Hudson Strait and this is important information for attempting to predict where and when pressured ice and ridges are going to be formed in the future. As well, the long time span of the research allows for comparisons to be made between the SLP, winds and ice coverage patterns for each of the years and the ridging patterns observed in those years in order to understand which factors influence ridging the most.

The research described in Chapter 3 builds on the foundation outlined in Chapter 2; it investigates the impacts of ridges and pressured ice on an ice strengthened vessel. The results describe the ship's voyages through the Hudson Strait over nine winter seasons. Because several years were included, as opposed to only one single incident or season, comparisons could be made between years in terms of where and when the vessel became beset. The longer time period provided more context than previous studies where only one voyage was examined and used as a basis for modeling ship besetting. Finally, when the ridges were included in the analysis, it allowed for understanding exactly what type of ridging conditions might cause a Polar Class 4 ice strengthened vessel to become beset.

There have been few attempts to relate actual observations of ridges and pressured ice to besetting incidents; most have been based on modeled ice conditions (see Kubat et al., 2009; Kubat et al., 2012; Kubat et al., 2013). As well, the results of the research, the cluster analysis in particular, validates observations made by captains of where and when ridges occur in the Hudson Strait by identifying statistically significant clusters of ridges.

Together, the research in these two Chapters address the need for more information on pressured ice and ridges as they relate to shipping. Ridging patterns were identified temporally and spatially, potential factors leading to those ridging patterns were posited and the impacts these conditions have on an ice strengthened vessel were investigated. This holistic approach covers regional ice dynamics and ice dynamics at a ship scale, which many studies fail to do, focusing on one or the other. The results demonstrate the potential use of ridges as predictors of difficult ice conditions, which can be used in the development of future shipping lanes, and if repeated with other vessel types, could characterize which ridge patterns and densities lead to the besetting events of particular vessel types.

4.3 LIMITATIONS

In each of the methods described in these two Chapters there are limitations that need to be acknowledged. In Chapter 2, there are several limitations due to the scale of the data included in the research. The accuracy of the identification of ridges was decreased by the low spatial resolution of the RADARSAT images used. Ridges are typically 3-4m wide while the images used had a 200m pixel^{-1} resolution (Johnston and Flett, 2001). Ridges were even more difficult to identify in densely crowded areas where ridges ran into one another. For these reasons, it was not possible to measure accurately ridge length or ridge width, these measurements could have given insight into ridge thickness and therefore, ridge strength. However, using ScanSAR Wide ensured that a much larger area could be covered with more frequent repeat passes. While ideally, larger scale images would have been used, they would have entailed a smaller study area with fewer passes over the same area by the satellite and a longer time period between passes.

Additionally, there are issues of scale using the NCEP reanalysis data, which has a scale of 25km, whereas the ScanSAR Wide images have a scale of 200m pixel^{-1}. However, the NCEP data was used to understand the broader scale patterns in SLP, air temperature and winds that affect the Hudson Strait and was used at a seasonal level.

Though smaller resolution imagery that covered a larger swath area was used, the corridor covered in Chapter 2 was fairly limited compared to the entire Strait. A more comprehensive, but time-consuming, study might have included a greater variety of conditions experienced by the ice, especially a longer area of coastline, which is highly variable and plays an important role in the creation of pressured ice. However, this was not possible given the extensive time required for the manual identification of ridges. The studied corridor did include some coastline included, as well as a bottleneck area and the middle of the strait, which provided some variety in terms of conditions the ice experienced.

In Chapter 3, the greatest limitation is that the comparison between ridging patterns and ships were done at the annual scale. Therefore, the precise impacts of those ridges on the vessel aren't known. The most accurate approach would have been to compare individual images closest to the date of the voyage to the locations where the vessel was beset in order to see exactly what conditions it was experiencing at the time. As well, some of the logbooks were missing and therefore there are some years where there was only voyage or part of a voyage available for analysis. The ship locations are limited by two hour increments and to the location of decimal degree minutes.

Another important limitation was the difficulty in determining where one besetting began and the next began. Notes in the logbooks simply stated if the vessel was beset or not, so it wasn't possible to know if the ship had gotten loose and then gotten stuck again within the two hours between the logbook notations. Location doesn't always resolve this issue as the ship can be moved quite a bit in the currents, tides and winds even if its beset so the track it leaves might be quite variable despite being stuck. This is especially of concern in the shear zone where the ship could become beset for days but might have actually gotten free, but still not have been able to cross the shear zone and so had gotten stuck or had retreated to wait for more favourable conditions rather than risk becoming beset and then being driven over the shoals that are present on either side of the entrance to Deception Bay. Individual besettings were identified to the best of my knowledge based on ship location, and notes made in the logbooks.

Finally, these results are limited to Polar Class 4 vessel, which is the rating of the MV Arctic. A vessel with a lower or higher ice class rating might have had a very different experience in the particular ice conditions present in the Hudson Strait.

4.4 Recommendations for Future Work

It is highly important that research is continued to better understand the processes that lead to ridged and pressured ice. There are several ways in which the work described in this thesis could be used as a foundation for future work.

To begin, the ridge identification process using ScanSAR Wide images should be validated. This could be done through 'on ice ridge analysis', or from a vessel. This would improve the accuracy of ridge identification from satellite images in the future and allow for the calculation of an error value. The described method could also be attempted with finer scale imagery, but this would limit the area covered and increase the image processing time. Finally, automated identification of ridges in satellite images is key to developing a faster method for mapping ridge densities. There has been some progress in this area but most has focused on classifying sea ice types, rather than identifying ridges. Automated classification would greatly enhance further studies of ridges and pressured ice (see Kwok et al.. 1992; Bogdanov et al., 2005; Yu et al., 2012; Leigh et al., 2014). Neural networks have been used in other areas to develop automated classification systems and this could potentially be implemented for the identification of ridges in satellite imagery (see Zakhvatkina et al.. 2013 for example).

More in-depth study is needed of the conditions leading to ridged ice in the Hudson Strait. Looking at the impacts of SLP, air temperature and winds at a finer temporal scale could reveal greater connections between these factors and the formation of ridges. Other factors could be included such as tidal patterns and currents. Additionally, further work could attempt the same methodology in a larger study area, one that includes a greater variety of conditions for the ice to encounter, such as islands, peninsulas, strong tides and winds. Including more coastline in the study area, rather than the short extent included in this study, could lead to a better understanding of ridge formation along shear zones and land-fast ice, and of where more treacherous shear zones might occur. Finally, using the

tools for deriving ice motion from RADARSAT would be an excellent next step for understanding ridging patterns and predicting areas of pressured ice. By tracking the convergent motion of the ice, pressured areas could be forecasted and identified without needing to individually identify ridges. Much work has already been done on ice motion from RADARSAT and SSM/I images including the development of feature tracking in RADARSAT2 images (Komarov and Barber, 2014). Kwok (2015) has used SSM/I and ASCAT images to track ice motion and convergence on the coasts of the Canadian Arctic Archipelago and Greenland in order to understand ice dynamics and its relationship to ice thickness distributions.

Further work that would build on the results of Chapter 3 could be conducting the same analysis in another location using a variety of ship types could provide better insight into how ridges might impact an icebreaker as opposed to a vessel with a lower Polar Class rating. As well, conducting the comparison between ridges and ship besetting events at a finer scale, such as monthly or even daily would provide a much better idea of how specific ridge conditions impact the vessel's voyage. Further work could include calculating fuel usage and carbon emissions based on voyage durations and their relationships to high and low ridge years. Another possible project would be creating least cost pathways through the Strait based on known areas of high ridge densities.

REFERENCES

Amundrud, T.L., Melling, H., Ingram, R.G. (2004). Geometrical constraints on the evolution of ridged sea ice.*Journal of Geophysical Research: Oceans.* 109(C06005) doi: 10.1029/2003JC002251

Bogdanov, A.V., Sandven, S., Johannessen, O.M., Alexandrov, V.Yu, Bobylev, L.P. (2005). Multisensor approach to automated classification of sea ice image data.*IEEE Transactions on Geoscience and Remote Sensing,* 43(7) 1648-1664

Choi, M., Chung, H., Yamaguchi, H., Nagakawa, K.(2015). Arctic sea route planning based on an uncertain ice prediction model. *Cold Regions Science and Technology.* 109:61-69

Ekeberg, O.-C., Høyland, K., Hansen, E. (2015) Ice ridge keel geometry and shape derived from one year of upward looking sonar data in the Fram Strait. Cold Regions Science and Technology. 109: 78-89

Gorbunova, K., Shkhinek, K. (2015). Engineering Properties of Sea Ice Ridges in the Barents Sea in 2012-2014 Years for Evaluation of Ice Loads on Offshore Structures. *Applied Mechanics and Materials*, (725-726) 263-269

Hopkins, M.A. (1998). Four stages of pressure ridging.*Journal of Geophysical Research: Oceans.* 103(C10) 21883-21891

Johnston, M. (2001). Validation of RADARSAT imagery using in situ measurements from first year ridged ice. Proceedings of the 16th International Conference on Port and Ocean Engineering under Arctic Conditions POAC'01 August 12-17 2001, Ottawa, Ontario, Canada.

Johnston, M. and D. Flett. (2001). First year ridges in RADARSAT ScanSAR imagery: influence of incidence angle and feature orientation. Proc. of 4th Int. Symp.On Remote Sensing, Int. Glac.Soc., 4 – 8 June 2001, College Park, U.S.A.,

Komarov, A.S., and D. G. Barber (2014).Sea Ice Motion Tracking From Sequential Dual-Polarization RADARSAT-2 Images. *IEEE Transactions on Geoscience and Remote Sensing.* 52(1), 121-136, doi:10.1109/TGRS.2012.2236845.

Kubat, I. and Sudom, D. (August 2008). Ship Safety and Performance in Pressured Ice Zones: Captains' Responses to Questionnaire. Canadian Hydraulics Centre. TP 14847E

Kubat, I., M. Hossein Babaei, M. Sayed (2012). Quantifying Ice Pressure Conditions and Predicting the Risk of Ship Besetting. Paper No. ICETECH12-130-R0

Kubat, I., M. Sayed, M. H. Babaei (2013).Analysis of Besetting Incidents in Frobisher Bay During 2012 Shipping Season.Proceedings of the 22nd International Conference on Port and Ocean Engineering under Arctic Conditions. June 9-13,2013, Espoo, Finland.

Kubat, I., Watson, D., Collins, A., Sayed, M. (2009).Modelling of ice pressure build-up in the Strait of Belle Isle and Northeast Coast of Newfound.Canadian Hydraulics Centre. CHC-TR-065

Kwok, R., E. Rignot, B. Holt, and R. G. Onstott (1992) Identification of Sea Ice Type in Spaceborne SAR Data. *J. Geophys. Res*., 97 (C2), 2391-2402

Kwok, R. (2014). Declassified high-resolution visible imagery for Arctic sea ice investigations: An overview.*Remote Sensing of Environment*. 142:44-56

Kwok, R. (2015). Sea ice convergence along the Arctic coasts of Greenland and the Canadian Arctic Archipelageo: Variability and extremes (1992-2014). *Geophysical Research Letters*, 42*, doi:*10.1002/2015GL065462.

Lasserre, F. (2015). Simulations of shipping along Arctic routes: comparison, analysis and economic perspectives. *Polar Record*. 51 (258) 239-259

Leigh, S., Z. Wang, D. A. Clausi (20134. Automated ice-water classification using dual polarization SAR satellite imagery, *IEEE Transactions on Geoscience and Remote Sensing*. 52(9) 5529-5539, doi: 10.1109/TGRS.2013.2290231

Montewka J., Goerlandt, F., Kujala, P., Lensu, M. (2015). Towards probabilistic models for the prediction of a ship performance in dynamic ice.*Cold Regions Science and Technology*. 112: 14-28

Parmerter, R.R., Coon, M.D. (1972). Model of pressure ridge formation in sea ice.*Journal of Geophysical Research.*77(33) 6565-6575

Vesecky, J.F., Samadani, R., Smith, M.P., Daida, J.M., Bracewell, R.N. (1988). Observations of Sea-ice dynamics using synthetic aperture radar images:

Automated analysis. *IEEE Transactions on Geoscience and Remote Sensing.* 26(1) 38-48

Vesecky, J.F., M.P. Smith, R. Samadani (1990). Extraction of lead and ridge characteristics from SAR images of sea ice. IEEE Transactions on Geoscience and remote sensing. 28(4) 740-744

Xue, C., X. Wen, Q. Dong, X. Wang (2011). Tracking the dynamic sea ice process with RADARSAT-2 Imagery.Proceedings of the Twenty-first (2011) International Offshore and Polar Engineering Conference. Maui, Hawaiim USA, June 19-24, 2011

Yu, P., D. A. Clausi, K. Qin, (2012). Unsupervised polarimetric SAR image segmentation and classification using region growing with edge penalty., *IEEE Transactions on Geoscience and Remote Sensing*, 50(4) 1302 - 1317

Zakhvatkina, N.Y., Alexandrov, V.Y., Johannessen, O.M., Sandven, S., Frolov, I.Y. (2013). Classification of sea ice types in ENVISAT synthetic aperture radar images. *IEEE Transactions on Geoscience and Remote Sensing.*51(5) 2587-2600